DESIGN, FABRICATION AND PERFORMANCE INVESTIGATION OF A DUAL CONVERTER FED VARIABLE SPEED D.C. DRIVE SYSTEM

178389
26-4-85

A DISSERTATION

submitted in partial fulfilment of the requirements for the award of the degree

of

MASTER OF ENGINEERING

in

ELECTRICAL ENGINEERING

(Power Apparatus and Electric Drives)

By

PRAMOD AGARWAL

DEPARTMENT OF ELECTRICAL ENGINEERING
UNIVERSITY OF ROORKEE
ROORKEE - 247 667 (INDIA)

January, 1985

CANDIDATE'S DECLARATION

I hereby certify that the work which is being presented in the dissertation entitled "DESIGN, FABRICATION AND PERFORMANCE INVESTIGATION OF A DUAL CONVERTER FED VARIABLE SPEED D.C. DRIVE SYSTEM" in partial fulfilment of the requirements for the degree of MASTER OF ENGINEERING IN ELECTRICAL ENGINEERING (Power Apparatus And Electric Drives) submitted in the Department of Electrical Engineering, University of Roorkee, Roorkee is an authentic record of my own work carried out during a period of six months from July 1984 to January 1985 under the supervision of Dr. V.K.Verma, Professor, Electrical Engineering Department, University of Roorkee, Roorkee.

The matter embodied in this dissertation has not been submitted for the award of any other degree or diploma.

Pramod Agarwal
(PRAMOD AGARWAL)

This is to certify that the above statement made by the candidate is correct to the best of my knowledge.

ROORKEE

DATE:January 21,1985

(DR. V.K.VERMA)
Professor
Electrical Engineering Department
University of Roorkee
Roorkee

A C K N O W L E D G E M E N T

I wish to express my profound sense of gratitude and indebtness to Dr. V.K.Verma, Professor of Electrical Engineering, for invaluable assistance, excellent guidance and sincere advice given by him during the course of investigations reported herein. It was a pleasure and a privelege to have worked under him during the tenure of this work. The care with which he examined the manuscript is thankfully acknowledged.

I am highly thankful to Dr. M.P.Dave, Professor and Head, Electrical Engineering Department, University of Roorkee, Roorkee, for providing computer and laboratory facilities.

I am deeply grateful to all the laboratory staff for their cooperation during the practical hours.

Thanks are also due to those who helped me directly or indirectly in preparing this dissertation.

Pramod Agarwal

(PRAMOD AGARWAL)

A B S T R A C T

The dissertation describes the design, analysis and experimental studies of a 4-quadrant, variable - speed d.c. drive fed from a single phase dual converter ;the d.c. motor field is seperately excited.

The various conventional schemes of adjustable speed d.c. drive are given in introduction. Different types of converters available are also described in the same chapter. Chapter 2 concerns the literature review in which the present status specifically in the field of dual converter controlled d.c. drive has been described. The basic dual converter and its types are discussed in chapter 3. The necessity of closed-loop control and description of the system designed in the present work are given in chapter 4. Chapter 5 deals with the mathematical model of the drive system and the state model of the system. The system design has been described in chapter 6. Experimental and theoretical results are compared in chapter 7. Conclusion and scope for further work are given in chapter 8. In appendix 'A', the parameter plane synthesis method and frequency scanning technique have been discussed. The measurement of d.c. motor constants and transducers gain have been given in appendix 'B'. The appendix 'C' deals with the discription of various chips. A listing of all computer programmes has been given in appendix 'D'.

NOMENCLATURE

The detailed list of the symbols used in the present work is given below. Lower-case letters have been used for instantaneous values of the quantities, and upper-case letters are used for constant, direct, average or rms values.

i_a	Motor armature current
e_a	Motor armature voltage
e_b	Motor generated voltage (or back emf.)
ω_m	Motor speed (rad/sec)
I_a	Average motor armature current
E_a	Average motor armature voltage
E_b	Average motor back emf.
ϕ	Average flux per pole
V	3-ϕ mains voltage (r.m.s. value)
R_a	Armature resistance (ohms)
L_a	Armature inductance (henrys)
K_b	Back emf constant
J	Moment of inertia of motor and loading generator
B	Viscous friction constant (including that of load on the motor)
T	Torque developed by the motor
T_L	Load torque
τ_m	Mechanical time constant (JR_a/K_b^2)

τ_a	Electrical time constant of the motor armature circuit
I_f	Field current
K_f	Field constant
V_R	Speed reference voltage
V_{c1}	Current controller output voltage
V_{c2}	Speed controller output voltage
K_1	Current controller gain
K_2	Speed controller gain
T_{c1}	Current controller time constant
T_{c2}	Speed controller time constant
ϵ_{c1}	Current error voltage
v'_{c1}	Voltage output of current error integrator
ϵ_{c2}	Speed error voltage
v'_{c2}	Voltage output of speed error integrator
V_c	Control voltage
A	Thyristor converter gain
T_{ca}	Converter delay time
ω_r	Reference speed
ω_f	Speed feedback
H_i	Current transducer gain
V_i	Current feedback voltage
H_ω	Tachogenerator gain

T_f	Tachogenerator filter time constant
V_ω	Speed feedback voltage
i_c	Circulating current
$I_{c\ max}$	Maximum circulating current
I_c	Average circulating current
α	Firing angle
s	Complex frequency
σ	Relative stability constant
ξ	Damping ratio
G,H,F	Functions of s
x	State variable
t	Time in second
L	Reactor coil inductance
V_{cc}	Supply voltage to firing circuit
ω_s	Supply frequency (rad/sec)
η	Efficiency
ω_d	Damping frequency

C O N T E N T S

Chapter - 1

INTRODUCTION

The growth of electric drives has closely paralleled the growth of automation in industry. In early periods, electric motors were operated directly from supply line under their own inherent torque - speed characteristics and at operating conditions determined by the mechanical load. Now, in most applications, motors are provided with control equipment by which their operating conditions are varied with respect to the mechanical load to suit the particular drive requirements. Electric drive systems provide a convenient means for controlling the operation of industrial machinery. In size, electric drives range all the way from fraction of one h.p. upto thousands of h.p. Speeds range from stalled positioning systems upto 15000 rev/min and higher [2].

D.C. motors are easily controllable and have dominated the adjustable speed drive field. A.C. motors are more expensive to control and are used in drive systems when special features of the a.c. motors, such as absence of commutators and brushes, must be utilized [1]. A.C. motors stall at loads above about twice their rated torque and can not start on loads above 150% of the rated torque. On the other hand, d.c. motors can start at higher loads and also can take up over loads upto 300 to 400 % of rated load for a short period. Regenerative or dynamic braking is easily obtainable with the d.c. motors for applications requiring quick stopping or speed reversal [24].

The basic equation of speed of d.c. motor is given by $\omega_m = \frac{E_a - I_a R_a}{K\phi}$. The speed of the separately excited d.c. motor can be controlled by following three methods:

(i) Varying resistance in the armature circuit

(ii) Varying motor excitation current

(iii) Varying the armature voltage.

Using the first method, the speed of the motor can be controlled in the downward direction from the rated speed at the expense of power loss in the armature circuit resistance. The second method is used for varying the speed above rated speed. This, in turn, produces severe problems of sparking at commutator and the consequent limitations on the life of brushes and commutators. Also, in this method torque decreases with increase in speed, therefore h.p. output above the rated speed remains constant. Smooth variation of speed over a wide range can be achieved by using the third method i.e. armature voltage control. In this method the flux of the motor is kept constant and h.p. is directly proportional to speed.

Ward Leonard speed control, first introduced about 85 years back, is the most familiar method of obtaining adjustable voltage for speed control of d.c. motor using the third method. It makes use of the motor - generator set and provides a smooth speed control over a wide range down to a very low value, which is limited by the residual magnetism of the generator. At lower speed, the stability of operation is affected by a demagnetization of the armature reaction. In this method, the power is automatically regenerated to the a.c. line through the M-G set when speed is reduced. The short time overload capacity is also large. The main disadvantages are:

(i) capital cost is high because of extra M-G set,

(ii) overall efficiency is less than 80 %,

(iii) large amount of space is required for the setup, and

(iv) periodic inspection and lubrication are necessary due to number of rotating machines [26].

Electricity is now a days distributed exclusively by 3 - Ø network at constant voltage and frequency. Therefore, a controlled electric drive always requires an additional power supply device in which the 3 - Ø supply is converted to d.c. of variable voltage. Conversion is achieved either with rotary converters or static devices, which include magnetic amplifiers, and mercury arc and semiconductor converters.

The heart of semiconductor converter is the thyristor, which was first introduced by General Electric Company, U.S.A. in 1957. It works on a similar principle of the gas - filled tube and thyratron. Once triggered, the thyristor must be restored to the blocking condition by some external means. In practice, this is done by natural or forced commutation. If we compare the most important types of power supply equipment for use with controlled drives, semiconductor converters are found in many respect to have significant and often decisive advantages.

In contrast to the rotary converters the semiconductor converter has no parts subjected to mechanical wear. Also efficiency is higher, response is better and cost of foundation is not considerable.

The semiconductor converter is far superior to the magnetic amplifier as regards speed of response. Its efficiency is usually higher, it weighs less and with the appropriate circuitry permits power reversal.

Mercury arc converters are of equal merit as far as response is concerned, but require various ancilliary devices for triggering and excitation etc. which are not needed with semiconductor equipment. Semiconductor converter works over a wider range of temperature. In addition, they are immediately ready for use, insensitive to vibration, have a higher overall efficiency and hence a small coolant requirement, they require less space and are easily replaced and stored [3].

Therefore, thyristor converters are the mostly used converters and provide variable armature voltage for the drive motor. The three basic methods: phase control, integral cycle control and chopper control for obtaining a variable d.c. voltage output from a fixed supply voltage (a.c. or d.c.) are illustrated in Fig. 1.1.

In all these methods, SCR connects the supply current to and disconnects it from the motor terminals. The frequency of switching is rapid, therefore, the motor responds to the average voltage output and not to the individual voltage pulses.

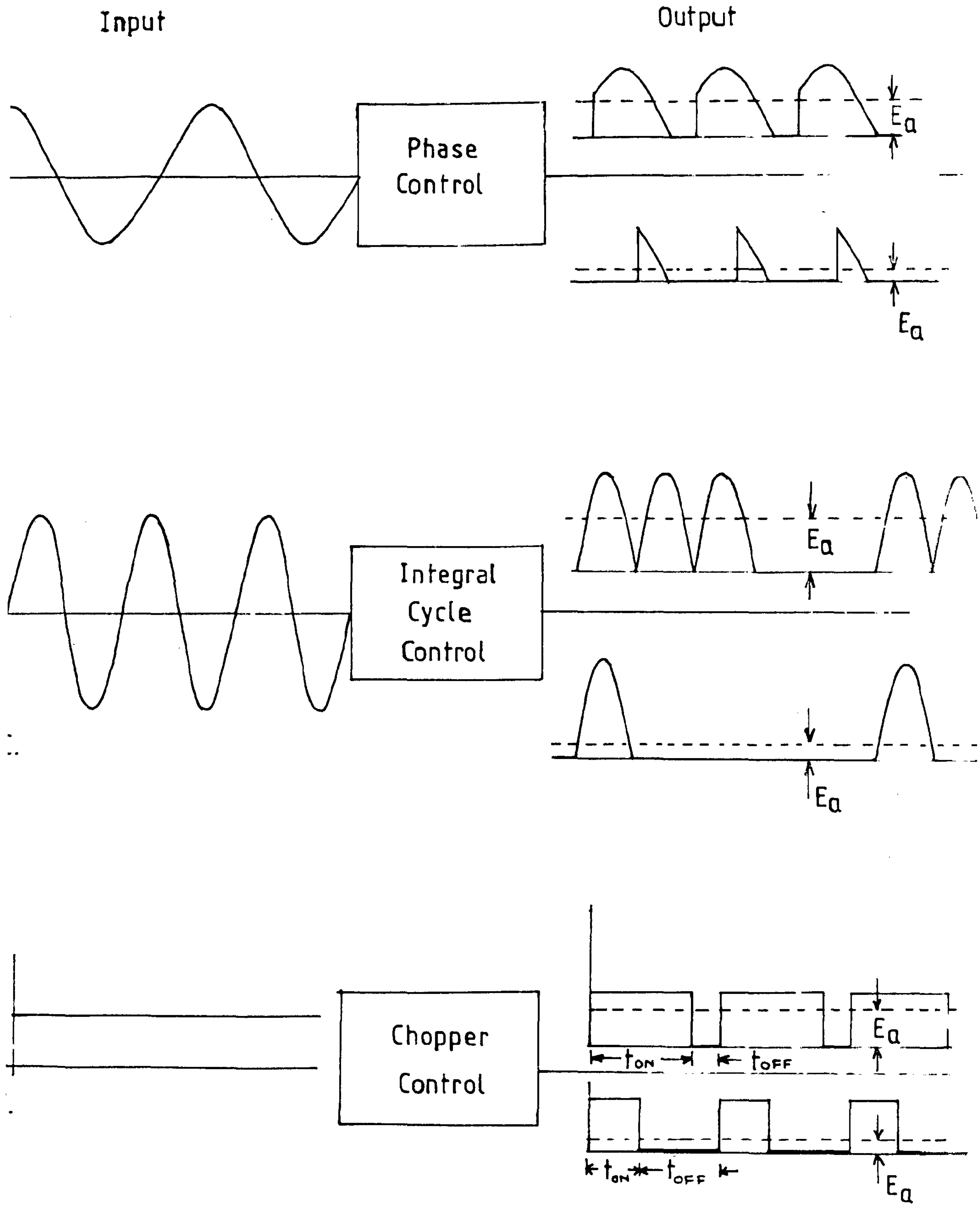

FIG.1.1 VARIOUS CONTROL METHODS

In both phase control and integral cycle control schemes, the conversion from a.c. to d.c. is achieved by rectification. In phase control, the SCR connects the supply to the motor during certain period in each half cycle and disconnects the motor from the supply for the remainder of each half cycle. In such converters, thyristor commutation (i.e. transfer of current from one SCR to the other) is easily achieved by a process referred to as natural or line commutation. When an incoming thyristor is turned ON, it immediately reverse biases the outgoing thyristor and turns it OFF. Therefore, no commutation circuit is necessary. These schemes are, therefore, simple and inexpensive, and hence widely used.

In the integral cycle control the SCR connects the supply to the motor for few half cycles and disconnects the motor for several half cycles. This scheme is satisfactory if the supply frequency is high and motor inertia is large, otherwise the motor will oscillate about its mean speed. This scheme has not been found satisfactory for speed control of motors.

If the supply is d.c., then chopper control scheme is used, in which SCR switches ON or OFF rapidly and provides a chopped voltage for the drive motor. The average value of the chopped voltage can be controlled by the ratio of the conduction time t_{ON} to the blocking time t_{OFF} of the thyristor. This scheme requires auxiliary circuits to turn off the SCRs. Choppers are operated at higher switching frequency to reduce the ripple content in the motor current. High speed switching requires special SCRs of low turn off time i.e. of inverter grade.

Therefore, chopper control is relatively complex, but nevertheless it is widely used [26, 27].

Now, since the dissertation concerns with phase controlled converters, therefore, these converters are discussed in great detail. Various alternative drive systems for d.c. machine using thyristor converter to control the applied armature voltage are illustrated in Fig. 1.2. The field winding of the machine is separately excited and steady state field current is fixed. Thus, by continuously controlling the armature voltage the speed of the motor is varied smoothly with a constant-torque characteristic.

In Fig. 1.2(a), a single quadrant converter is used to provide a unidirectional speed control of the motor. Due to incapability of converter to operate in inverting zone, it is not possible for energy to be returned from the motor to the supply and hence, the drive system does not have the facility of regenerative braking.

In Fig. 1.2(b), a 2-quadrant (fully controlled) converter is connected to the armature of the d.c. motor in which the voltage polarity can reverse but current remains unidirectional because of the unidirection thyristors. Regeneration of power is possible with fully controlled converter. In these two methods, it is not possible to control the speed in both directions.

In Fig. 1.2(c), a 2-quadrant converter is connected to the armature of a d.c. motor through a reversing switch.

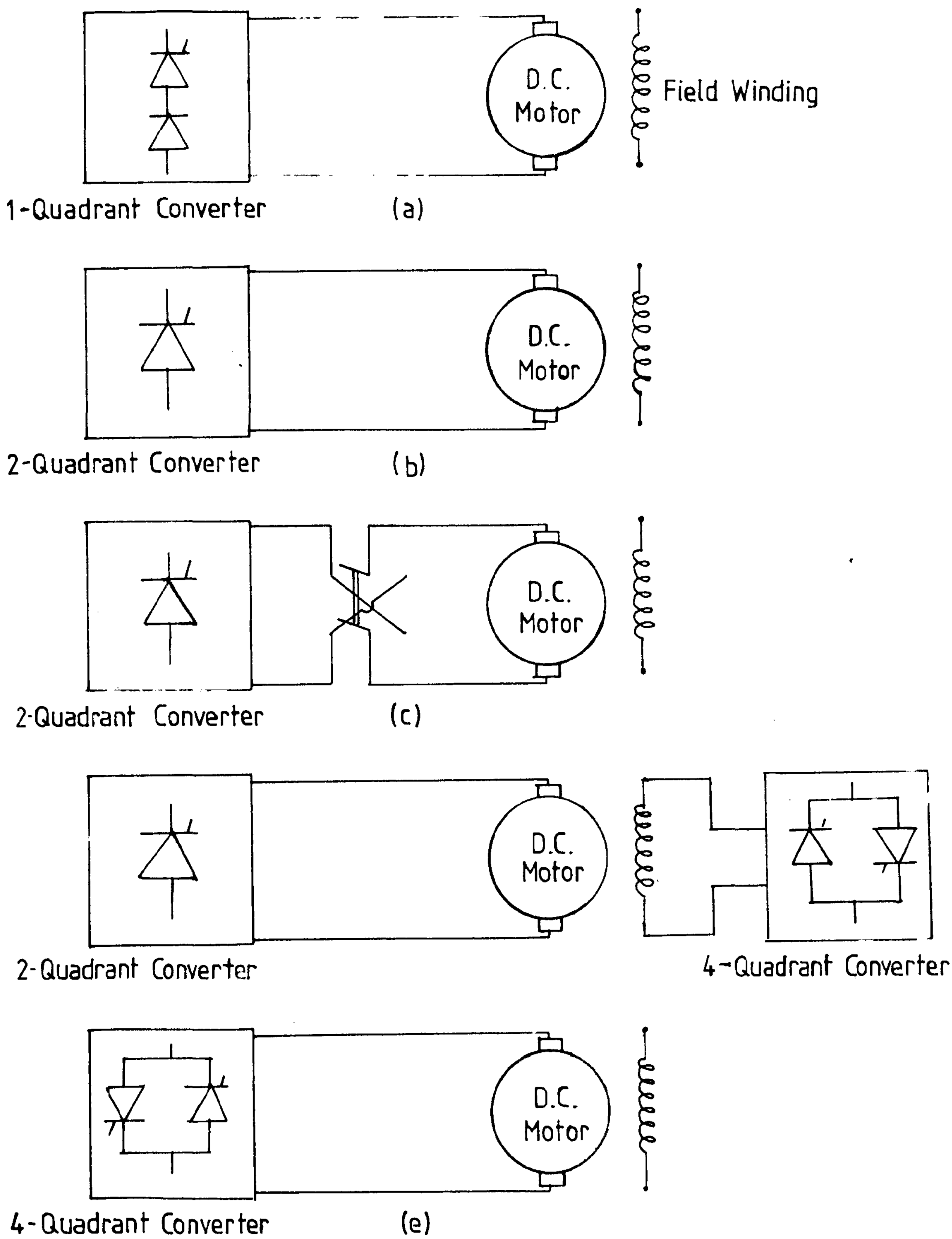

FIG.1.2. PHASE CONTROLLED CONVERTERS

Thus, by reversing the switch it is possible to control the speed in both directions, with the facility for regenerative braking. This method is satisfactory if the time delay associated with the mechanical change over of the reversing switch is small and acceptable. During this time, the machine coasts freely and is not under the control of converter.

In Fig. 1.2(d), a 2-quadrant converter is connected to the armature of d.c. motor and relatively low power 4-quadrant dual converter is connected to the field winding. Thus, by suitable control of dual converter the field current can be made to flow in either direction. Therefore, a full 4-quadrant operation is possible and speed of the motor can be controlled in both forward and reverse directions, with the facility for regenerative braking. The control circuit and the time response for current reversal cannot be as fast as that in the armature current reversal system because field winding is highly inductive.

In Fig. 1.2(e), a 4-quadrant dual converter is connected to the armature of d.c. motor. This system provides a fully reversing drive with regenerative braking without changing the armature circuit connections or field current polarity. Thus, by means of suitable control circuit it is possible to achieve very repid reversal of speed and torque with little or no time lag [22, 27].

The author has used single phase dual converter for speed control of d.c. motor in the present work.

Chapter - 2

LITERATURE REVIEW

A rapid growth of thyristor controlled d.c. drive applications has resulted from the many benefits derived by these equipments and replaced the conventional Ward Leonard M-G set. SCR drives are not exact equivalents of M-G sets and require special considerations regarding their successful utilization. Jacobs and Walsh [4] discuss some of them. The first part of the paper describes the static power conversion equipment, their characteristics and benefits as well as the effect on the d.c. drive motor. According to them, the pulsating voltage and current waveforms generated by an SCR power supply adversely affects the heating and commutation of a d.c. motor. The effect of SCR power conversion equipment on the power distribution system is described in the second part. The undesirable side effects of SCR drives are also described by Robinson [5]. According to him, these effects are due to high ripple content in the rectified voltage output of the converters, which causes increased heat generation in the d.c. drive motor and adversely affects its ability to commutate armature currents without sparking at the brushes. These effects are described and analysed for several basic configurations of converter power circuits. He has suggested that electrical design features of low sparking factor, sufficient inductance to minimize ripple currents, laminated interpole and frame structures along with large interpole airgaps, unsaturated interpole and frame magnetic circuits, high grade electrographitic brushes and smooth commutators contribute to good transient characteristic necessary to operate on rectified power and provide good transient response.

The degree of controllability provided by static converters is mostly determined by the speed and accuracy of information available from the transducers. This is the subject matter of research by Arrilage and Hisha [6]. The effect of providing fast ON/OFF detection of SCR is also discussed and a method based on continuous monitoring of gate to cathode voltage is suggested which provide sufficiently reliable fast ON/OFF information for the purpose of direct digital control of the converter plant.

Operating diagrams are developed for 1 - Ø as well as 3 - Ø half controlled thyristor converters connected to a general resistive, inductive and emf load in the paper by **Palenichamy and Subbiah** [7]. With the help of circuit equations, the mode of operation of such converters are identified and analyzed. Minimum inductance necessary in the load circuit for continuous current operations is also evaluated.

Simard and Raj Gopalan describe a simple equidistant pulse firing scheme [8] which is found quite economical for industrial application but its disadvantage is the minimum delay of at least a period necessary to provide any firing angle corrections; this is in contrast to the delay of one - sixth of a period in all the other schemes.

The theoretical relations between currents, fluxes and pulse duration in a d.c. motor energized by power pulses are described by Franklin [9]. From their values the average torque, speed, and their instantanceous variations are calculated. The non-linearity of the magnetic circuit is considered by a suitable approximation of the magnetization curve and the resulting error evaluated.

Rectifier performance with the low inductance counter emf load of a large d.c. motor is different from that of the performance resulting from a highly inductive load. The effect of rectifier discontinuous current on motor performance is discussed by K.G. Black [10]. If, at low average values the current is not continuous but flow in pulses, both the static and dynamic characteristics of the rectifier motor system are affected. He has suggested that addition of a series saturating reactor to the armature circuit overcomes these effects.

Farag and others [11] describe their analytical and experimental studies on a variable speed d.c. shunt motor driven by a single phase full wave rectified power supply using SCRs. They recommend that as motor current may be continuous or discontinuous the use of laminated stator is a must to reduce losses due to harmonic effect. Mathematical model expressions for the torque speed characteristics are derived for these two modes of operation. Experimental studies show that the calculated characteristics coincide very well with the measured characteristics over a wide range of speed. System stability has also been discussed by the second method of Liapunov. The calculated stability limits compare favourably with the experimental results.

Brill and Rammamorthy in part I of their paper [12] describe a reversible drive control for elevator doors, using a d.c. motor with phase-controlled power supply. The speed reversal is obtained by changing the polarity of the field voltage. Due to the large inductance of the field circuit the the complete reversal requires 4-cycle of the input line frequency. This tends to make the dynamic response of the motor a bit sluggish. The performance could have been improved by controlling the polarity of the armature voltage for speed reversal. The motor also hunts due to large gain in the feed back path and therefore has limited stable operating region. The problem could have been removed if the speed control is operated in open loop and feedback is used to limit the armature current in the extreme operating region.

In part II, the same authors [13] have described a modified control scheme using a d.c. shunt motor with armature control scheme for reversible operation and feedback control for current limits. This control provides a soft start during opening of door and dynamic braking reduces the door speed at the limit. Adjustable torque limit control the door force speed reversal is fairly instantaneous.

Krishnan and Ramaswami [14] in their paper describe a practical speed control system for a d.c. motor using a 1 - Ø controlled thyristor amplifier. The non-linear system is approximated by a low-order linear model as a good approximation. The main feature of their scheme is the inner current loop which protects the thyristor from over current and also provides fast response against disturbances such as variation in supply voltage. The speed control scheme discussed in their paper is useful for one direction of rotation.

The design, construction and operation of a 4-quadrant speed control scheme for separately excited d.c. motor fed from a dual converter has been discussed by the same authors [15]. The have used only one firing circuit and the firing pulses are directed to the appropriate converter by a master controller i.e. the dual converter is operating in discontinuous mode. PI controllers have been used to achieve good dynamic and steady state response. The main disadvantage of this scheme is the delay time between the switching over the controllers.

Sen and Machnald [16] presented a systematic procedure for analysis, design and testing of a SCR controlled separately excited d.c. motor drive system. The closed loop control scheme is analyzed using transfer function technique and the necessity of an inner current control loop is demonstrated. Armature reconnection is used to enable regenerative braking and speed reversal. Design of both proportional and proportional integral controller is outlined, and experimental results are given. While designing the controllers the system dynamic model is considerably simpified. This requires neglecting some smaller time constants.

Eswaramma and others [17] present a closed-loop control scheme of d.c. motor using dual converter operating in circulating current mode. The dual converter incorporates cosine firing circuit using integrated circutry. The method of speed control is found to be more economical. The fast reversal of speed is feasible because of the dual converter operating in circulating current mode. Circulating current is found more in 1 - Ø converter but can be reduced if 3 - Ø dual converter is used.

Duff and Ludbork [18] describe a technique for the design of reversible armature power supplies which results in a very high performance system and retains the high conversion efficiency of a single converter bridge. A unique firing circuit and regulator design allows the transfer characteristics of the two converter bridges to be coincident. Logic circuit is used to select the operating bridge dependent on system requirements.

Revanker and Subnis [19] analyse the dual converter system feeding separately excited d.c. motor load for both steady state and transient performance characteristics. Both the circulating current mode and circulating current free mode of operation are considered. Further, normalized circuit equations are derived and solved on digital computer for typical values of circuit parameters. They have concluded that circulating current free mode of operation is superior from the point of view of better power factor, efficiency and cost but the main drawback is the discontinuous conduction and consequent drop in the speed regulation characteristics.

Also, a dead zone is inevitable during the reversal of motor. Good speed regulation characteristics are possible with circulating current mode of operation and also fast reversal of load current is possible because of natural freedom for the load current to flow in either direction. However, if large circulating current is allowed, the p.f. and efficiency are poor. The improvement in transient response of the dual converter system in circulating current mode of operation is possible by using magnetically coupled reactors only if the armature inductance is very small.

In 1981, Mittal and Chatterjee [20] have described a simple method for the calculation of circulating current in a dual converter operating on no load. They have also shown that the injection of d.c. offset voltage in the gate circuit of dual converter reduces circulating current very much between positive and negative converters. The study of computed results shows that with this method it is possible to reduce the size of circulating current reactor by 66% for same level of circulating current between the converters.

Another method of controlling the circulating current between two reverse parallel connected converters (i.e. dual converter) is described by Srivastava and Davies [21]. According to them, completely suppressing the gate firing pulses of one converter to reduce circulating current often leads to failure of commutation on inversion due to inevitable difference in the instants of reappearance of these pulses on all bridge arms. The circulating current flows for the duration when successive phases are short - circuited during recurrent cycle of operation. This duration is reduced by biasing both the bridges in inverter region by an angle β. The duration of short circuit is eliminated for $\beta = 60^{o}$. In this arrangement, the regenerative braking is not possible until the back emf of motor is more than motor terminal voltage and therefore greater firing pulse movement is necessary.

Author's Contribution

The author has developed a thyristorized single-phase dual converter operating in circulating current mode for closed loop speed control of a separately excited d.c. motor for 4-quadrant motor operation. The dual converter incorporates cosine firing technique using integrated circuitry. A speed loop with PI controller maintains the desired speed irrespective of the load variation on the motor. An inner current control loop, again incorporating a PI controller, protects the thyristors from over currents. This loop also provides fast response overcoming the effects of disturbances such as variation in supply voltage. This system has the advantage of simple circuit controllability and smooth variations of speed control over a wide range by merely varying a single parameter in both the directions. The circulating current mode of operation gives fast response of speed. The method effectively replaces the Ward - Leonard system. The parameters of the

PI controllers are designed on the basis of system stability and response of the drive system. D-decomposition technique is used for finding the region of parameters for stable drive system and this is checked using Mikhilov criterion. Runga Kutta fourth order method is used for solving simultaneous differential equations to see the response of the drive. The dual converter is tested at resistive, inductive and motor loads.

Chapter - 3

DUAL CONVERTER

The principle and operation of single phase dual converter is described in this chapter. The circulating current and non-circulating mode of operation of dual converter with their advantages and disadvantages are considered in detail. The basic principle of obtaining cosine firing scheme is developed. The waveforms of various voltages and currents are discussed. Finally, the expressions for circulating current are developed.

3.1 Introduction

A dual converter consists of two similar fully-controlled phase converters which are connected in antiparallel as shown in Fig. 3.1. With this arrangement current can flow in either direction at the d.c. terminals, positive load current being carried by positive converter and negative load current by negative converter.

The converters are assumed ideal and they produce pure d.c. output voltage i.e. there is no ripple at the d.c. output terminals. The magnitude of the d.c. voltage varies as the cosine of the firing angles of the converters. The average voltage output at d.c. terminals of the 1 - Ø converter is given by:

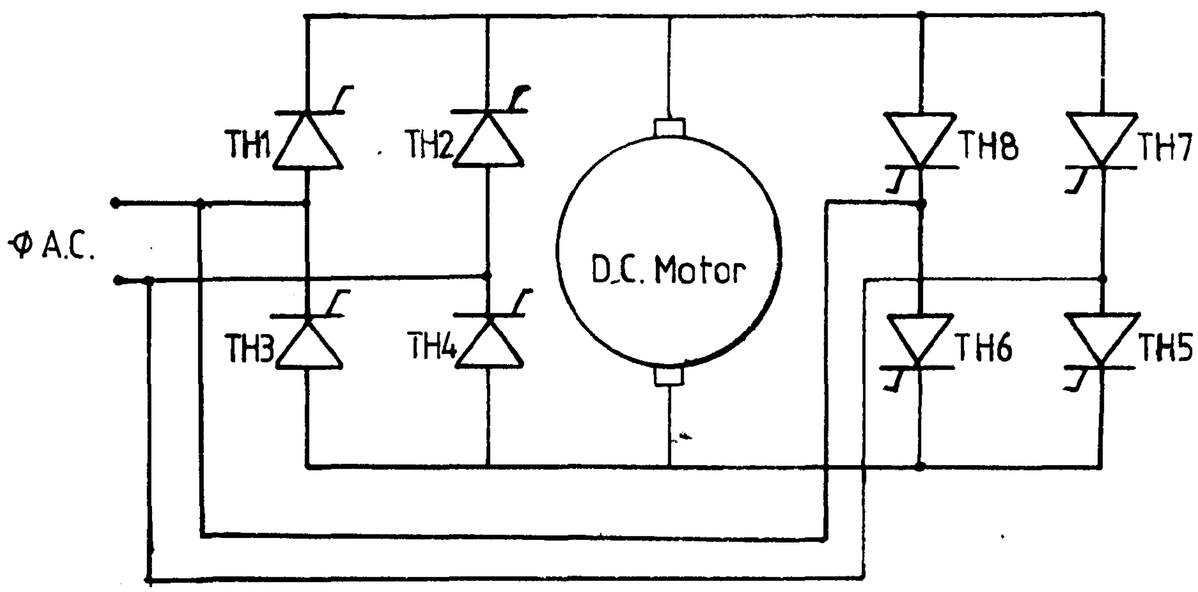

FIG. 3.1 DUAL CONVERTER

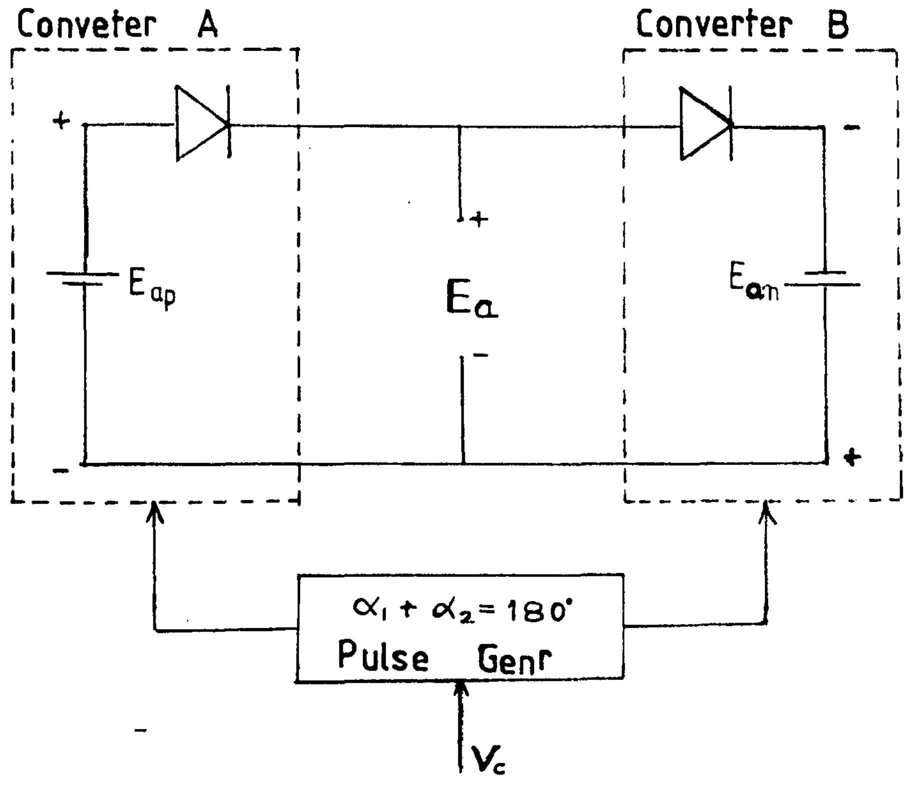

FIG. 3.2 REPRESENTATION OF DUAL CONVERTER

$$E_a = \frac{2\sqrt{2}}{\pi} V \cos\alpha$$

$$= E_{max} \cos\alpha \qquad \ldots(3.1)$$

where,

V = r.m.s. value of supply voltage

α = firing angle of the converter.

The converters can be replaced as shown in Fig. 3.2 by a d.c. voltage source in series with diodes that represent unidirectional current flow characteristic of the converters.

The firing angle of both the converters are regulated by a control voltage V_c so that their d.c. voltage outputs are equal and of the same polarity. Therefore,

$$E_{ap} = E_{max} \cos\alpha_1$$

$$E_{an} = E_{max} \cos\alpha_2 \qquad \ldots(3.2)$$

Where E_{ap} and E_{an} are the average d.c. voltage outputs of positive and negative converters respectively, and α_1 and α_2 are their firing angles.

In an ideal dual converter,

$$E_{ap} = -E_{an} = E_a \qquad \ldots(3.3)$$

From equations (3.2) and (3.3),

$$E_{max} \cos\alpha_1 = -E_{max} \cos\alpha_2$$

$$\text{or} \quad \cos\alpha_1 + \cos\alpha_2 = 0$$

$$\alpha_1 + \alpha_2 = 180^\circ \qquad \ldots(3.4)$$

Therefore, if the firing angle of one converter is less than 90° then, the firing angle of other converter will be more than 90°. Thus, both converters produce the same terminal voltage, one operating as rectifier (firing angle less than 90°) and other operating as inverter (firing angle more than 90°). Fig. 3.3 shows the terminal voltage as a function of firing angle for the two converters. The firing angle control circuit can be designed such that as the control voltage V_c changes, α_1 and α_2 change in such a way as to maintain $\alpha_1 + \alpha_2 = 180^{\circ}$.

In practice, with the firing angles of the converters controlled in this manner, only the mean d.c. terminal voltages of the two converters equal to one another, there are, however, inevitable instantaneous inequalities between the ripple voltages appearing at the d.c. terminals of the two converters. These ripple voltages are almost out of phase. If solid connection is made between the two converters, there would result theoretically an infinite circulating current that will not flow through the load. Therefore, circulating current between the converters must be controlled.

The first method for the above aim is to inhibit completely the flow of current through appropriate automatic control of the firing pulses, so that only that converter which carries the load current is in conduction and the other temporarily 'idle' converter is blocked. This is the so called circulating current free mode of operation. In

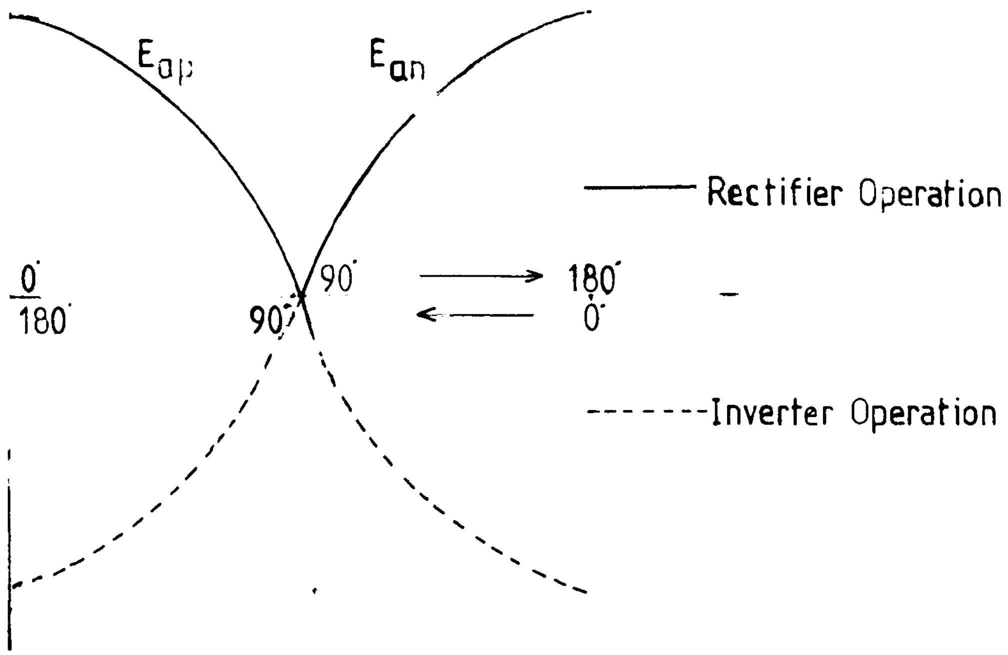

FIG.3.3 TERMINAL VOLTAGE VS FIRING ANGLE

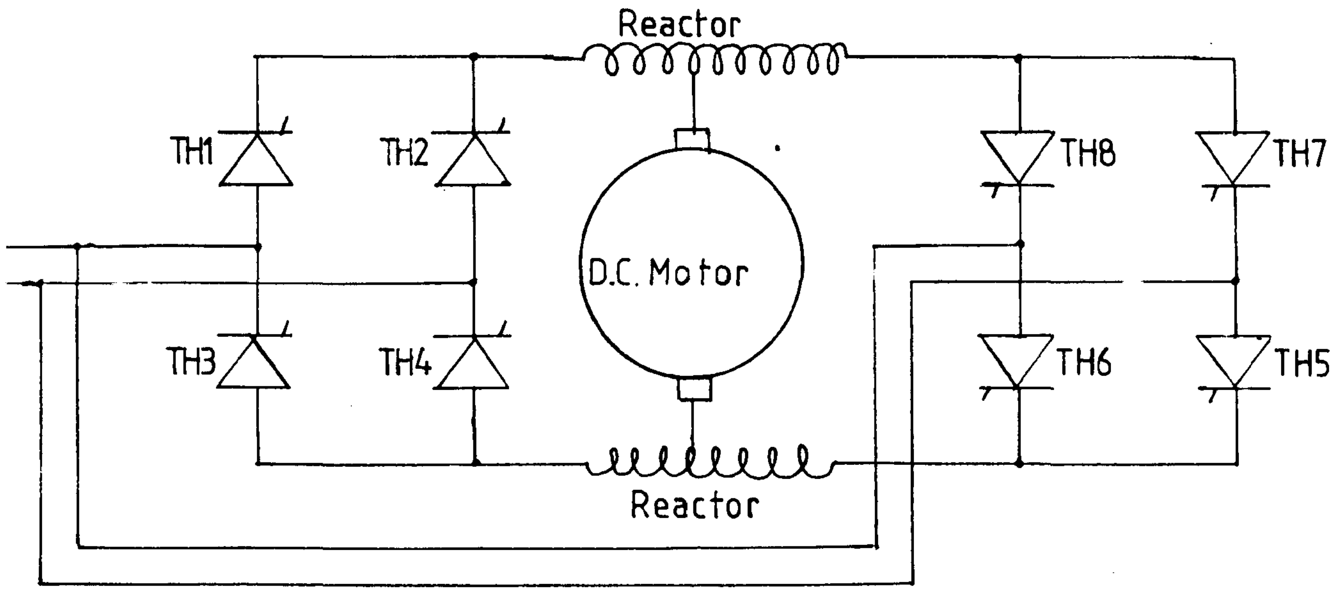

FIG.3.4 DUAL CONVETER WITH REACTORS

circuilating current free mode of operation, the various control strategies used are as mentioned below:

(a) Control signal polarity selects the converter.

(b) Load current selects the converter.

(c) Both control voltage and load current select the converter.

In the second method, the circulating current is limited to an acceptable level by means of the two reactors. This is the so called circulating current mode of operation and is shown in Fig. 3.4. The circulating current keeps both the converters in continuous conduction over entire control range in the loaded condition. However, in the no-load condition, the current is discontinuous except at $\alpha_1 = \alpha_2 = 90^o$. Table 3.1 gives merits and demerits of the circulating current and circulating current free mode of operation of a dual converter.

Table 3.1 Advantages and Disadvantages of Dual Converter with and without Circulating Current

S.No.	Consideration	With Circulating current	Without Circulating Current
1.	Current Mode	Converters operate in continuous current mode.	Converters operate in discontinuous current mode.

Table 3.1 (Contd.).

S.No.	Consideration	With Circulating Current	Without Circulating Current
2.	Transfer characteristic	Linear transfer characteristics are obtained with constant gain.	Non-linear transfer characteristics due to discontinuous current with reduced gain.
3.	Regulator response	Response is fast.	Response is sluggish
4.	Cross over technique	It is simple.	It is complex.
5.	Fault susceptibility	(a) Since one converter is always inverting, there is higher probability of converter faults.	(a) Inversion takes place only during regenerative braking and hence fault susceptibility is less.
		(b) Fault current between converters caused by spurious firing are restricted by presence of reactors.	(b) Faults between converters caused by spurious firing results in dead short circuit condition.
6.	Converter loading	The converter loading is higher than the output load.	The converter loading is same as the output load.
7.	Cost	Reactors are needed to limit circulating current. These reactors are costly.	Reactors may be needed to make load current continuous and to reduce ripple current.

Table 3.1 (Contd.)

S.No.	Consideration	With Circulating Current	Without Circulating Current
8.	Efficiency	Circulating current increases losses and hence, decreases efficiency.	Efficiency is higher.

Single-phase dual converter is used upto 20 h.p. and above 20 h.p. three-phase dual converter is used. The author has developed single-phase dual converter for speed control of a d.c. motor of 2 h.p. rating. The control circuitry is easy to fabricate in this case.

3.2 Basic Control Schemes

The basic principle of the firing control scheme is shown in Fig. 3.5. For single-phase dual converter the references for the triggering pulses of the SCRs are the zero voltage point of the a.c. line voltage. For SCR TH1 and TH4 (Fig. 3.4) the reference for triggering pulses is the instant t_1. If the $1-\phi$ dual converter is supplied with V_{RY} (line to line voltage of a 3-phase supply), and V_{BN} is used as synchronizing signal for firing circuit, this results in cosine firing scheme. The peak of V_{BN} coincides with the instant t_1. A control voltage V_c can be used to produce triggering pulses for TH1 at the crossing point with V_{BN}. Similarly, reverse voltage of V_{BN} i.e. V_{NB} can be used to

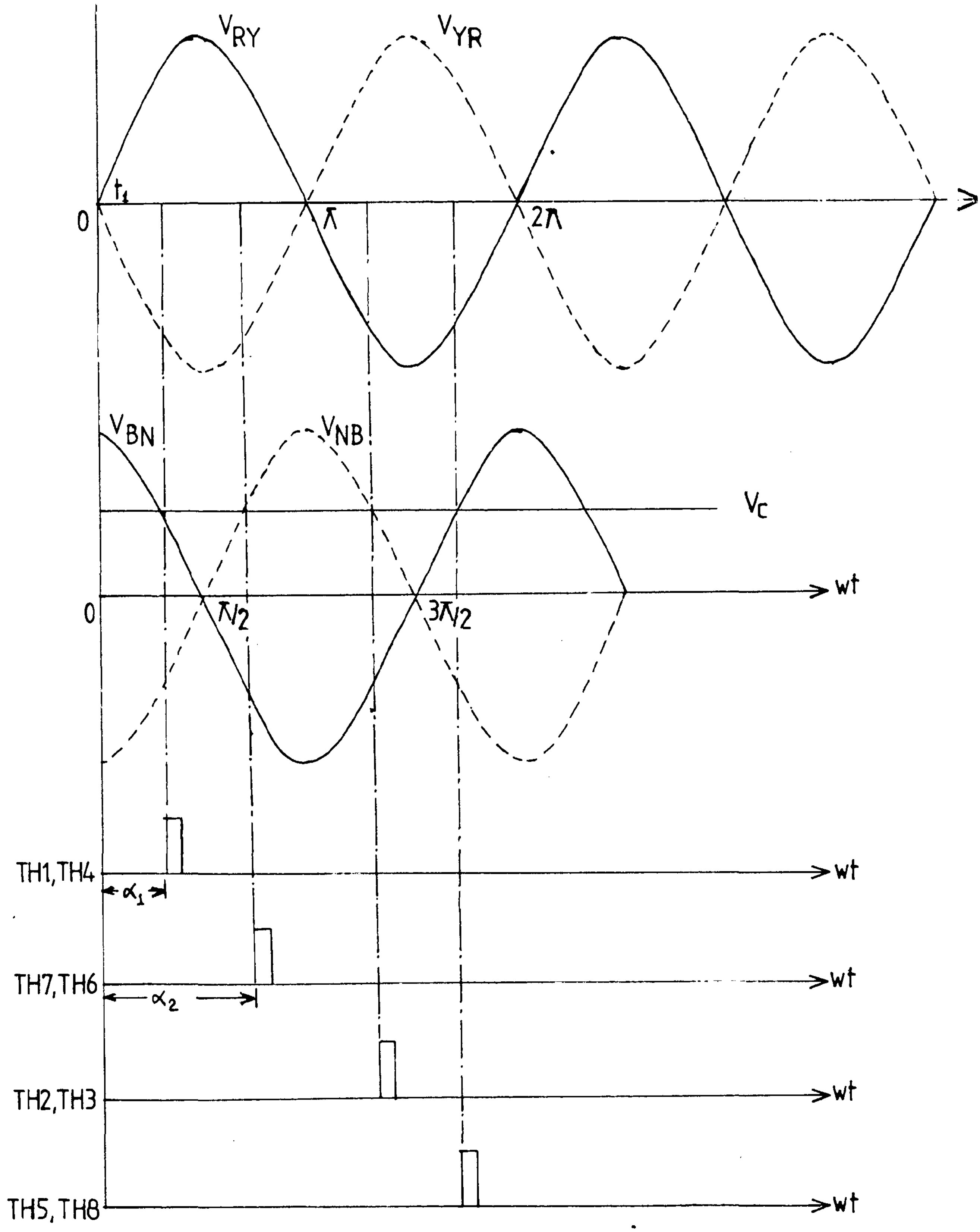

FIG.3.5 PRINCIPLE OF CONTROL SCHEME

generate triggering pulses for TH7 and TH6. If V_c is varied, the relationship $\alpha_1 + \alpha_2 = 180^o$ will be maintained. In case 3-phase supply is not available, single phase supply is directly given to the converter and the same voltage is advanced by 90^o using a phase-shift circuit for firing circuit to get cosine firing shceme.

Let

$$V_{BN} = K \cos\theta$$

$$\therefore V_{NB} = -K \cos\theta \qquad \ldots(3.5)$$

Then

$$V_c = K \cos\alpha_1$$

and also,

$$V_c = -K \cos\alpha_2 \qquad \ldots(3.6)$$

$$\therefore \quad K \cos\alpha_1 = -K \cos\alpha_2$$

$$\cos\alpha_1 + \cos\alpha_2 = 0$$

or

$$\alpha_1 + \alpha_2 = 180^o$$

$$\therefore \quad E_{ap} = E_{max} \cos\alpha_1 = \left(\frac{E_{max}}{K}\right) V_c \qquad \ldots(3.7)$$

$$E_{an} = E_{max} \cos\alpha_2 = -\left(\frac{E_{max}}{K}\right) V_c \qquad \ldots(3.8)$$

$$\therefore \quad E_a = E_{ap} = -E_{an} = \left(\frac{E_{max}}{K}\right) V_c \qquad \ldots(3.9)$$

Thus the d.c. terminal voltage is directly proportional to the control voltage V_c as shown in Fig. 3.6.

3.3 Operation and Waveforms

The operation of dual converter with circulating current is described below. The following assumptions are made:

(i) The reactors are lossless.

(ii) The firing angle of the two converters are controlled so that their sum is 180^o (i.e. $\alpha_1+\alpha_2=180^o$).

The waveforms for $\alpha_1 = 60^o$ and $\alpha_2 = 120^o$ are shown in Fig. 3.7. Because of the circulating current both the converters are in a state of continuous conduction under loaded condition. Hence, the waveforms are well defined. The instantaneous d.c. terminal voltage is the average of the instantaneous converter voltage. The instantaneous voltage across the reactors is the difference between the instantaneous converter voltages.

3.4 Circulating Current

The circulating current is obtained from the time integral of the voltage across the reactors.

Voltage applied to the converters = $\sqrt{2}\ V\ \mathrm{Sin}\omega_s t$

Instantaneous voltage across the reactors = $2\sqrt{2}\ V\ \mathrm{Sin}\omega_s t$

There are two operating conditions :

Case 1. When α_1 is less than 90^o, the voltage across the reactors varies from α_2 to $\pi+\alpha_1$.

Case 2. When α_1 is more than 90^o, the voltage across the reactors varies from α_1 to $\pi+\alpha_2$.

Let the inductance of each reactor be L and the circulating current be i_c.

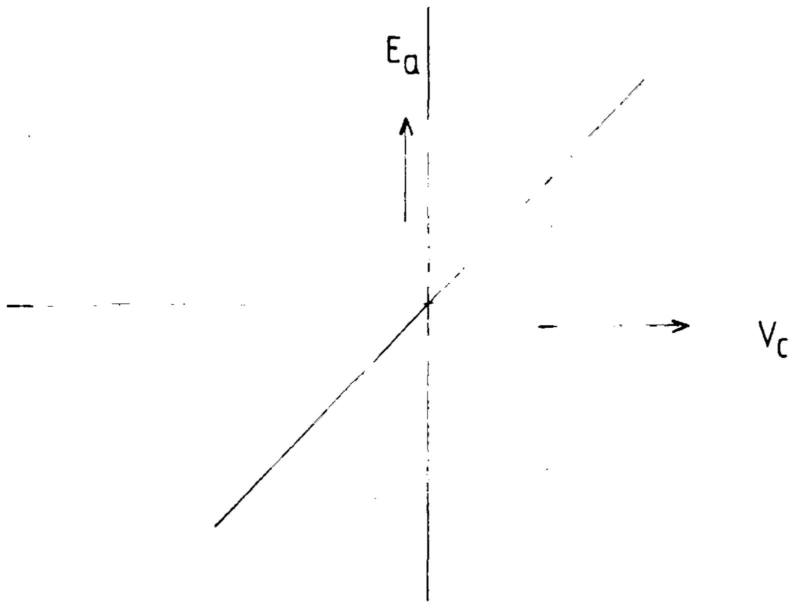

FIG.3.6 TERMINAL VOLTAGE VS CONTROL VOLTAGE

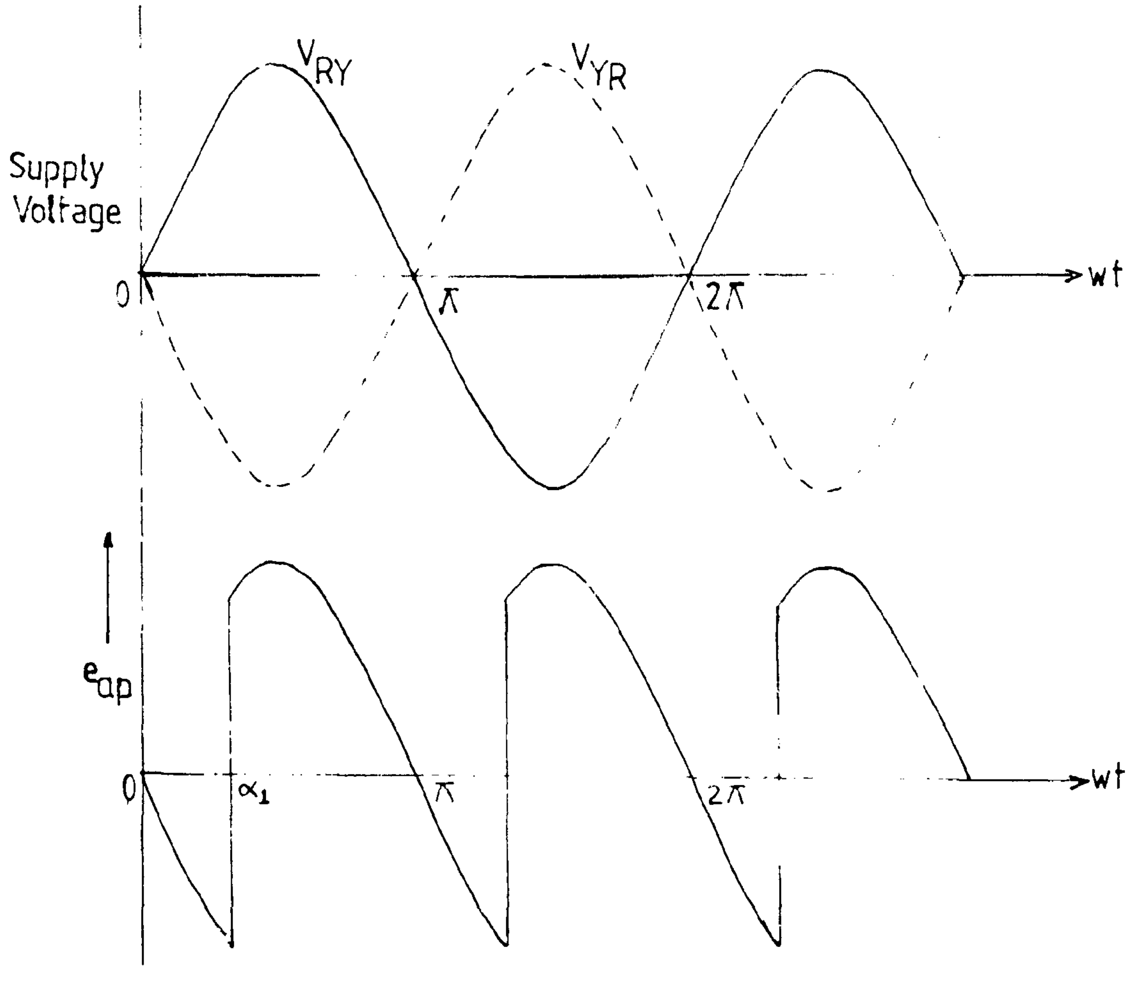

FIG.3.7 DUAL CONVERTER WAVEFORMS

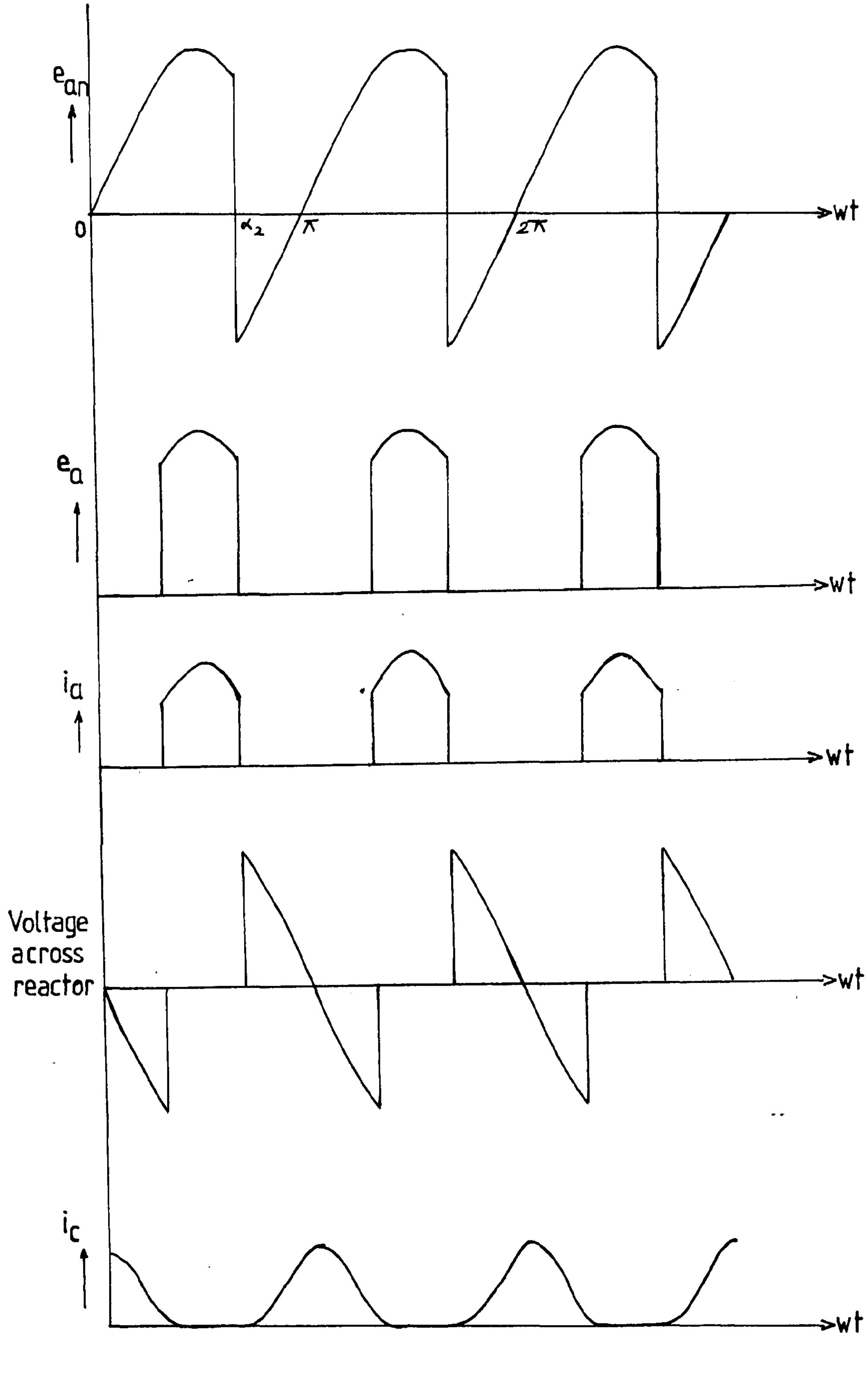

FIG. 3.7 DUAL CONVERTER WAVEFORMS (Contd.)

$$\therefore \quad 2L \frac{di_c}{dt} = 2\sqrt{2}\, V \, Sin\omega_s t$$

or

$$\frac{di_c}{dt} = \frac{\sqrt{2}\, V}{L} \, Sin\omega_s t$$

In case 1,

$$i_c = \frac{\sqrt{2}\, V}{L} \int_{\alpha_2/\omega_s}^{t} Sin\omega_s t \, dt$$

$$= \frac{\sqrt{2}\, V}{\omega_s L} \, (Cos\alpha_2 - Cos\omega_s t)$$

In case 2,

$$i_c = \frac{\sqrt{2}\, V}{L} \int_{\alpha_1/\omega_s}^{t} Sin\omega_s t \, dt$$

$$= \frac{\sqrt{2}\, V}{\omega_s L} \, (Cos\alpha_1 - Cos\omega_s t)$$

Maximum value of circulating current occurs at $\omega_s t = \pi$ with $\alpha_1 = \alpha_2 = 90^o$ and is given by

$$I_{cmax} = \frac{\sqrt{2}\, V}{\omega_s L}$$

The average value of the circulating current for the case 1, when $\alpha_1 \leqslant 90^o$, can be calculated as follows:

$$\text{Average value of } i_c = I_c = \frac{1}{\pi} \int_{\alpha_2}^{\pi+\alpha_1} i_c d(\omega_s t)$$

$$= \frac{1}{\pi} \int_{\alpha_2}^{\pi+\alpha_1} \frac{\sqrt{2}\, V}{\omega_s L} \, (Cos\alpha_2 - Cos\omega_s t) \; d(\omega_s t)$$

$$= \frac{2\sqrt{2}\, V}{\omega_s L} \, [- \alpha_1 \, Cos\alpha_1 + Sin\alpha_1]$$

Similarly, when $\alpha_1 > 90^o$

Average value of $i_c = I_c = \frac{1}{\pi} \int_{\alpha_1}^{\pi+\alpha_2} i_c \, d(\omega_s t)$

$$= \frac{1}{\pi} \int_{\alpha_1}^{\pi+\alpha_2} \frac{\sqrt{2}\, V}{\omega_s L} \left(\text{Cos}\alpha_1 - \text{Cos}\omega_s t\right) \, d(\omega_s t)$$

$$= \frac{2\sqrt{2}\, V}{\omega_s L} \left[- \alpha_2 \,\text{Cos}\alpha_2 + \text{Sin}\alpha_2\right]$$

The circulating current thus depends upon firing angles and is limited by the value of reactors. The variation of average value of circulating current with the firing angle α_1 is shown in Fig. 3.8.

Without the load current the converter current is the same as the circulating current and is due to the ripple voltages. The overall conduction of current is discontinuous.

With the load current in positive direction, the load current flows through positive converter for some portion in each half cycle and for the remaining portion in each half cycle circulating current flows. Thus, positive converter is in continuous conduction state. The negative converter carries only the circulating current and therefore, in discontinuous conduction state.

3.5 Conclusion

The principle of dual converter is described. The firing angle of both the converters are varied in such a manner so that their sum is always 180°. One converter

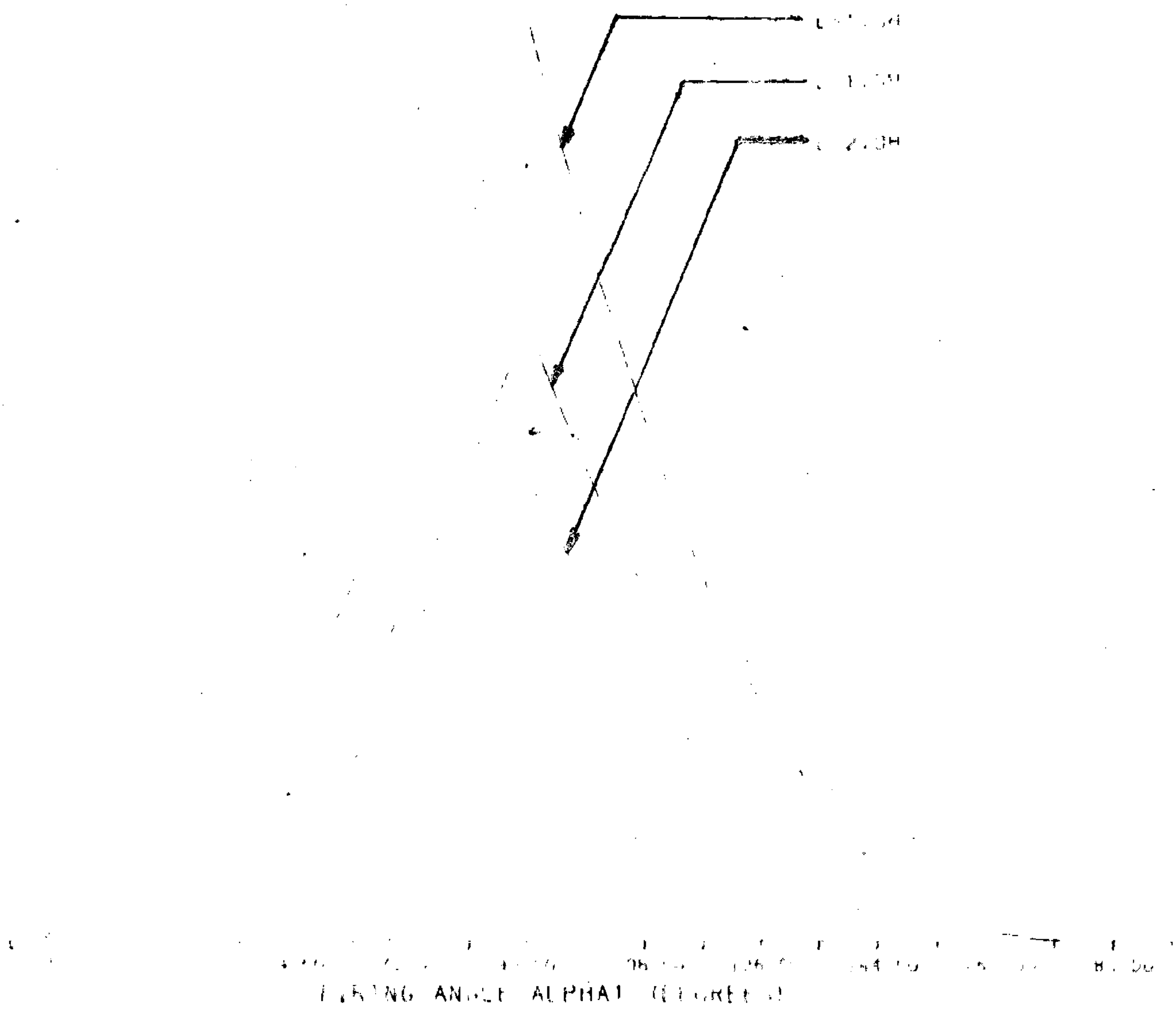

FIG 5B

operates in rectification mode and other operates in inversion mode. The advantages and disadvantages are discussed. In circulating current mode of operation, the circulating current is limited to an acceptable value using reactors. The cosine firing scheme is such that the d.c. terminal voltage is directly proportional to the control voltage. Circulating current keeps both the converters in continuous conduction under loaded condition. The circulating current is maximum at firing angles equal to 90°.

Chapter - 4

CLOSED-LOOP CONTROL SCHEME

In this chapter, the closed-loop control scheme for speed control of a separately excited d.c. motor is described. speed controller and current controller are discussed in great detail. The basic components of cosine firing circuit and the waveforms at each point are described. The dv/dt protection of thyristor is considered. The operation of experimental setup is also described.

4.1 Introduction

The open loop operation of a d.c. motor may not be satisfactory in many applications. If the firing angle is kept constant and the torque applied to the motor is increased, the speed changes. If the drive requires constant speed operation, the firing angle of the converter must be changed to maintain a constant speed. This can be achieved in a closed-loop control system. The basic block diagram of such a system is shown in Fig. 4.1.

If the motor speed decreases due to application of the additional load torque, the speed error ϵ_{c2} increases which increases the control voltage signal V_c. This, inturn, changes the firing angle of the converter and increases the motor armature voltage E_a, and hence, restore the speed of the system. The system passes through a

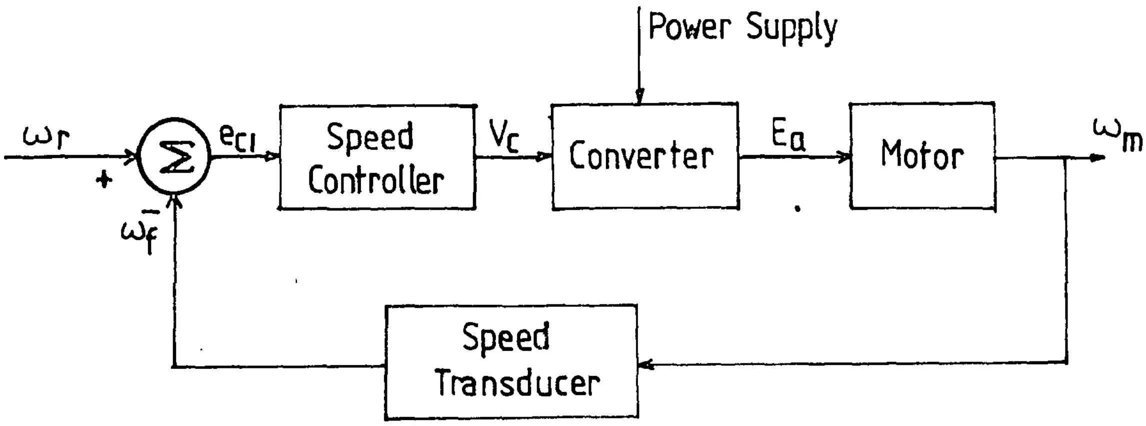

FIG.4.1 BASIC CLOSED LOOP CONTROL SYSTEM

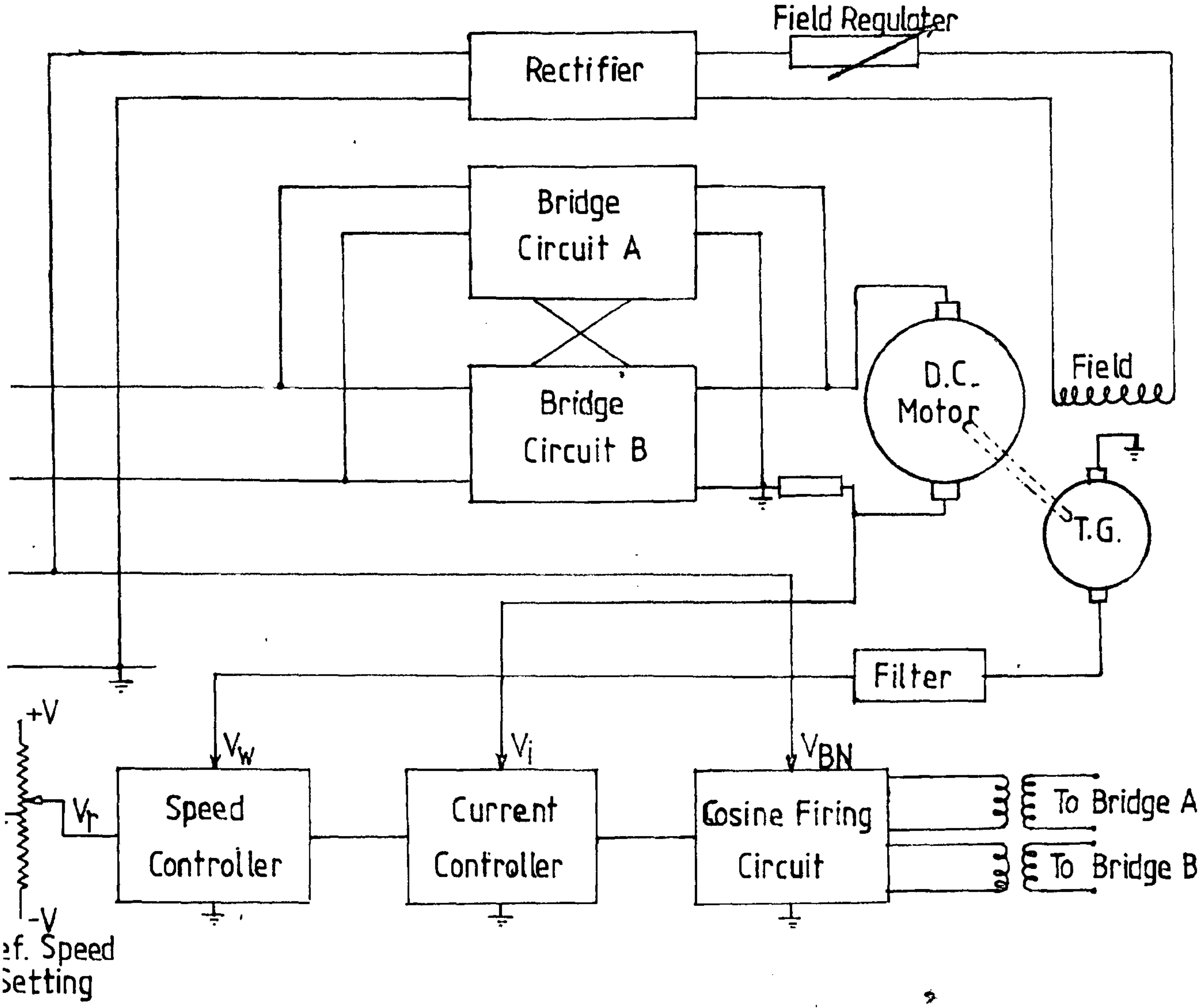

FIG.4.2 BLOCK DIAGRAM OF EXPERIMENTAL SYSTEM

transient period until the developed torque matches the applied torque. A closed-loop control has the advantages of greater speed accuracy, improved dynamic response and reduce effects of disturbances such as loading, supply voltage variation etc. When the drive requires rapid acceleration and deceleration, closed - loop control is a must.

4.2 Description of System

The basic scheme is shown schematically in Fig. 4.2. A separately exicited d.c. motor driving a separately-excited d.c. generator is the plant, the speed of which is to be controlled. The armature of the d.c. motor is fed from a single - phase fully controlled dual converter. Four integrated firing circuits are fabricated for firing the thyristors and the firing angle is controlled by V_{c1}, the output of the current controller. The armature current is sensed by means of a low resistance in the armature circuit. The speed is sensed by means of a tacho - generator mounted on the motor shaft.

4.3 Control Scheme

The control scheme consists of

4.3.1 Speed and current controllers

4.3.2 Cosine firing circuit

4.3.3 Dual converter

4.3.4 Field circuit rectifier

4.3.1 Speed and Current Controllers

(a) Reference Speed Setting

It is provided through a centre-tapped potentiometer and can vary from positive reference speed to negative reference speed.

(b) Speed Controller

The speed loop is required to provide zero steady-state error and fast response. Therefore, a proportional plus integral controller (PI) is used for speed control. The reference speed set by the potentiometer (V_R) and the tachogenerator output voltage (V_ω) are compared, and error ($V_R - V_\omega$) is amplified in the PI controller. The speed-controller output V_{c2} automatically sets the current reference such that the desired speed is maintained independent of the load on the motor. The saturation feature in the speed controller is used for providing the current limiting in both the directions.

(c) Current Controller

A PI controller is again used as current controller to regulate the current. While starting the motor, or reversing its direction of rotation, the converter putput is maximum as the control input to the firing circuit is at its maximum value. This causes a very heavy current to flow after the drop in speed is integrated out by the speed (PI) controller to give a new firing angle α. Hence, for the corrective action to take place, a change in speed has to accompany a change in the supply voltage and the response is poor on account of the large mechanical time constant involved. With a current loop present, a fall in armature current itself results in a new firing angle α and fall in supply voltage is counter - acted by correcting the armature current at a fast rate. This results in a fast response with zero steady - state error.

4.3.2 Cosine Firing Circuit

The block diagram of cosine firing circuit and the output waveforms at each stage of the circuit are shown in Fig. 4.3.

The circuit uses the principle of cosine wave crossing control which determines the firing point of each SCR from the crossing point of synchronizing signal with the analog reference signal or control voltage V_{c1}. The firing angle is made to respond to this control voltage V_{c1} such that the cosine of firing angle α is proportional to control voltage V_{c1} i.e. $\cos\alpha \propto V_{c1}$.

The circuit consists of a comparator, differentiator, monostable (pulse stretcher), oscillator and output stages. The control signal and the cosine time wave (synchronizing signal) are compared in a comparator. The output of comparator is differentiated. A pulse stretching circuit which is

4.3.1 Speed and Current Controllers

(a) Reference Speed Setting

It is provided through a centre-tapped potentiometer and can vary from positive reference speed to negative reference speed.

(b) Speed Controller

The speed loop is required to provide zero steady-state error and fast response. Therefore, a proportional plus integral controller (PI) is used for speed control. The reference speed set by the potentiometer (V_R) and the tachogenerator output voltage (V_ω) are compared, and error (V_R - V_ω) is amplified in the PI controller. The speed-controller output V_{c2} automatically sets the current reference such that the desired speed is maintained independent of the load on the motor. The saturation feature in the speed controller is used for providing the current limiting in both the directions.

(c) Current Controller

A PI controller is again used as current controller to regulate the current. While starting the motor, or reversing its direction of rotation, the converter putput is maximum as the control input to the firing circuit is at its maximum value. This causes a very heavy current to flow in the armature which might damage the motor as well as the SCR converter. Also overload will result in overcurrents. To avoid these problems, a current control loop is provided to limit the armature current to a safe value, and protect the converter and motor from overcurrents. This is achieved by sensing the armature current using a low resistance in series with motor armature and feeding voltage drop across it to the input of PI current controller. The references signal V_{c2} for motor armature current and current feed back signal V_i are compared in this controller. The output of current controller V_{c1}, sets the firing angle of the converters. The output V_{c1} is limited in both directions (+ve and - ve) such that firing angle α lies between two limits α_{min} and α_{max}. This can be achieved by providing saturation feature in the current controller output.

The current controller also provides fast response overcoming the effect of disturbances such as variation in supply voltage.

Suppose the supply voltage falls. Since the electrical time constant τ_a of the armature is small compared to the mechanical time constant, the armature current rather than speed drops almost instantaneously. In the absence of the current loop, the motor decelerates to cope with the load torque. The speed comes back to the original speed only after the drop in speed is integrated out by the speed (PI) controller to give a new firing angle α. Hence, for the corrective action to take place, a change in speed has to accompany a change in the supply voltage and the response is poor on account of the large mechanical time constant involved. With a current loop present, a fall in armature current itself results in a new firing angle α and fall in supply voltage is counter - acted by correcting the armature current at a fast rate. This results in a fast response with zero steady - state error.

4.3.2 Cosine Firing Circuit

The block diagram of cosine firing circuit and the output waveforms at each stage of the circuit are shown in Fig. 4.3.

The circuit uses the principle of cosine wave crossing control which determines the firing point of each SCR from the crossing point of synchronizing signal with the analog reference signal or control voltage V_{c1}. The firing angle is made to respond to this control voltage V_{c1} such that the cosine of firing angle α is proportional to control voltage V_{c1} i.e. $\cos\alpha \propto V_{c1}$.

The circuit consists of a comparator, differentiator, monostable (pulse stretcher), oscillator and output stages. The control signal and the cosine time wave (synchronizing signal) are compared in a comparator. The output of comparator is differentiated. A pulse stretching circuit which is

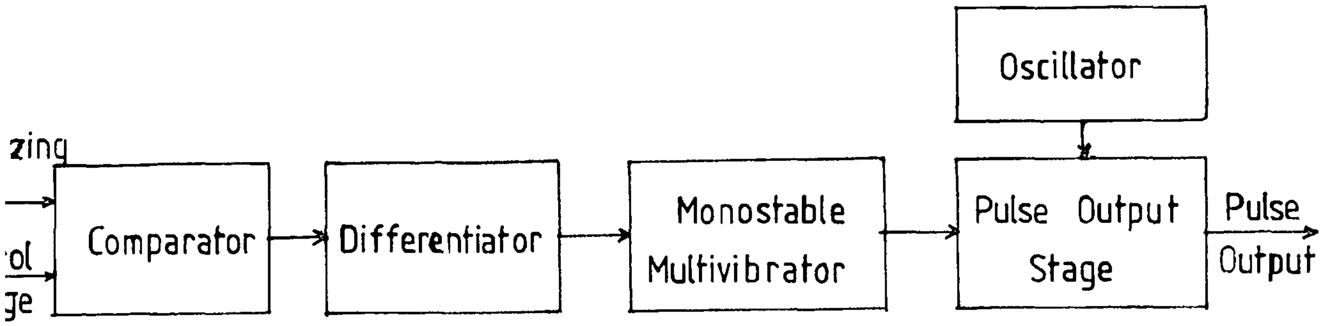

FIG.4.3(a) COSINE FIRING CIRCUIT

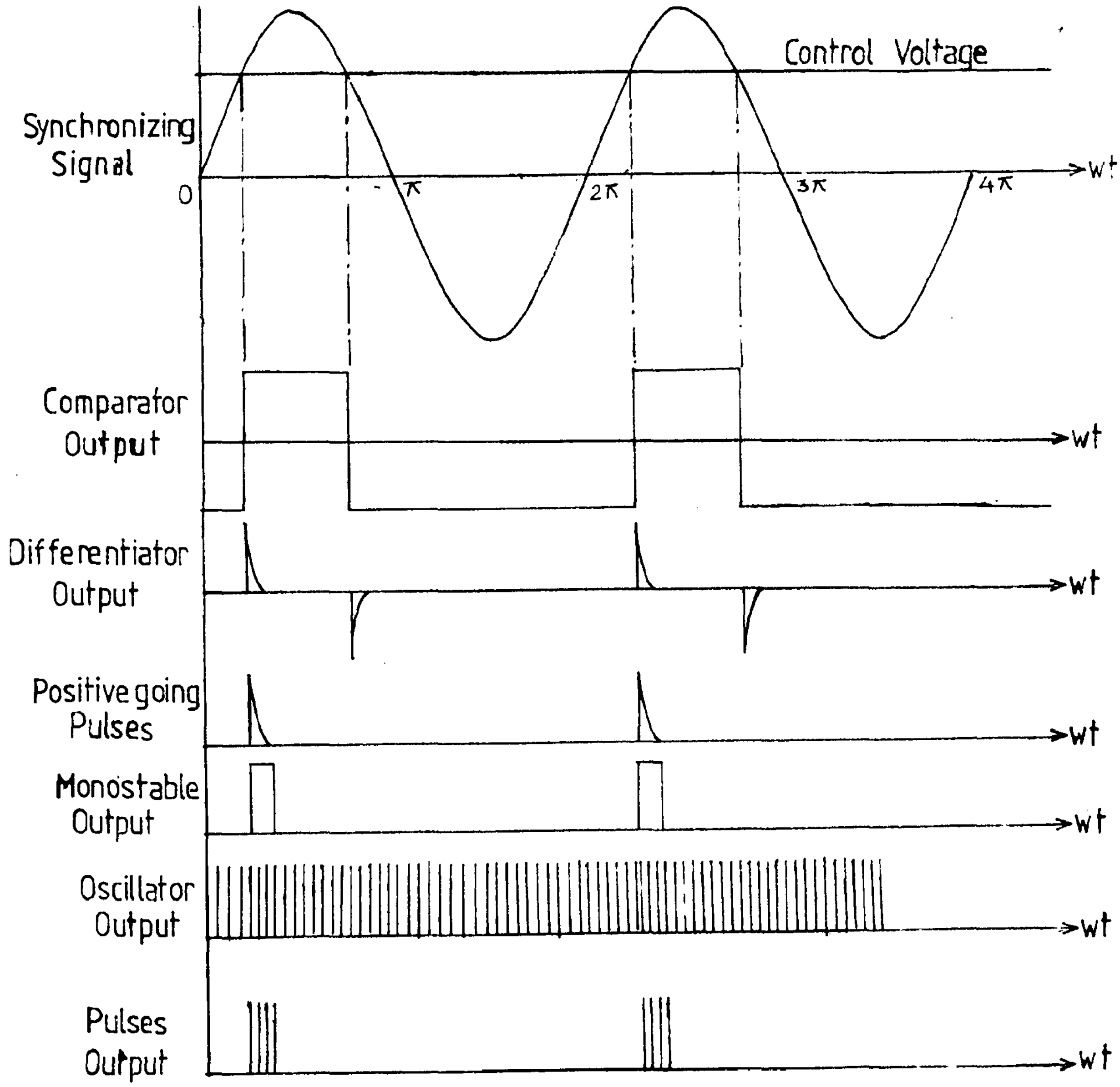

FIG.4.3 (b) FIRING CIRCUIT WAVEFORMS

triggered by the output of the differentiator output pulse (either positive going or negative going) generates a single pulse of constant width irrespective of magnitude of signal input. An oscillator is used to a produce a high frequency carrier wave. The oscillador output is ANDed with the monostable output and the output pulses are given to the gate of SCRs after amplification. The significance of this circuit is that the cosine relationship between the firing angle and control voltage is the most natural one for a steady-state d.c. output.

Since the synchronizing signal is taken directly from the supply through a step-down transformer, it might be possible that if supply voltage decreases sufficiently, then the maximum control voltage V_{cl} may exceed the peak value of the synchronizing signal and hence no output pulse will appear. To avoid this situation an end - stop pulse is produced at the peak of synchronizing signal as shown in Fig. 4.4. The author has developed a simple circuit to achieve it. The phase voltages V_{RN} and V_{YN} are compared in a comparator and the rectangular wave output is differentiated. The stepped-down synchronizing signal (V_{BN}) and differentiator output are added directly. The end-stop pulses are exactly at the peak of synchronizing signal because the voltages V_{RN} and V_{YN} are equal only at the peak of V_{BN}.

4.3.3 Dual Converter

The dual converter has been already discussed in

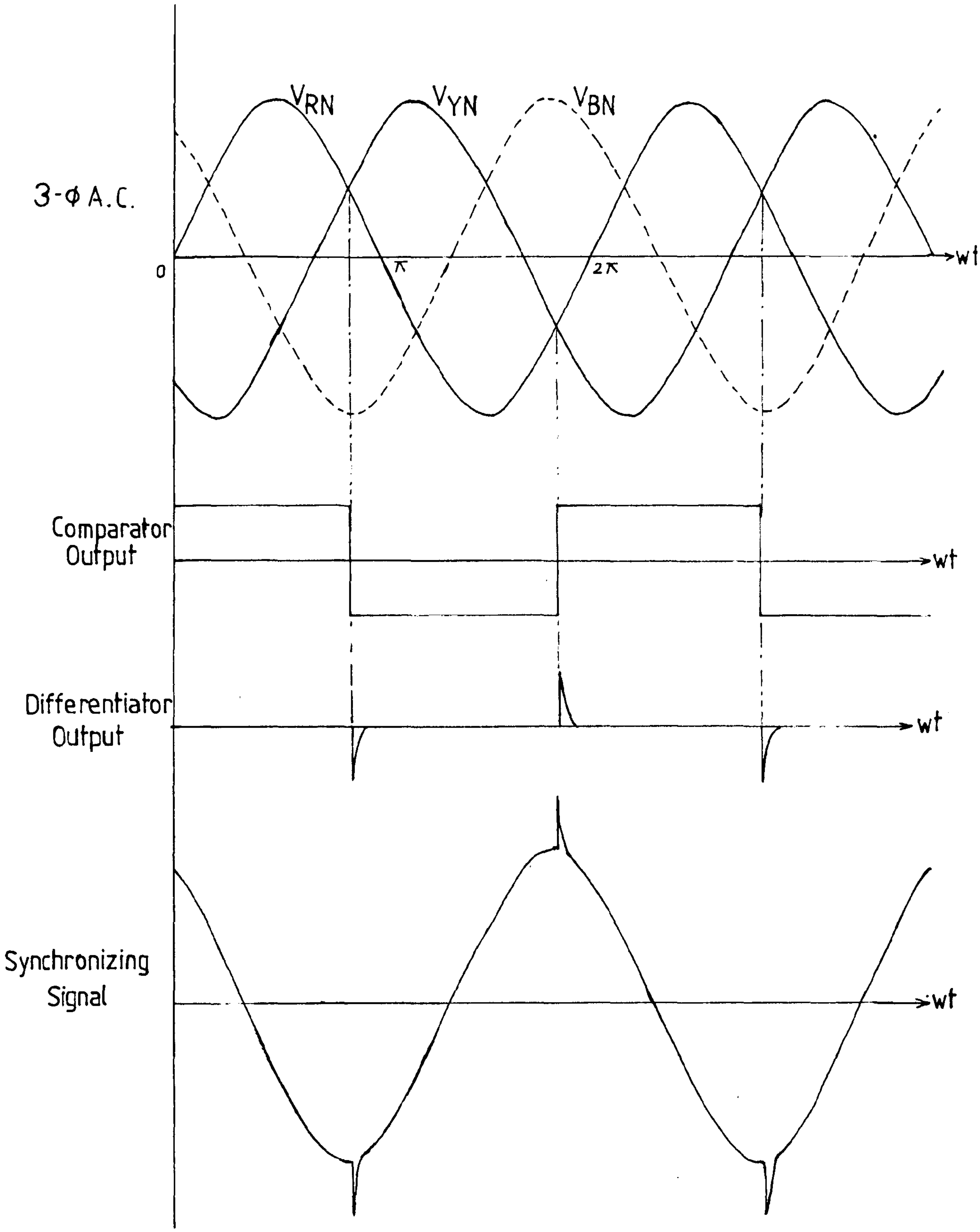

FIG.4.4 SYNCHRONIZING SIGNAL WITH END STOP PULSES

chapter - 3 in detail. If the dv/dt (i.e. rate of rise of the positive anode to cathode voltage) is very large, the thyristor will turn on without application of the gate signal. This may occur even though the applied forward voltage amplitude is considerably below the peak anode forward voltage (PFB) rating of the thyristor. Such an unscheduled turn on usually results in excessively large currents which cause thyristor fuse to interrupt or may cause thyristor to fail. To protect the thyristor against large dv/dt, a snubber circuit (R - C series circuit) is used across each thyristor as shown in Fig. 4.5.

4.3.4 Field Circuit Regulator

The conventional full-wave uncontrolled bridge rectifier is employed for field excitation of the motor. The ripple contents in the output of rectifier will not affect the operation because field winding, being much in-ductive in nature, acts as a filter.

4.4 Operation of Experimental Speed Control System

The schematic block diagram of the entire experimental system is shown in Fig. 4.6. A potentiometer is calibrated in terms of speed and is set to the desired speed. The control signal V_{c1} is generated in response to the speed error and fed to the cosine firing circuit. The synchronizing signal is obtained from B and N terminals of a 3 - Ø supply as

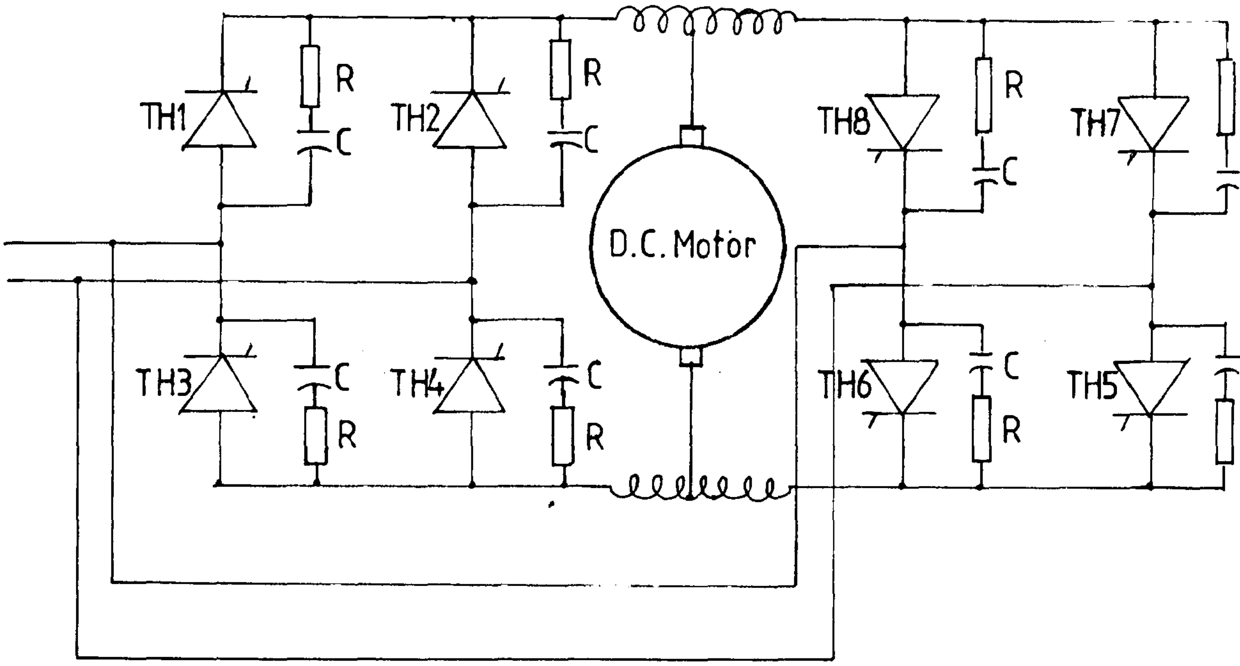

FIG.4.5 DUAL CONVERTER WITH dv/dt PROTECTION

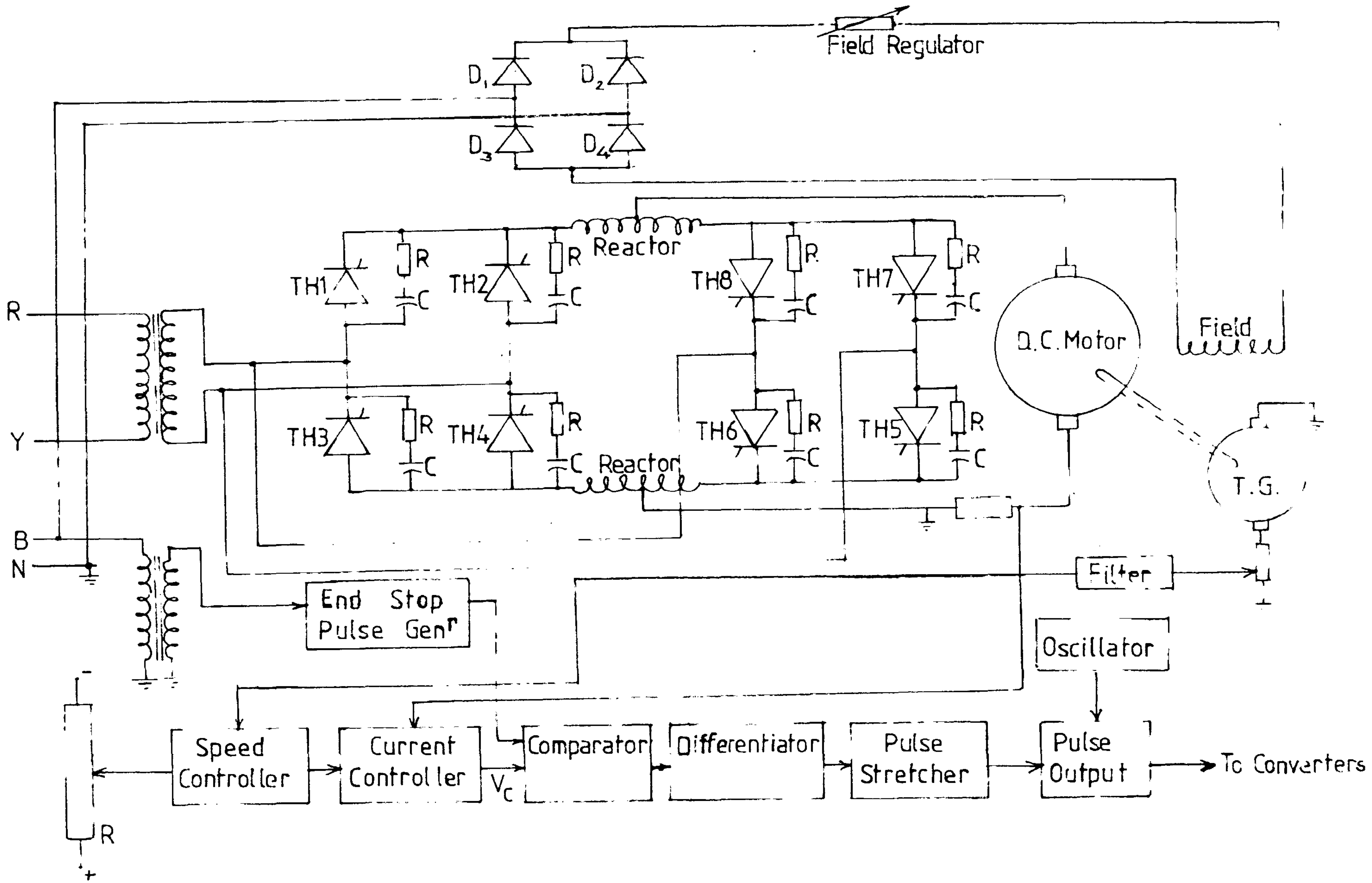

FIG.4.6 SCHEMATIC BLOCK DIAGRAM OF EXPERIMENTAL SYSTEM

explained earlier. The required firing pulses for the cosine firing circuits are generated. The supply for bridges are taken from R-Y terminals of the 3 - Ø supply through an isolation transformer. The bridge circuits are fired from the output pulses of cosine firing circuit through pulse transformers. The field supply is also obtained from B and N terminals, and is rectified and regulated.

4.5 Conclusion

The necessity of closed-loop operation for speed control of d.c. motor is essential. The PI speed controller gives zero steady-state error. The PI current controller gives fast response and protects the thyristors from over currents. To protect the thyristors against dv/dt turn ON, snubber circuits are used. The operation of complete system is described.

Chapter - 5

THE MATHEMATICAL MODEL OF DRIVE SYSTEM

The mathematical model of the closed-loop control scheme for speed control of d.c. motor is developed in this chapter. The transfer functions of various elements are derived separately. The system state model has been developed in simplest possible form.

5.1 Introduction

The closed-loop control scheme for speed control of d.c. motor has been discussed in the previous chapter. To design both the PI current controller and speed controller, the mathematical model of the drive system is necessary and then only any stability criterion can be used. Also, the mathematical model of the overall system is necessary to study the effect of load variation or speed reference changes. The complete schematic block diagram of the speed control system is shown in Fig. 5.1.

5.2 Transfer Function of Various Elements

5.2.1 D.C. Motor

The differential equation of armature circuit of a separately-excited d.c. motor, with constant field excitation is as follows:

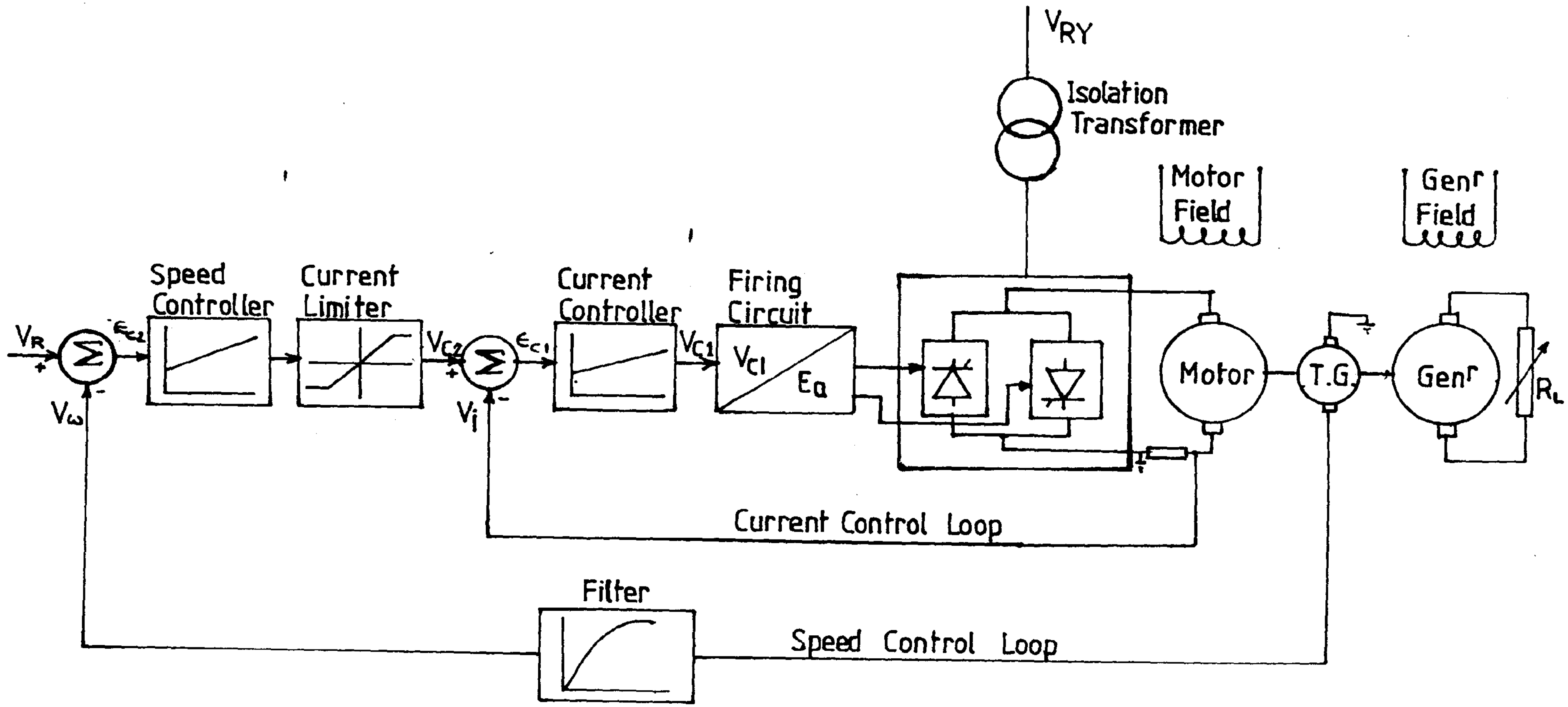

FIG.5.1 SCHEMATIC DIAGRAM OF SPEED CONTROL SYSTEM

$$e_a = e_b + R_a i_a + L_a \frac{di_a}{dt}$$

where Back emf $e_b = K_b \omega_m$ Volts

with $K_b = K_f I_f$ = constant ...(5.1)

and I_f = constant field current.

The torque balance differential equation is

$$\frac{J d\omega_m}{dt} = T - T_L$$

where, Load torque $T_L = B\omega_m$ Nw- m and electromagnetic torque $T = K_b \, i_a$ Nw-m- ...(5.2)

The coulomb and static frictions are neglected for getting a linear model. The viscous friction is included in the load torque T_L. In a experimental setup, the d.c. motor i is loaded by means of a d.c. generator supplying power to a resistive load. Neglecting the electrical time constant of armature circuit of the d.c. generator, it can be shown that the load torque on the d.c. motor is proportional to speed. The viscous friction only increases this proportionality constant. For the operating condition, this proportionality constant is determined experimentally.

Taking Laplace transform of equations (5.1) and (5.2)

$$E_a(s) = E_b(s) + R_a I_a(s) + sL_a I_a(s)$$

$$E_b(s) = K_b \omega_m(s)$$

$$sJ\,\omega_m(s) = T(s) - T_L(s)$$

$$T_L(s) = B\,\omega_m(s)$$

$$T(s) = K_b I_a(s)$$

$$(sJ + B)\,\omega_m(s) = T(s) = K_b I_a(s) \qquad \ldots(5.3)$$

The block diagram of d.c. motor using above equations can be drawn as shown in Fig. 5.2. From the block diagram the transfer function of the motor is determined as follows:

$$\frac{\omega_m(s)}{E_a(s)} = \frac{G(s)}{1 + G(s)\,H(s)}$$

$$= \frac{\dfrac{K_b}{(sL_a+R_a)\,(sJ+B)}}{1+\dfrac{K_b^2}{(sL_a+R_a)(sJ+B)}}$$

$$\frac{\omega_m(s)}{E_a(s)} = \frac{1/K_b}{1 + \dfrac{JR_a}{K_b^2}\,(1 + s\dfrac{L_a}{R_a})\,(s + \frac{B}{J})}$$

Now defining,

$\tau_a = \dfrac{L_a}{R_a} =$ electrical time constant of the motor armature circuit

$\tau_m = \dfrac{JR_a}{K_b^2} =$ mechanical time constant.

the transfer function becomes,

$$\frac{\omega_m(s)}{E_a(s)} = \frac{1/K_b}{1 + (\ + s\tau_a)\,(s + B/J)\,\tau_m} \qquad \ldots(5.4)$$

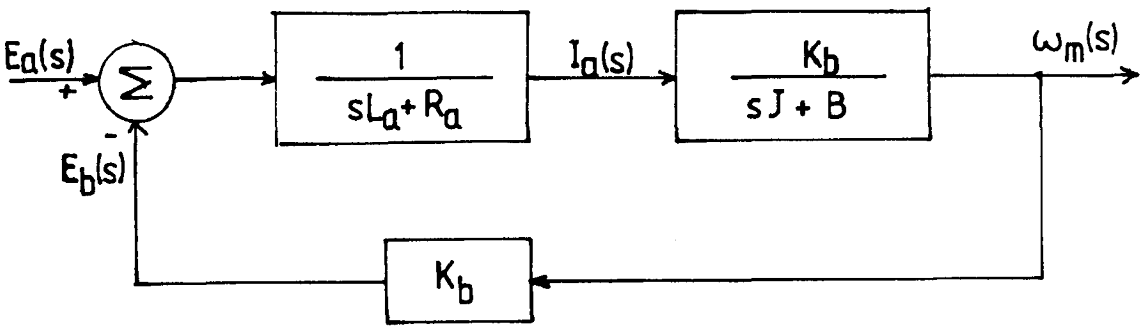

FIG.5.2 BLOCK DIAGRAM OF D.C. MOTOR

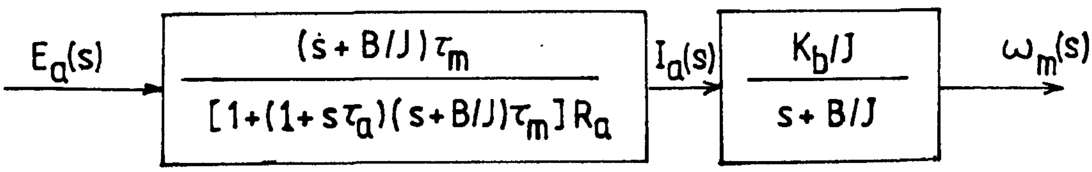

FIG.5.3 REDUCED BLOCK DIAGRAM OF D.C. MOTOR

Also,

$$\frac{\omega_m(s)}{I_a(s)} = \frac{K_b}{sJ + B} = \frac{K_b/J}{(s + B/J)}$$

$$\frac{I_a(s)}{E_a(s)} = \frac{I_a(s)}{\omega_m(s)} \times \frac{\omega_m(s)}{E_a(s)}$$

$$= \frac{(s + B/J)}{K_b/J} \times \frac{1/K_b}{1+(1+s\,\tau_a)\,(s+B/J)\,\tau_m}$$

$$= \frac{(s+B/J)\;J/K_{bb}^2}{1+(1+s\,\tau_a)\,(s+B/J)\,\tau_m}$$

$$= \frac{(s+B/J)\,\tau_m}{[1+(1+s\,\tau_a)\,(s+B/J)\,\tau_m]\;R_a} \qquad \ldots(5.5)$$

The block diagram of d.c. motor can be redrawn as shown in Fig. 5.5.

5.1.2 Thyristor Converter

The output voltage of thyristor converter is given by

$$E_a = \frac{E_{max}}{K} \quad V_{cl} \qquad \ldots\ (5.6)$$

This equation shows that the firing circuit provides a linear relationship of E_a for variation of V_{cl}. Therefore, the thyristor converter gain (A) is constant and is given by $(\frac{E_{max}}{K})$.

Although the output is proportional to V_{cl}, the firing of the bridge is not instantaneous. Once the firing occurs, the information in V_{cl} is of no value until the instant next firing occurs. To make the analysis simpler, the delay in the firing unit is approximated by a simple first order time lag with a time constant equal to half the period between consecutive firing pulses (T_{ca}) [14].

Thus, the thyristor power amplifier (consisting of the bridge and the firing unit) is approximated by a linear continuous element although it is a non-linear sampled data element in reality. The transfer function of the thyristor power amplifier is given by

$$\frac{E_a(s)}{V_{c1}(s)} = \frac{A}{1+sT_{ca}} \qquad \ldots(5.7)$$

5.2.3 Current Controller

A PI controller has been choosen for current control since this provides quick response with zero steady state error. Its transfer function can be written as

$$\frac{V_{c1}(s)}{\epsilon_{c1}(s)} = \frac{K_1\ (1+T_{c1}s)}{T_{c1}\ s} \qquad \ldots(5.8)$$

5.2.4 Speed Controller

To provide zero steady state error in speed, PI controller has been chosen for speed control. The transfer function of speed controller can be written as

$$\frac{V_{c2}(s)}{\epsilon_{c2}(s)} = \frac{K_2(1+T_{c2}s)}{T_{c2}\ s} \qquad \ldots(5.9)$$

5.2.5 Current Transducer

Since the current signal is directly taken through a resistance in the armature of the d.c. motor, therefore, the gain of current transducer is constant. Thus, the transfer function of current transducer is

$$\frac{V_i(s)}{I_a(s)} = H_i \qquad \ldots(5.10)$$

5.2.6 Speed Transducer

The output of the tachogenerator is directly proportion to speed of the motor. Therefore, the gain of the tachogenerator is constant. A filter is used to reduce the ripples in the output voltage. The transfer function of speed transducer can be written as

$$\frac{V_\omega(s)}{\omega_m(s)} = \frac{H_\omega}{1+sT_f} \qquad \ldots(5.11)$$

The complete block diagram is shown in Fig. 5.4.

5.3 System State Model

To analyse the response of the drive for a step input, the system state model should be established. The block diagram of Fig. 5.4 is modified, as shown in Fig. 5.5, so that state variables are easily identified.

The state variable set chosen is given below:

$$x_1 = v'_{c2}$$

$$x_2 = v'_{c1}$$

$$x_3 = E_a$$

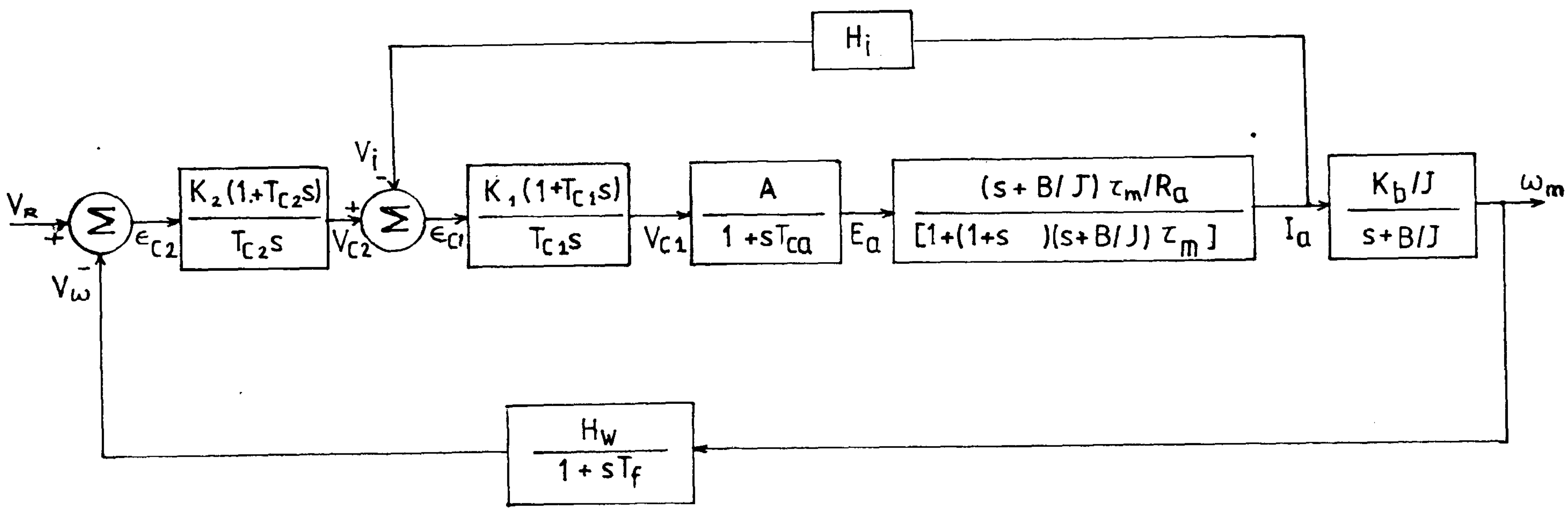

FIG.5.4 SYSTEM BLOCK DIAGRAM

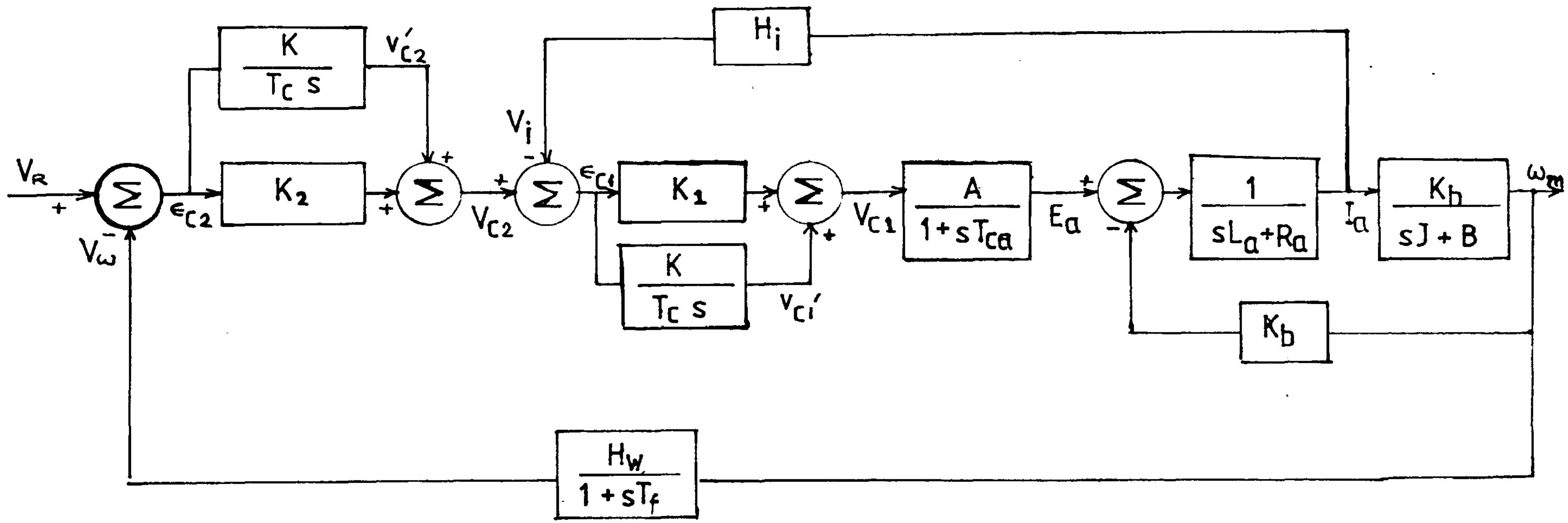

FIG.5.5 SYSTEM BLOCK DIAGRAM WITH ALL STATE VARIABLES

$$x_4 = I_a$$

$$x_5 = \omega_m$$

$$x_6 = V_\omega \qquad \text{...(5.12)}$$

Now, from the block diagram 5.5

$$x_1 = \frac{K_2}{T_{c2}s} \epsilon_{c2} \qquad \text{(a)}$$

$$x_2 = V_R - x_6 \qquad \text{(b)}$$

$$V_{c2} = x_1 + K_2\epsilon_{c2} \qquad \text{(c)}$$

$$x_2 = \frac{K_1}{T_{c1}s} \epsilon_{c1} \qquad \text{(d)}$$

$$\epsilon_{c1} = V_{c2} - H_i x_4 \qquad \text{(e)}$$

$$V_{c1} = x_2 + K_1\epsilon_{c1} \qquad \text{(f)}$$

$$x_3 = \frac{A}{1+sT_{ca}} V_{c1} \qquad \text{(g)}$$

$$x_4 = \frac{1}{sL_a+R_a} (x_3-K_b x_5) \qquad \text{(h)}$$

$$x_5 = \frac{K_b}{sJ+B} x_4 \qquad \text{(i)}$$

$$x_6 = \frac{H_\omega}{1+sT_f} x_5 \qquad \text{(j)} \qquad \text{...(5.13)}$$

On substitution of equation (5.13 b) in equation (5.13 a) and equation (5.13 c),

$$x_1 = \frac{K_2}{T_{c2}s} (V_R - x_6)$$

or

$$sx_1 = \frac{K_2}{T_{c2}} (V_R - x_6)$$

Taking inverse Laplace transform,

$$\frac{dx_1}{dt} = \frac{K_2}{T_{c2}} (V_R - x_6) \qquad 5.14(a)$$

$$V_{c2} = x_1 + K_2 (V_R - x_6) \qquad 5.14(b)$$

On substitution of equation (5.12 e) in equation (5.13 d) and equation (5.13 f),

$$x_2 = \frac{K_1}{T_{c1}s} (V_{c2} - H_i\ x_4)$$

or

$$sx_2 = \frac{K_1}{T_{c1}} (V_{c2} - H_i\ x_4)$$

Taking inverse Laplace transform,

$$\frac{dx_2}{dt} = \frac{K_1}{T_{c1}} (V_{c2} - H_i\ x_4) \qquad (5.14\ c)$$

$$V_{c1} = x_2 + K_2 (V_{c2} - H_i\ x_4) \qquad (5.14\ d)$$

From equation (5.13 g)

$$x_3 = \frac{A}{1+sT_{ca}} V_{c1}$$

or

$$x_3 + sx_3T_{ca} = A\ V_{c1}$$

or

$$sx_3 = \frac{A\ V_{c1} - x_3}{T_{ca}}$$

Taking inverse Laplace transform

$$\frac{dx_3}{dt} = \frac{A\ V_{c1} - x_3}{T_{ca}} \qquad (5.14\ c)$$

From equation (5.13 h)

$$x_4 = \frac{1}{sL_a+R_a} (X_3 - K_b x_5)$$

$$sx_4L_a + R_ax_4 = x_3 - K_bx_5$$

$$sx_4 = \frac{x_3 - K_bx_5 - R_ax_4}{L_a}$$

g inverse Laplace transform,

$$\frac{dx_4}{dt} = (x_3 - K_bx_5 - R_ax_4)/L_a \qquad .(5.14\ f$$

equation (5.13 i)

$$x_5 = \frac{K_b}{sJ+B}\ x_4$$

$$sx_5J + Bx_5 = K_bx_4$$

$$sx_5 = \frac{K_b\ x_4 - Bx_5}{J}$$

inverse Laplace transform,

$$\frac{dx_5}{dt} \quad \frac{K_bx_4 - Bx_5}{J} \qquad (5.14\ g)$$

quation (5.13 j)

$$x_6 = \frac{H_\omega}{1+sT_f}\ x_5$$

$$x_6 + sx_6T_f = H_\omega\ x_5$$

$$sx_6 = \frac{H_\omega x_5 - x_6}{T_f}$$

inverse Laplace transform,

$$\frac{dx_6}{dt} = \frac{H_\omega x_5 - x_6}{T_f} \qquad (5.14\ h)$$

The equations (5.14 a) to (5.14 h) describe the state model of the drive system. The identity of V_{c1} and V_{c2} is required to incorporate the saturation characteristic of the controllers later.

5.4 Conclusion

The closed-loop control scheme has been mathematically modelled. The transfer function of all elements of the drive are established. Also the system state model is developed. These mathematical models will be used later to design the system and study its response for particular inputs and load variations.

Chapter - 6

SYSTEM DESIGN

In this chapter, the complete system is designed. This includes design of power circuit, reactors, field circuit rectifier, firing circuit, and speed and current controllers. Controllers are designed on the basis of relative stability using the D-decomposition method and the frequency scanning technique.

6.1 Introduction

The earlier chapters describe the various blocks of system in their analytical and operational forms. The system is now designed in complete detail. The d.c. motor selected has rating as follows:

Specification of the motor

D.C. motor

Power = 2 h.p. or 1.592 KW

Voltage = 220 Volts

Speed = 1050 rpm.

Supply available - 3 Ø a.c. 440 V, 50Hz

6.2 Design of Power Circuit

For 1 - Ø dual converter the voltage at the d.c. terminals is given by

$$E_a = \frac{2\sqrt{2}}{\pi} V \cos\alpha \qquad (6.1)$$

where,

V = r.m.s. value of supply voltage

For $\alpha = 0^o$,

$$E_a = \frac{2\sqrt{2}}{\pi} \times 440$$

$$= 396 \text{ volts}$$

The theoretical maximum output volta e is above the maximum motor voltage rating and therefore, the full range speed control is possible.

The minimum firing angle is fixed by limiting the value of control voltage V_{cl} in both directions at $\pm$ 9V such that the minimum firing angle is 10^o and maximum firing angle is 170^o. Beyond the firing angle 170^o, there is danger of commutation failure in inversion mode. Therefore, from 10^o to 170^o the output of dual converter is directly proportional to control voltage V_{cl}.

At $V_{cl} = 9V$, $\alpha = 10^o$

$$\therefore E_a = \frac{2\sqrt{2}}{\pi} 440 \text{ Cos} 10^o$$

$$= 390.12 \text{ volts}$$

$$\therefore \text{Gain of the dual converter} = A = \frac{390.12}{9}$$

$$= 43.34$$

The supply frequency is 50 Hz. Therefore, time period of the supply voltage is 20 msec. In each cycle two firing pulses are required to trigger the positive/negative converter. Therefore, time lag T_{ca} between two consecutive firing pulses will be $\frac{1}{2}(\frac{20}{2}) = 5$ msec.

Thyristors Voltage Rating

The supply voltage available to the power amplifier is 440 volts, a.c., therefore, the peak inverse voltage (PIV) across each arm of the thyristor bridge will be given by

$$PIV = \frac{\pi}{2} \times V = \frac{\pi}{2} \times 440$$

$$= 691.15 \text{ volts}$$

Allowing a safety factor of about 2, so that the thyristor can easily take a reasonable transient over voltage a thyristor with 1200 PIV rating are used.

Thyristors Current Rating

The full - load d.c. motor armature current is determined as below:

$$\text{D.C. motor armature current} = \frac{\text{h.p.} \times 746}{\eta \times \text{volts}}$$

$$= \frac{2.0 \times 746}{0.90 \times 220}$$

$$= 7.53 \text{ amps.}$$

Efficiency is assumed to be 90 %.

SCRs of rating 10 amps. can easily take the motor full load current. The thyristors available are of 16 amps. current rating.

The thyristors used has following specifications:

Thyristor Type SS1012

Current Rating 16 amps.

Maximum Reverse Repetitive Voltage 1200 V

The SCR must be mounted on a heat sink. It will enable the heat generated within the thyristor to be transferred from the cathode junction to the surrounding atmosphere without allowing the cathode junction temperature to rise above the maximum allowable value for the thyristor used.

To protect the thyristor againt $\frac{dv}{dt}$ turn ON, a snubber circuit which is a R-C series circuit is used across each thyristor. The accepted value of R and C available are 50 ohms, 5 watts and 0.25 µf, 1800 volts respectively.

6.3 Design of Reactors

The maximum circulating current is given by

$$I_{cmax} = \frac{\sqrt{2}V}{\omega_s L}$$

The maximum circulating current allowed is assumed to be 1.5 Amps.

$$\therefore L = \frac{\sqrt{2}V}{\omega_s I_{cmax}}$$

$$= \frac{\sqrt{2} \times 440}{2 \times \pi \times 50 \times 1.5}$$

$$= 1.32 \text{ H}$$

Therefore, two reactor coils of 1.32 H each are required.

6.4 Design of Field Circuit Rectifier

For field circuit BY126 rectifier diodes are selected because their current rating is 3.0 Amps. which is sufficient to meet the field current requirement. They are connected in bridge form.

6.5 Design of Firing Circuit

The firing circuit consists of end-stop pulse generator, comparator, differentiator, pulse stretcher (monoslable multivibrator), oscillator, AND gate and the output stage. The design of these components is described below.

6.5.1 End Stop Pulse Generator

178389

The phase to neutral voltages V_{RN} and V_{YN} are stepped down using 220V/3-0-3 V transformers and the outputs are compared in an OPAMP IC741 through 10K resistance as shown in Fig. 6.1. The description of IC741 is given in Appendix 'C'. The output wave is differentiated using a capacitor of 0.01 µf in series with output. The pulse outputs are directly in synchronism with the stepped-down voltage V_{BN} at the peak points and are added to the same voltage through 10 K resistances directly. Thus, the required synchronizing signal is obtained. Two such circuit are developed, one for V_{BN} synchronizing voltage and another for V_{NB} synchronizing

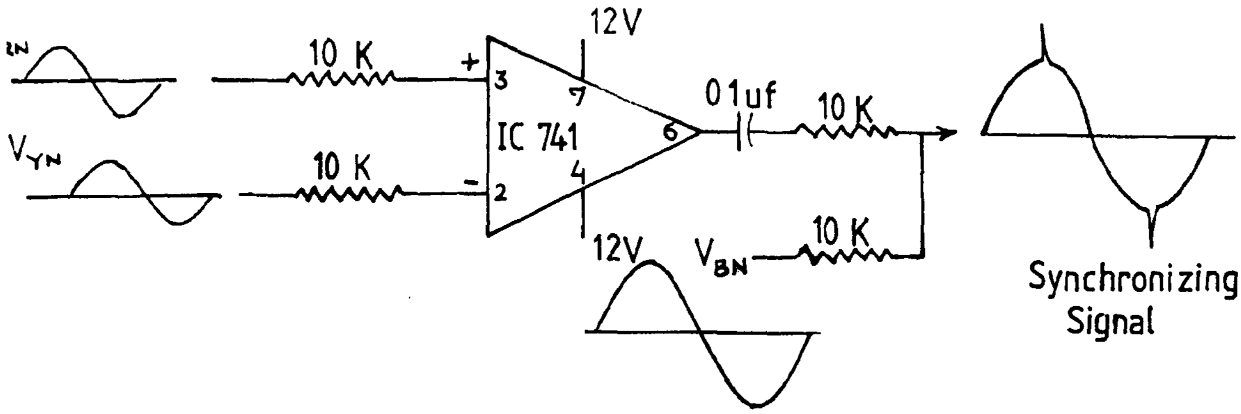

FIG. 6.1 END STOP PULSE GENERATOR

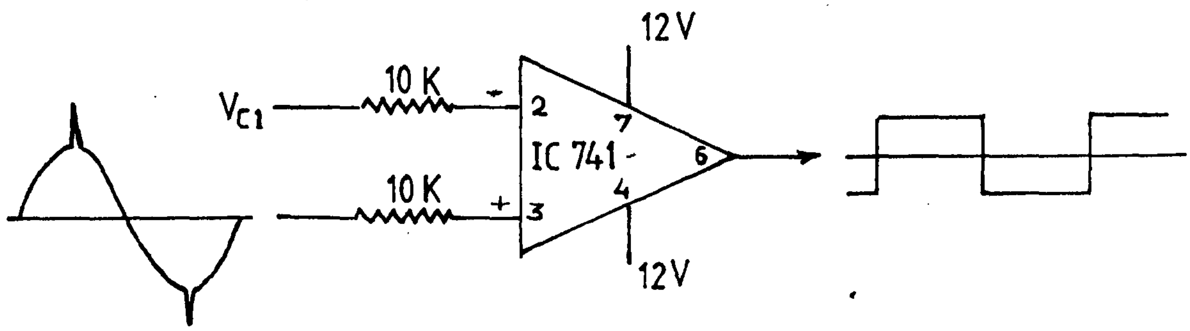

FIG. 6.2 COMPARATOR

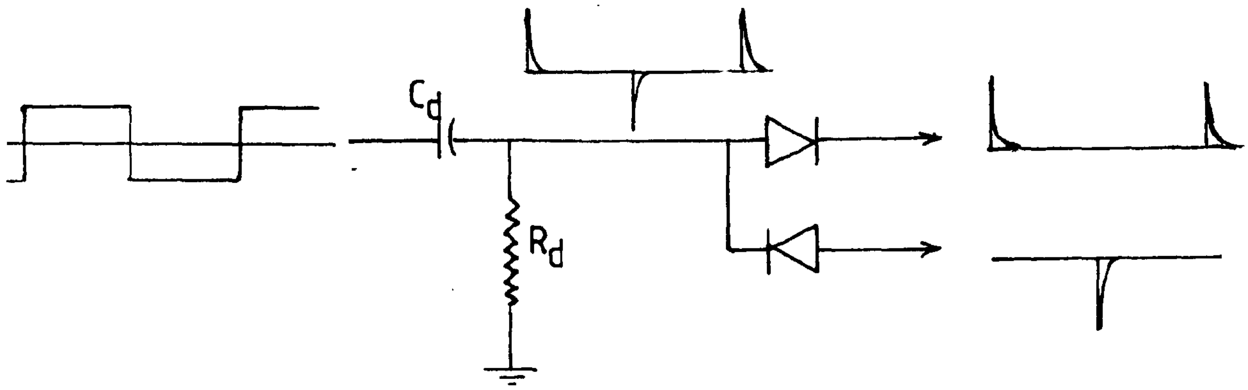

FIG. 6.3 DIFFERENTIATOR

voltage.

6.5.2 Comparator

The comparator circuit is made with the help of operational amplifier IC741 as shown in Fig. 6.2. The output of current controller (V_{c1}) is given to the inverting terminal (pin 2), and the synchronizing signal is given at non-inverting terminal (pin 3) through 10 K resistance. As V_{c1} varies from +9V to -9V, the firing angle changes from 10^{o} to 170^{o}. Two such comparators are used. In one synchronizing signal voltage V_{BN} and in other voltage V_{NB} is used.

6.5.3 Differentiator

A R-C differentiator is used for differentiation as shown in Fig. 6.3. The R_dC_d time constant is assumed as 1 msec. Therefore, R_d and C_d values selected are 10 K ohm and 0.01 μf respectively. Both the positive and negative going pulses are used to trigger two monostable multivibrators, and therefore, these pulses are sent through diodes IN4001 resulting in blocking either the positive pulses or negative pulses.

6.5.4 Monostable Multivibrator

The monostable is an electronic circuit which has a stable state and a quasi - stable state. The circuit remains in its stable state until an externally applied triggering signal switches it to a quasi - stable state.

The R - C time constant within the circuit determines the interval during which the circuit remains in the quasi - stable state. Upon completion of the time constant interval the circuit reverts to its original stable state and reamins in this state until another externally initiated triggering pulse is applied. The circuit is frquently called a one - shot multivibrator [32].

The author has used IC74121 which is a monostable chip. The details of IC74121 are given in Appendix 'C'. In order to trigger the monostable at negative going pulse output from the differentiator, both A_1 and A_2 inputs at pin 3 and 4 of the monostable IC are grounded and the positive going pulse is applied at input B (pin 5) as shown in Fig. 6.4(a). To trigger the monostable at positive going pulse output from the differentiator, both A_2 and B inputs are kept high and positive going pulse is applied at input A_1 as shown in Fig. 6.4(b). The duration of the output pulse is determined by the timing resister R_{ex} connected between pin 14 and 11. The timing resistance R_{ex} must be in the range of 1.4 K ohm to 40 K ohm. The maximum allowable value of timing capacitor is 1000 µf. The duration of the output pulse is seconds is given by

$$T_{ON} = 0.7\, R_{ex} C_{ex}$$

T_{ON} is assumed as 2.5 msec (approximately) so that reliable firing of thyristor is assured.

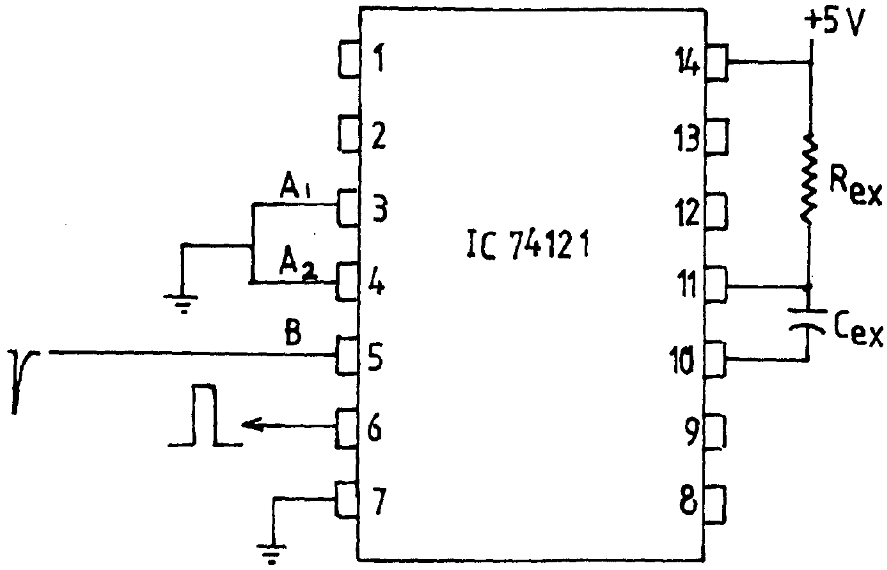

(a)

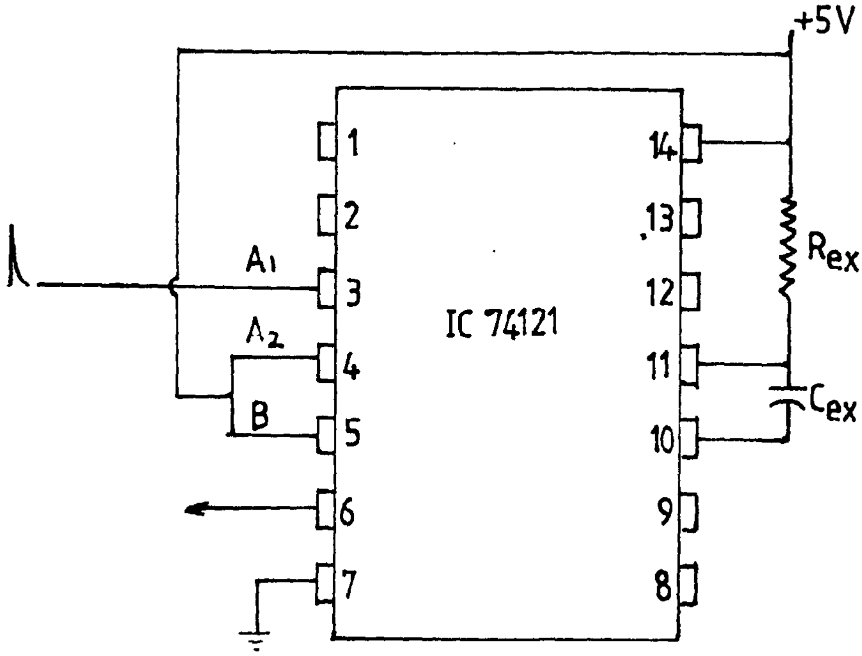

(b)

FIG.6.4 PULSE STRETCHER

Hence,

$$C_{ex}R_{ex} = \frac{2.5 \times 10^{-3}}{0.7} = 3.57 \times 10^{-3} \text{sec}$$

$$= 3.57 \text{ msec}$$

Values of R_{ex} and C_{ex} selected are 33 K ohm and 0.1 µf respectively to achieve the desired T_{ON} time.

6.5.5 Oscillator

IC555 is used as an oscillator. The details of IC555 are given in Appendix - 'C'.

The circuit is connected as shown in Fig. 6.5. It will trigger itself and free run as a multivibrator. The external capacitor C_T charges through R_A and R_B and discharges through R_B only. Thus the duty cycle may be set precisely by the ratio of these two resistances [35].

In this mode of operation the capacitor charges and discharges between $\frac{1}{3}$ V_{cc} and $\frac{2}{3}$ V_{cc}. The charging and discharging time and hence, the frequency is independent of the supply voltage. The charging time (output high) is given by

$$t_1 = 0.693 \ (R_A + R_B) \ C_T$$

The discharging time (output low) is given by

$$t_2 = 0.693 \ R_B C_T$$

Thus the total time period is given by

$$T = t_1 + t_2 = 0.693 \ (R_A + 2R_B) \ C_T$$

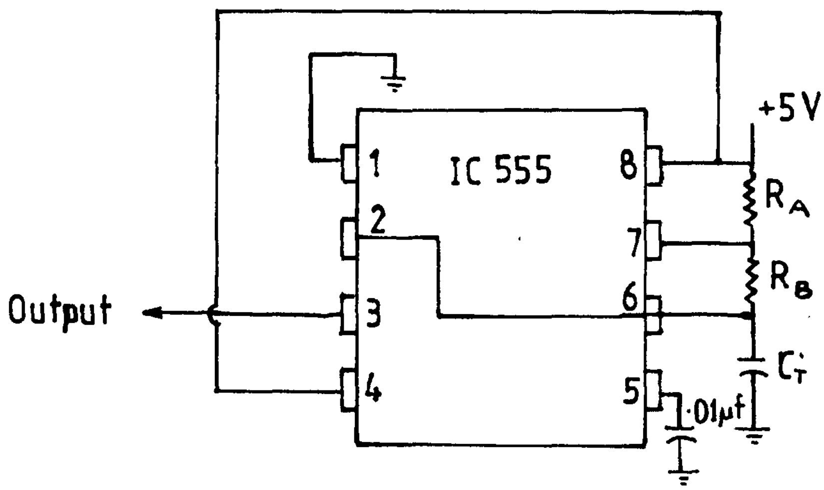

FIG.6.5 OSCILLATOR

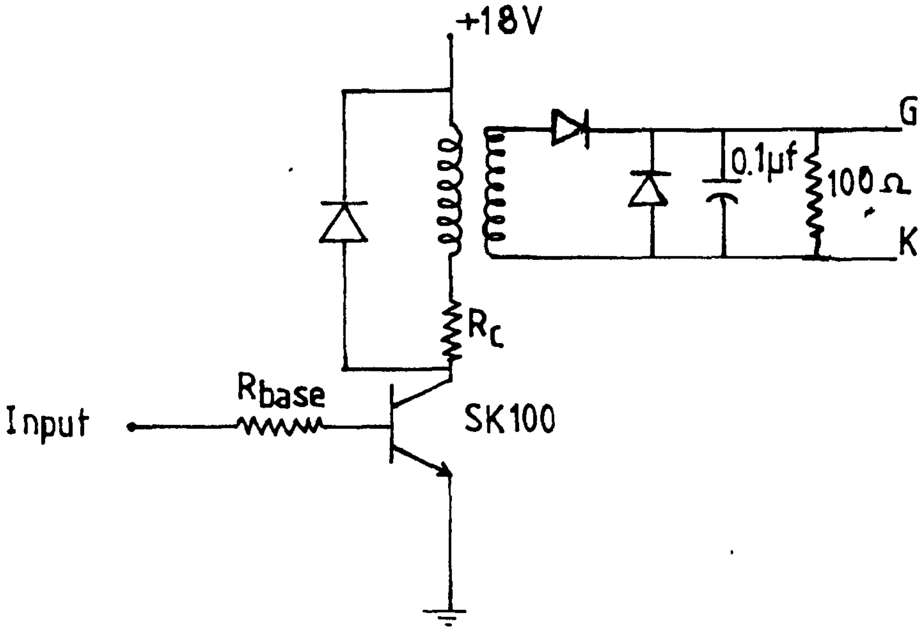

FIG.6.6 OUTPUT AMPLIFIER

and frequency of oscillation is therefore,

$$f = \frac{1}{T} = \frac{1.44}{(R_A + 2R_B)\ C_T}$$

Duty cycle D is given by

$$D = \frac{t_2}{T} = \frac{R_B}{R_A + 2R_B}$$

Oscillator frequency is selected as 750 H_z. High frequency of gating pulses reduce the gate losses sufficiently. Duty cycle is selected nearly equal to 0.5.

$$\therefore \frac{1.44}{(R_A + 2R_B)\ C_T} = 750$$

$$\frac{R_B}{R_A + 2R_B} \simeq 0.5$$

C_T is selected as 0.01 μf.

$$\therefore R_A + 2R_B = \frac{1.44}{750 \times 0.01 \times 10^{-6}} \text{ ohms}$$

$$= 192 \text{ K ohm}$$

also $R_A + 2R_B \simeq 2R_B$

Therefore, R_A is taken as 1 K ohm, and 100 K ohm present is used for R_B to adjust the desired frequency accurately.

6.5.6 AND Gate

The output of monostable multivibrator and oscillator are ANDed in an AND gate to get high frequency pulses during each monostable output pulse IC7408 (2-input AND gate) is used for ANDing operation. The details of IC7408 are given in Appendix 'C'.

6.5.7 Output Stage

The pulse output from AND gate may not be strong enough to turn ON and SCR. Therefore, the output of AND gate is amplified through an amplifier as shown in Fig. 6.6. A transistor SK100 is used for this purpose. The load resistance R_C is taken as 33 ohm and base resistance R_{base} as 4.7Kto achieve the desired amplification. The gate and cathode terminals are at higher potentials of the power circuit, therefore the control circuit should not be directly connected to the power circuit. A pulse transformer is used for physical isolation between control circuit and power circuit. A diode IN4001 is connected across R_C and pulse transformer primary winding to avoid the saturation of pulse transformer core. A diode IN4001 is connected in series with secondary of pulse transformer to block the negative pulses. Gate should also be protected against over voltages. This is achieved by connecting a diode IN4001 across gate-to-cathode.

A common problem encountered in the SCR circuitry is spurious (or noise) firing of the device. Trigger pulses may be induced at the gates due to turn ON or turn OFF of a neighbouring SCR or transients in the power circuit. These undesirable pulses may turn ON the SCR, thus causing improper operation of the circuit. Gates are protected against such spurious signals by connecting a capacitor (0.1 μf) and a resistance (100 ohm) across the gate-to-cathode to by pass the noise pulses [34, 26]. The waveforms at each point of the firing circuit are shown in Fig. 6.7.

6.6 Design of Controllers

6.6.1 Current Controller

A PI controller is used as a current controller to limit the armature current and for fast system response. The transfer function of the current controller is given by $\frac{K_1(1 + T_{c1}s)}{T_{c1}s}$. Therefore, the gain K_1 and time constant T_{c1} of the controller are to be designed. The current control loop is shown in Fig. 6.8.

The gain and time constant are selected on the basis of relative stability as well as the response of the current loop for a step current reference input. The parameter values for a **certain relative** stability is determined using the D-decomposition method as described in Appendix 'A'.

The characteristic equation of the current loop is given by

$$1+K_1\left(1+\frac{1}{T_{c1}s}\right)\frac{A\,H_i(s+B/J)\,\tau_m/R_a}{[1+(1+s\tau_a)\,(s+B/J)\tau_m](1+sT_{ca})} = 0 \qquad \ldots(6.1)$$

$$\frac{1}{K_1}+\left(1+\frac{1}{T_{c1}s}\right)\frac{A\,H_i(s+B/J)\,\tau_m/R_a}{[1+(1+s\tau_a)\,(s+B/J)\tau_m](1+sT_{ca})} = 0 \qquad \ldots(6.2)$$

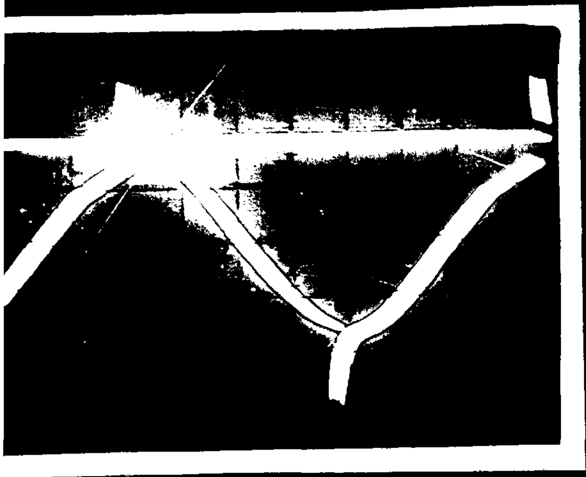

Fig.6.7(a)Synchronizing Signal & Control Voltage

Fig.6.7(b) Comparator Output

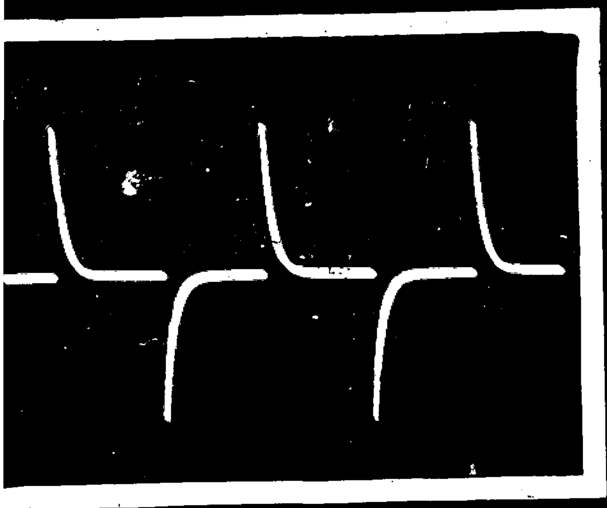

Fig.6.7(c)Differentiator Output

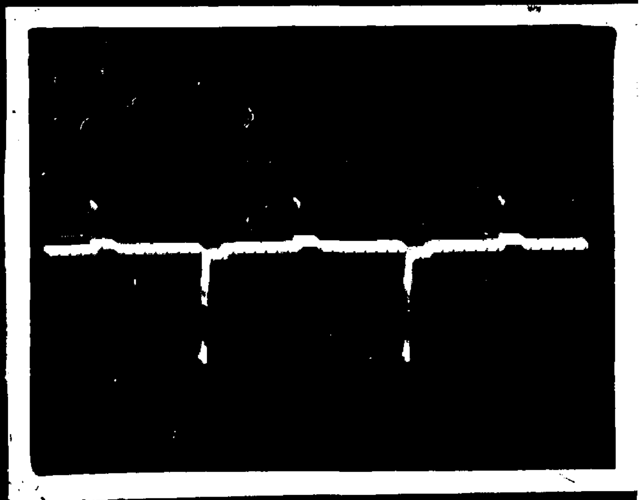

Fig.6.7(d)Negative Going Pulse Output

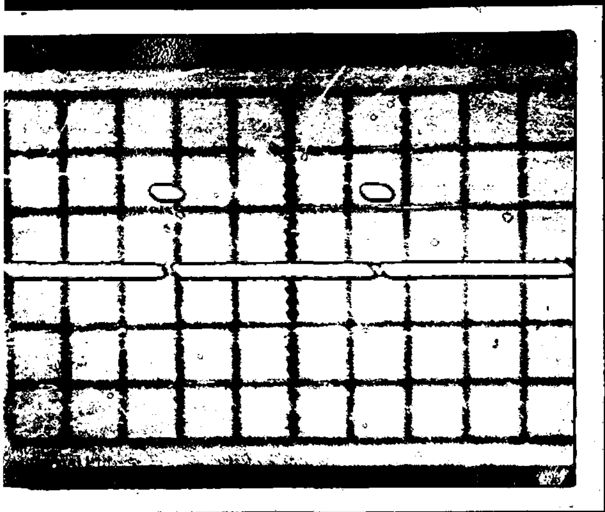

Fig.6.7(e)Pulse Stretcher Output

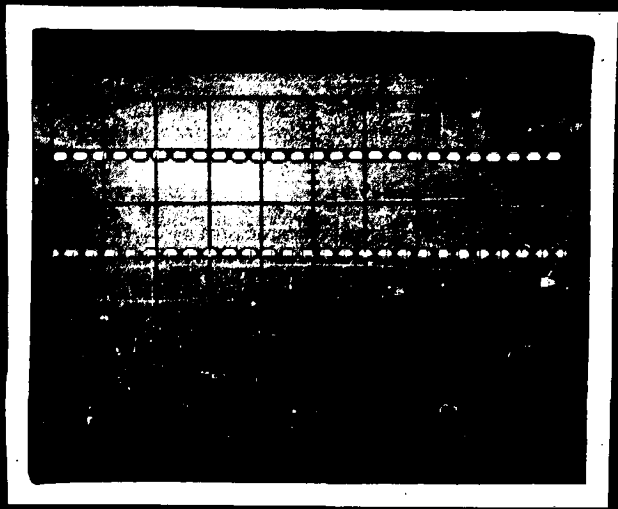

Fig.6.7(f)Oscillator Output

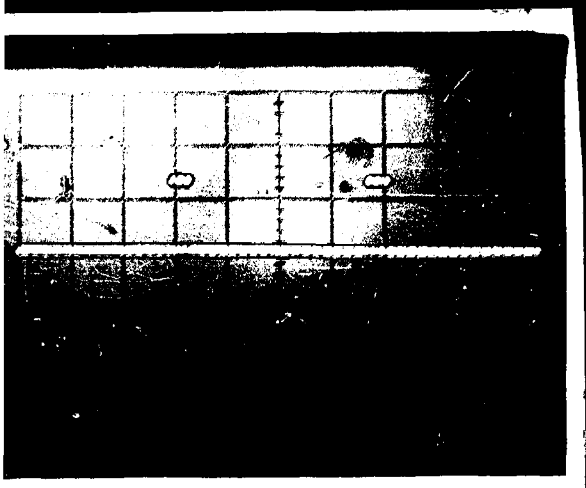

Fig.6.7(g)AND Gate Output

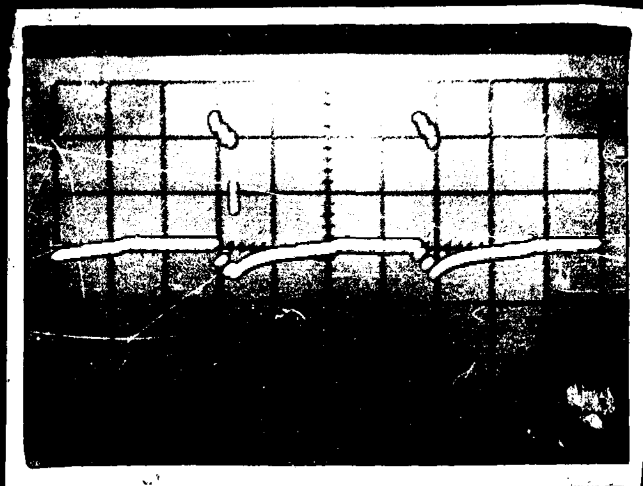

Fig.6.7(i)Pulse Amplifier Output

Putting $\alpha = \frac{1}{K_1}$ and $\beta = \frac{1}{T_{c1}}$, the equation (6.2) can be written as

$$\alpha+(1+\frac{\beta}{s})\quad \frac{A\ H_i(s+B/J)\tau_m/R_a}{[1+(1+s\tau_a)\ (s+B/J)\tau_m](1+sT_{ca})} = 0 \qquad \ldots(6.3)$$

Writing $F_1(s) = A\ H_i(s+B/J)\tau_m/R_a$,

and $F_2(s) = [1+(1+s\tau_a)\ (s+B/J)\tau_m]\ (1+sT_{ca})$ the equation (6.3) can be rewritten as

$$\alpha\ sF_2(s) + \beta\ F_1(s) + sF_1(s) = 0 \qquad \ldots(6.4)$$

Since 's' is a complex frequency, equation (6.4) can be expressed by following two equations, after equating real and imaginary terms separately to zero for any value of s:

$$\alpha\ \mathrm{Re}[sF_2(s)] + \beta\ \mathrm{Re}[F_1(s)] + \mathrm{Re}[sF_1(s)] = 0 \qquad \ldots(6.5)$$

$$\alpha\ \mathrm{Im}[sF_2(s)] + \beta\ \mathrm{Im}[F_1(s)] + \mathrm{Im}[sF_1(s)] = 0 \qquad \ldots(6.6)$$

Where 'Re' stands for real value and 'Im' stands for imaginary value of the bracketed quantities.

Solving equation (6.5) and (6.6), the values of α and β can be given by:

$$\alpha = \frac{\mathrm{Re}[F_1(s)].\ \mathrm{Im}[sF_1(s)] - \mathrm{Re}[sF_1(s)].\ \mathrm{Im}[F_1(s)]}{\mathrm{Im}[F_1(s)].\ \mathrm{Re}[sF_2(s)] - \mathrm{Im}[sF_2(s)].\ \mathrm{Re}[F_1(s)]}$$

$$\beta = \frac{\mathrm{Im}[sF_2(s)].\ \mathrm{Re}[sF_1(s)] - \mathrm{Im}[sF_1(s)].\ \mathrm{Re}[sF_2(s)]}{\mathrm{Im}[F_1(s)].\ \mathrm{Re}[sF_2(s)] - \mathrm{Im}[sF_2(s)].\ \mathrm{Re}[F_1(s)]}$$

Putting $s = -\sigma + j\omega_d$ or $s = -\xi\omega_n \pm j\omega_n\sqrt{1-\xi^2}$. two different sets of D-partition boundaries are obtained as shown in Figs.6.9, 6.10, 6.11. To ensure maximum relative stability, σ and ξ are increased from minimum value of zero. It is found that the region with higher degree of relative stability goes on decreasing as σ and ξ are increased. Computer programmes are given in Appendix 'D' for obtaining the D-partition boundaries. Thus, regions with highest possible σ and values are obtained. The stability of the probable most stable region is checked by frequency scanning technique as shown in Fig. 6.12 qnd 6.13. After ensuring stability of the probable most stable region, the final selection is made by comparing the time response of the current loop for a step current reference input at different points (i.e. different gain and time constants) in this stable region. For this purpose, the state model of the current loop is required.

The model of system is modified slightly for the transient response of the current loop. The back emf E_b will remain constant for a step current reference input because (i) the current loop is fast, and (ii) the motor has sufficient inertia. The modified current loop is shown in Fig. 6.14.

The selected state variables are:

$$v'_{c2} = x_1$$

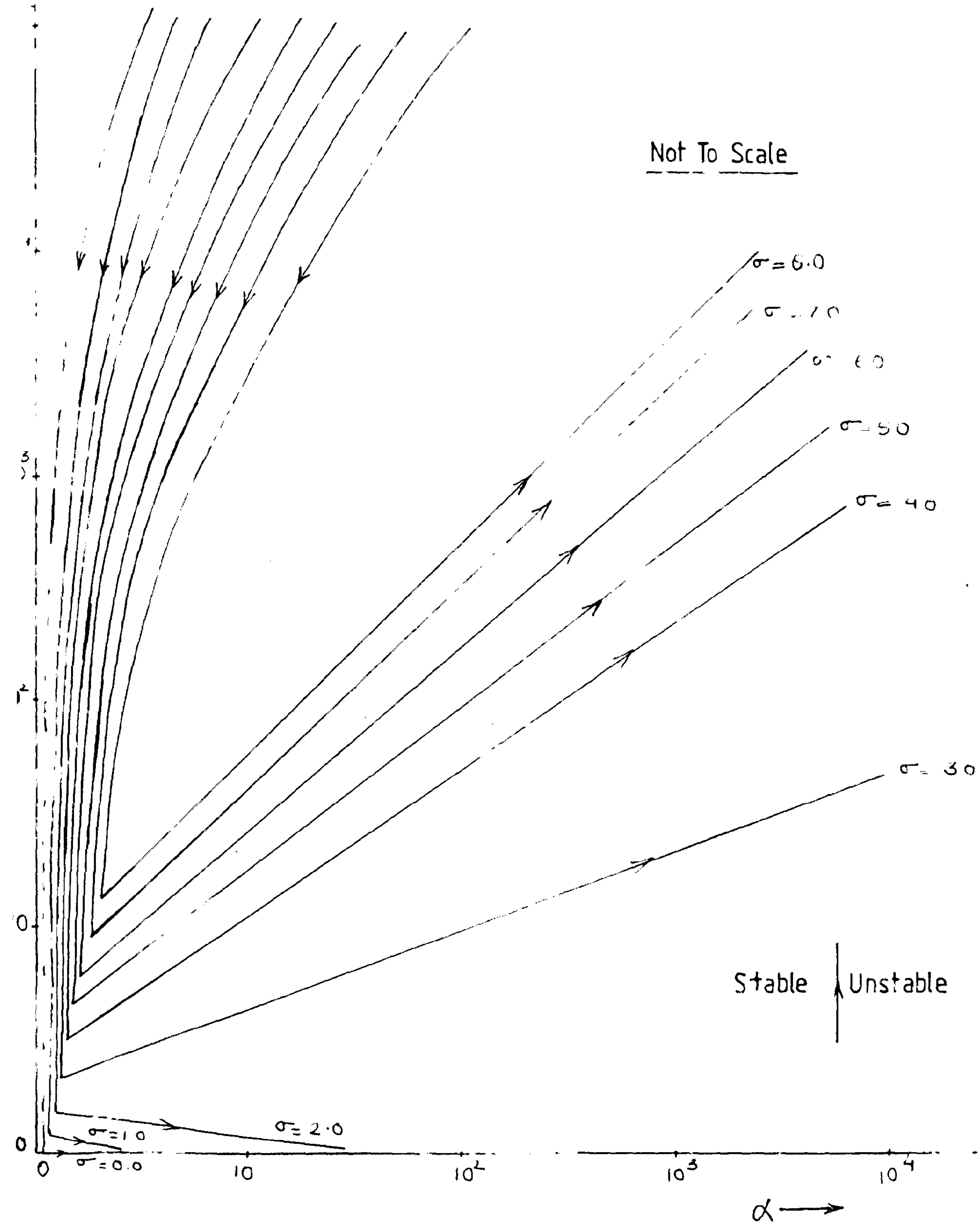

.6.9 D-PARTITION CURVE FOR CURRENT CONTROLLER WITH VARIATION IN σ

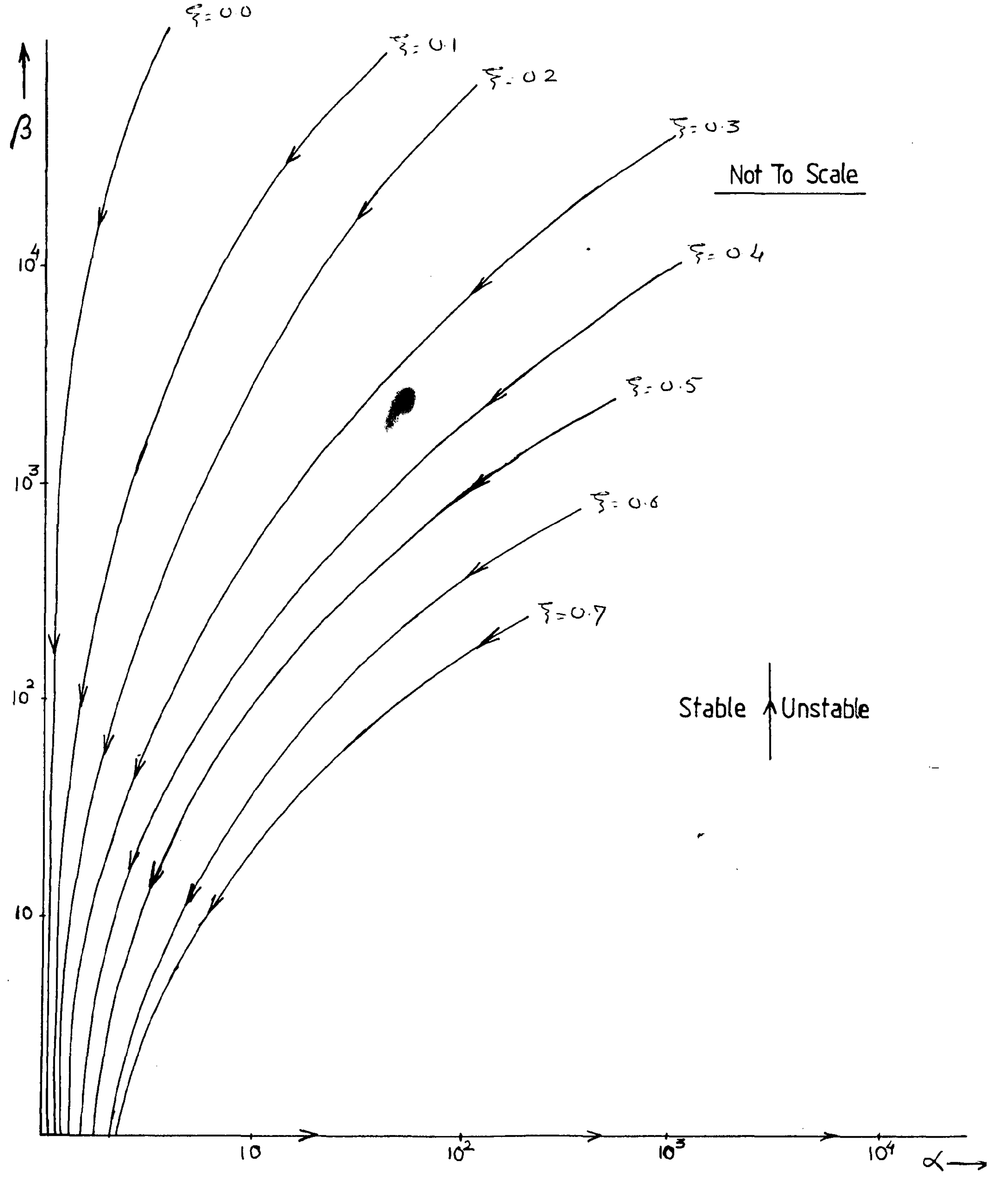

IG.6.10 D-PARTITION CURVE FOR CURRENT CONTROLLER WITH VARIATION IN ξ

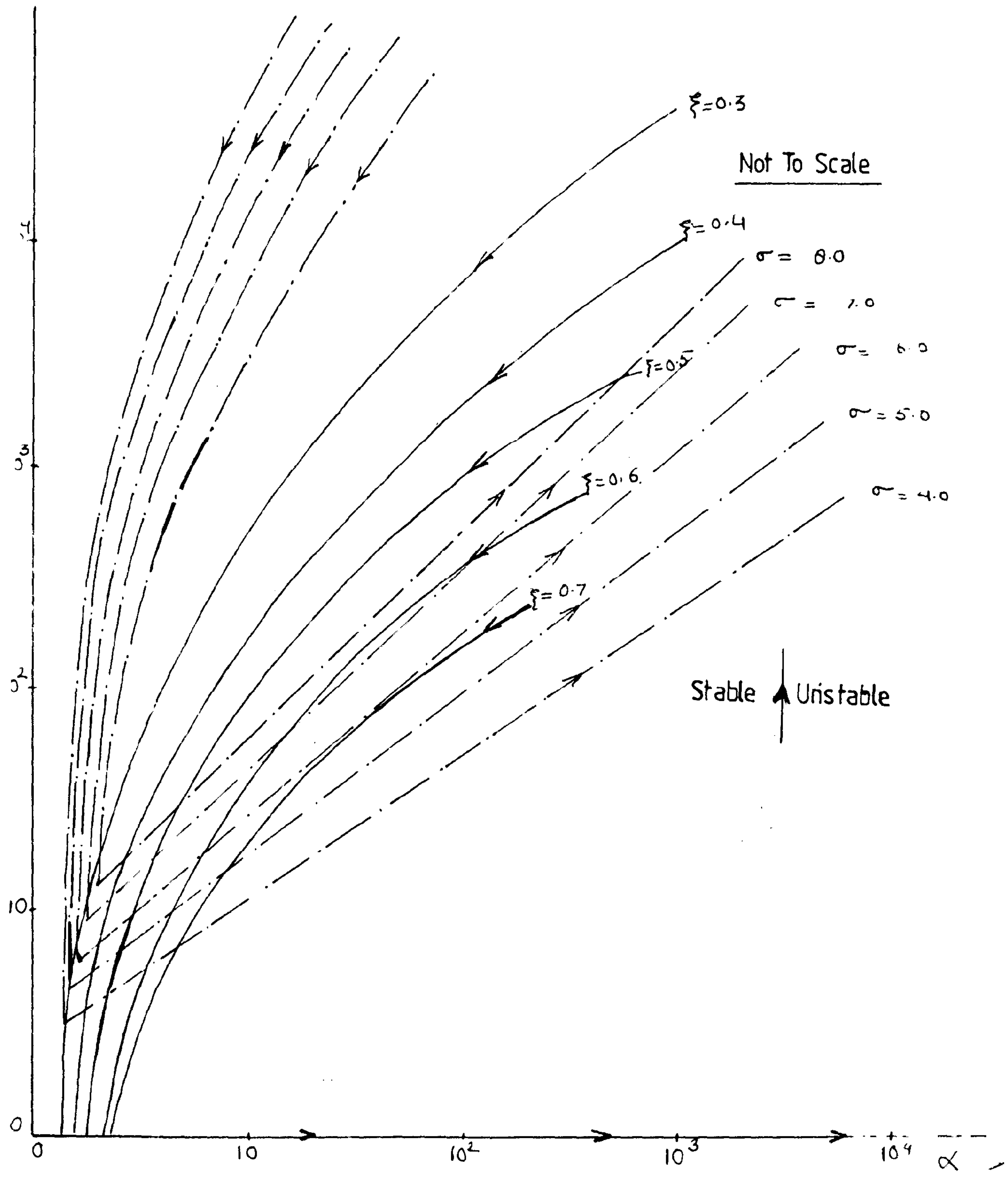

FIG.6.11 COMBINATION OF FIGS. 6.9 & 6.10

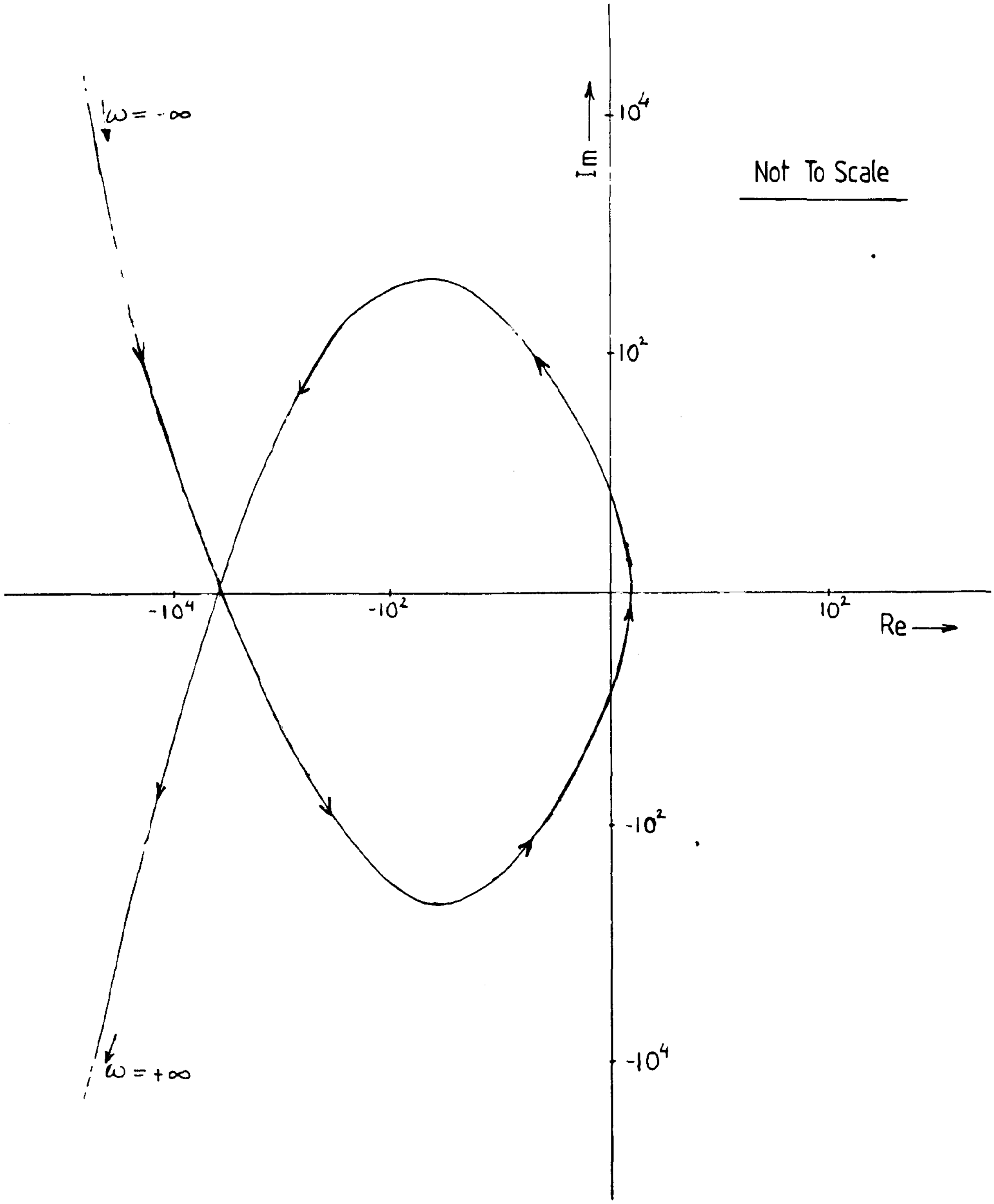

5.12 STABILITY CHECK FOR CURRENT CONTROLLER

($\sigma = 7.0$, $\alpha = 4.0$, $\beta = 12.0$)

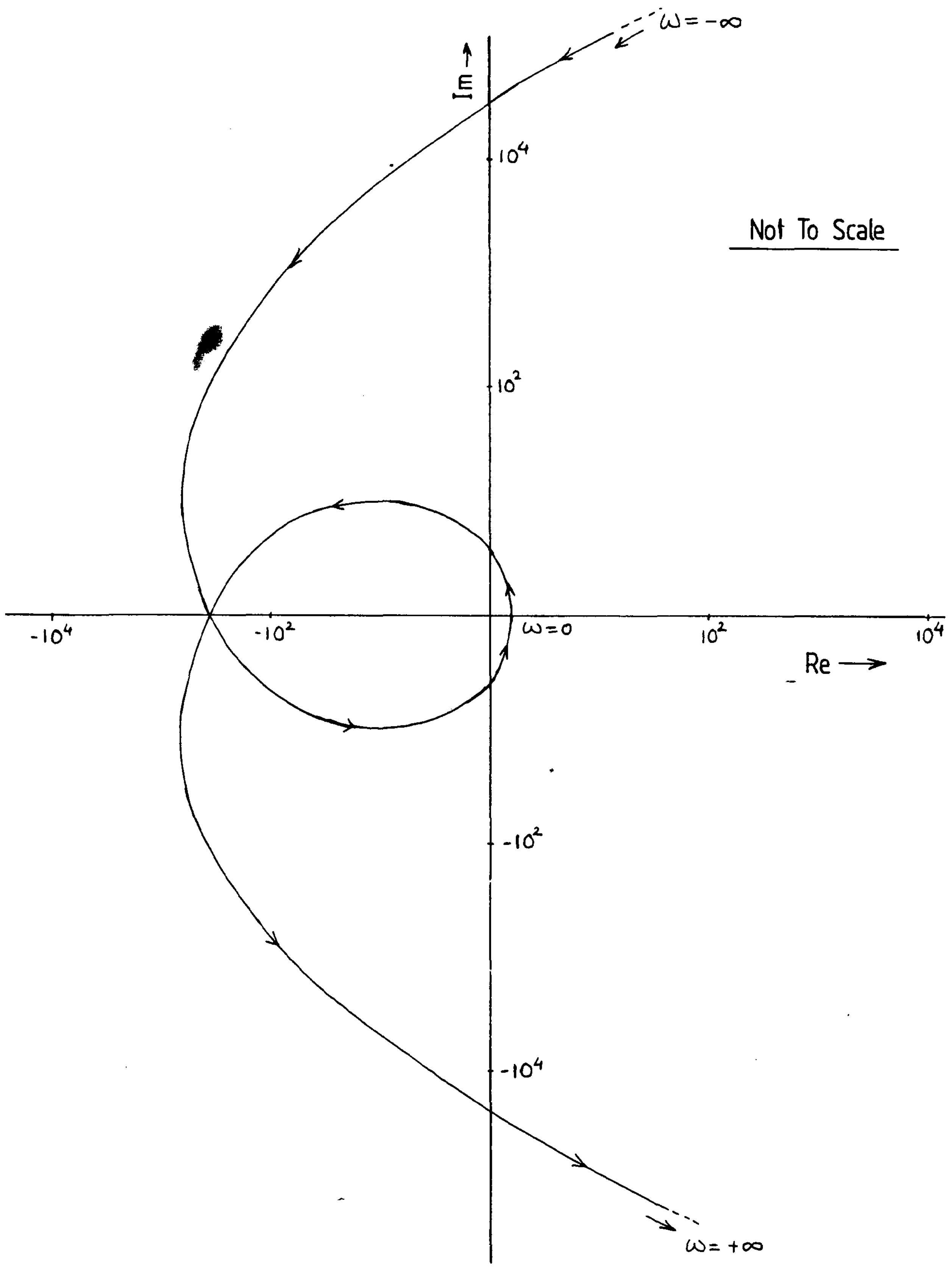

FIG.6.13 STABILITY CHECK FOR CURRENT CONTROLLER

($\xi = 0.5$, $\alpha = 4.0$, $\beta = 12.0$)

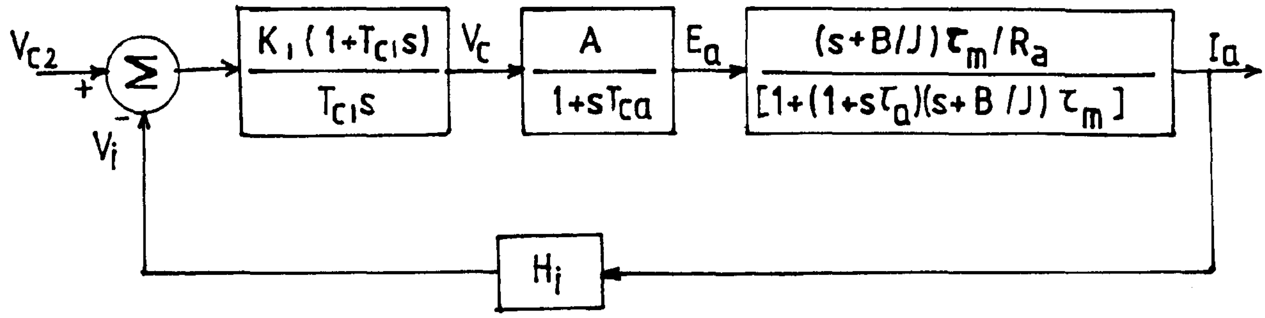

FIG.6.8 BLOCK DIAGRAM OF CURRENT CONTROL LOOP

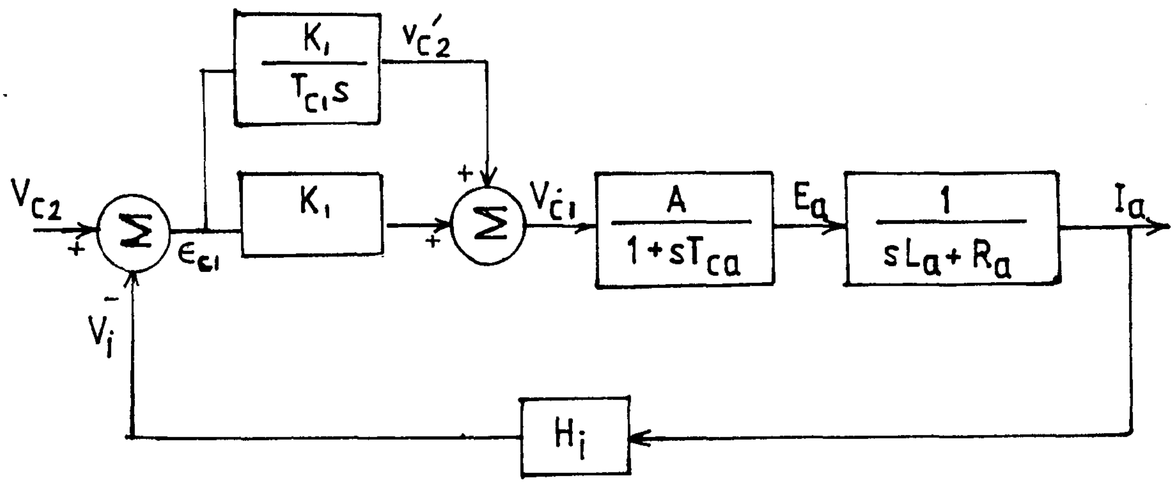

FIG.6.14 BLOCK DIAGRAM OF CURRENT CONTROL LOOP WITH ALL STATE VARIABLES

$$E_a = x_2$$

$$I_a = x_3$$

The reference current input is taken as

$$V_{c2} = 1.0$$

From the block diagram of Fig. 6.14

$$x_1 = \frac{K_1}{T_{c1}s} \epsilon_{c1}$$

$$\epsilon_{c1} = V_{c2} - H_i\, x_3$$

$$\therefore\; sx_1 = \frac{K_1}{T_{c1}} (V_{c2} - H_i\, x_3) \qquad \ldots(6.7)$$

Taking inverse Laplace transform of equation (6.7)

$$\frac{dx_1}{dt} = \frac{K_1}{T_{c1}}(V_{c2} - H_i\, x_3) \qquad \ldots(6.8)$$

Also,

$$x_2 = \frac{A}{1+sT_{ca}} V_{c1}$$

Hence,

$$sx_2T_{ca} = A\, V_{c1} - x_2 \qquad \ldots(6.9)$$

Taking inverse Laplace transform of equation (6.9)

$$\frac{dx_2}{dt} = \frac{A\, V_{ck} - x_2}{T_{ca}} \qquad \ldots(6.10)$$

Further,

$$x_3 = \frac{1}{sL_a + R_a} x_2$$

$$\therefore\; sL_a x_3 = x_2 - R_a x_3 \qquad \ldots(6.11)$$

Taking inverse Laplace transform of equation (6.11)

$$\frac{dx_3}{dt} = \frac{x_2 - R_a x_3}{L_a} \qquad \ldots(6.12)$$

Also,

$$V_{c1} = x_1 + K_1 \ (V_{c2} - H_i x_3) \qquad \ldots(6.13)$$

The limiting values of V_{c1} are $\pm$ 9V.

$$\text{i.e.} \quad +9V \leqslant V_{c1} \leqslant -9V \qquad \ldots(6.14)$$

Using equations (6.8), (6.9), (6.12), (6.13), and condition (6.14) the transient response of the current loop for a step current reference input are calculated using Runga--Kutta Fourth order method and the current (I_a) as a function of time (t) is plotted on CALCOMP plotter of DEC-20 Computer for different values of gain and time constants as shown in Fig. 6.15. It will be noted that for gain K_1 = 0.25 and time constant T_{c1} = 0.083 sec, the response is fast and the settling time is nearly 0.4 sec. Therefore

Gain of the controller K_1 = 0.25

Time constant of the controller (T_{c1}) = 0.083 sec

The transfer function of the current controller is now given by $\frac{0.25(1 + 0.083\ s)}{0.083\ s}$.

The realization of current controller is shown in Fig. 6.16. OPAMP 741 is used for this purpose. The non-inverting terminal (pin 3) is grounded through 1K resistance and error between reference and feedback signals is given at inverting terminal (pin 3). The output of the amplifier

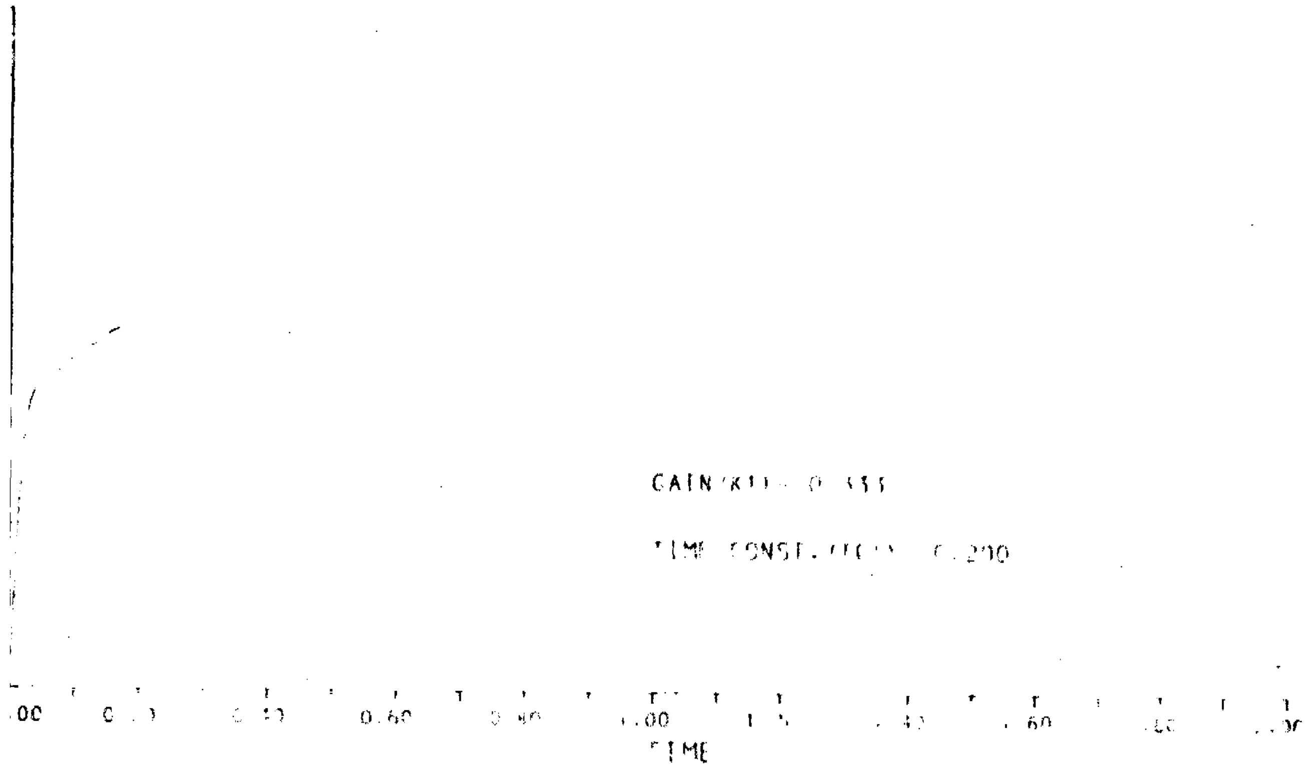

FIG. 6 15 (c)

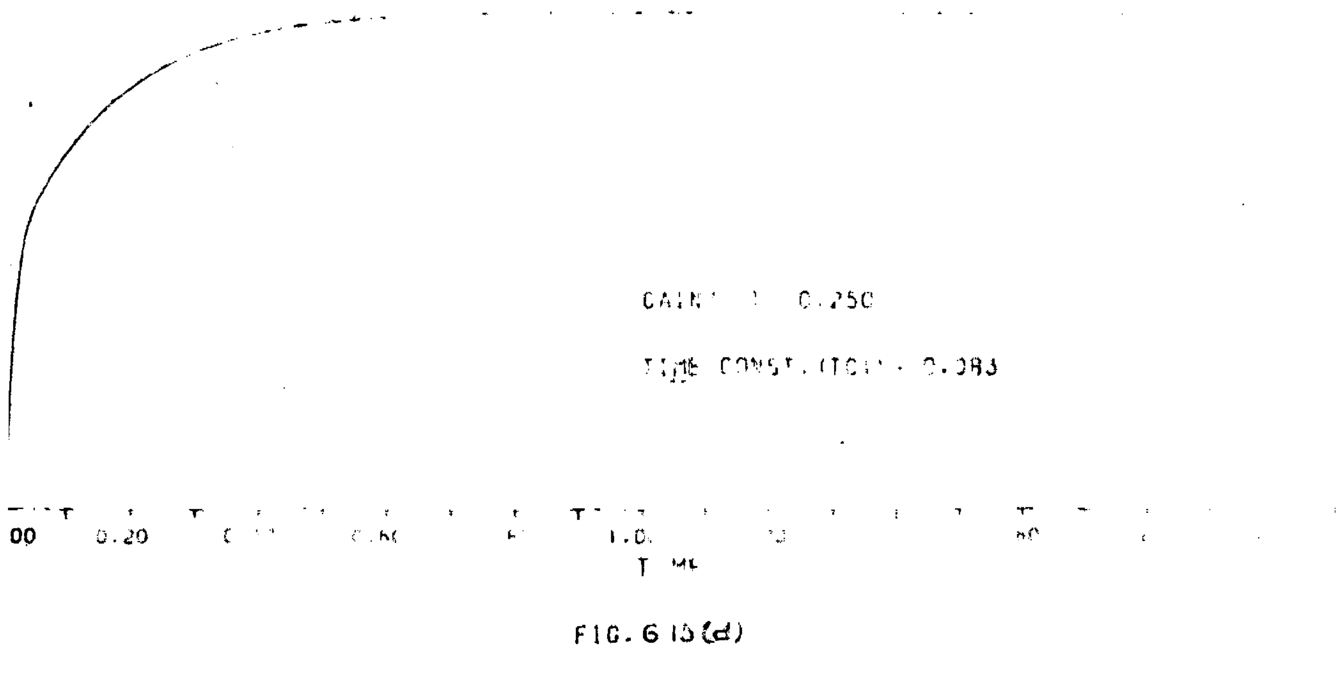

FIG. 6 15 (d)

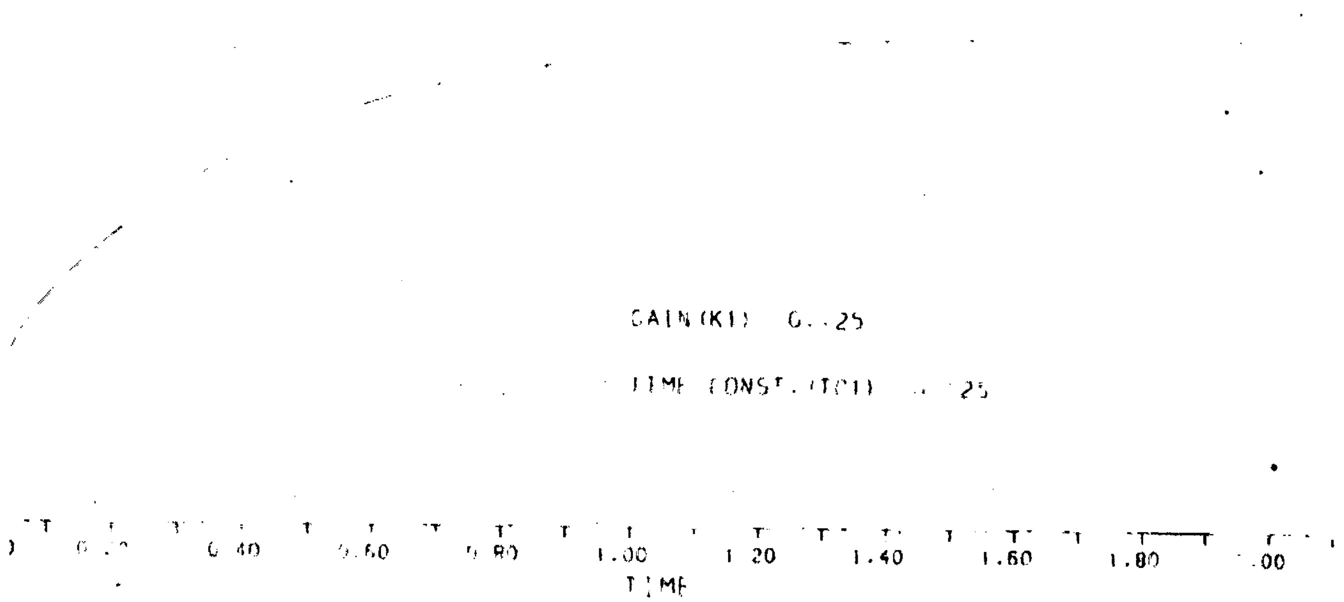

FIG. 6.15(e)

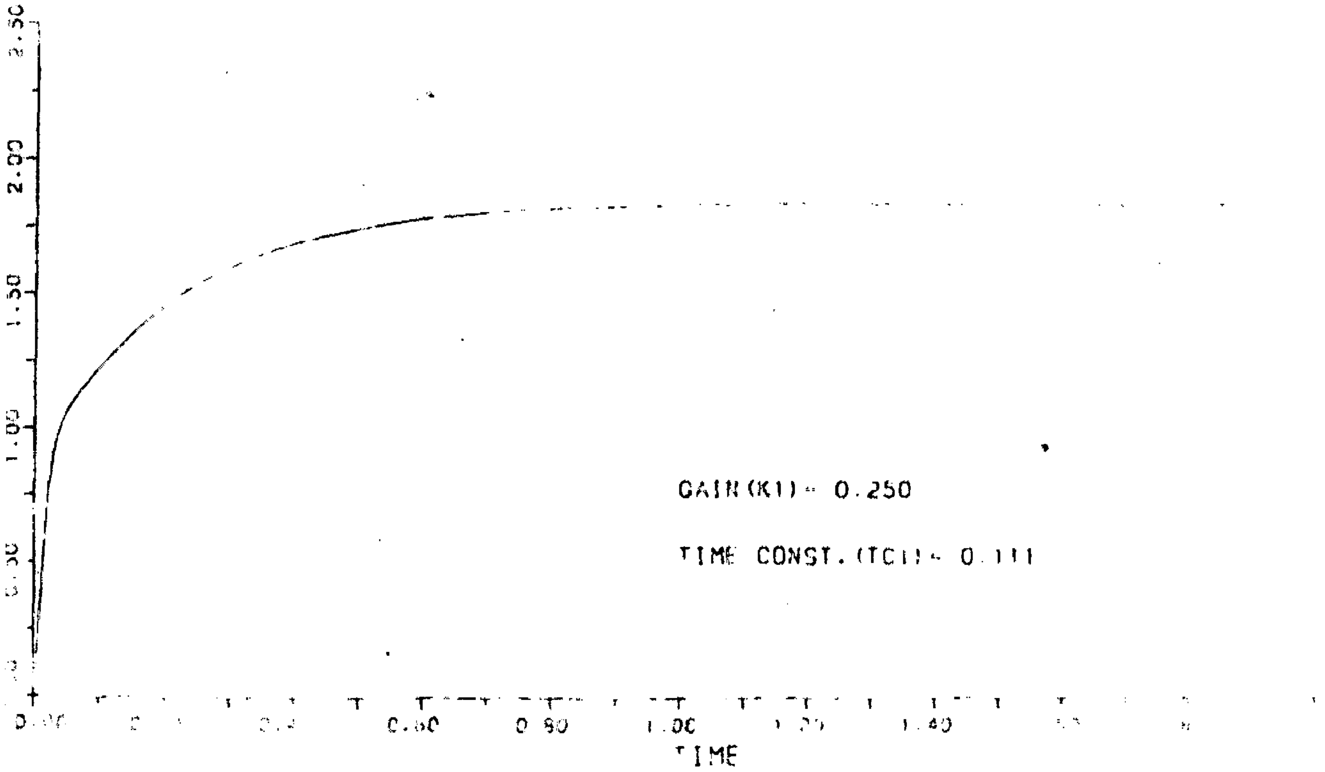

FIG 6.15(f)

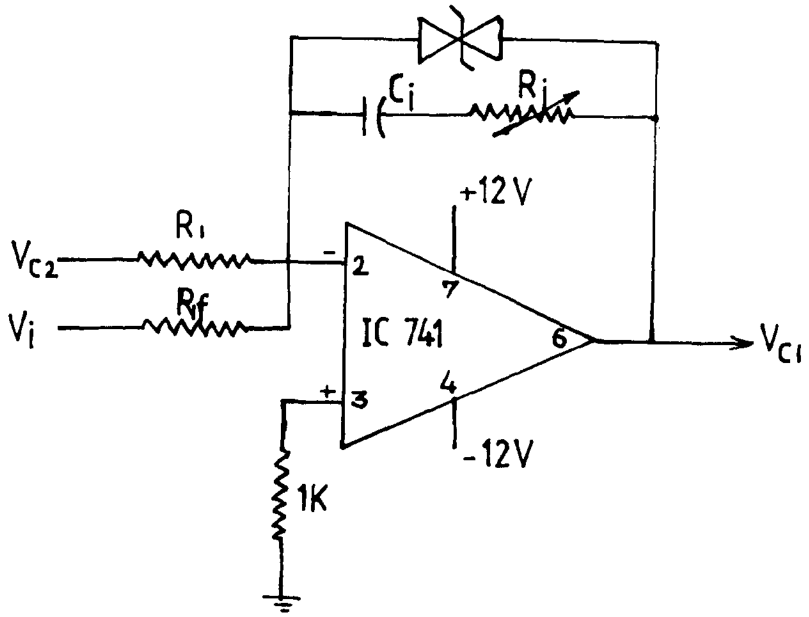

FIG.6.16 CURRENT CONTROLLER

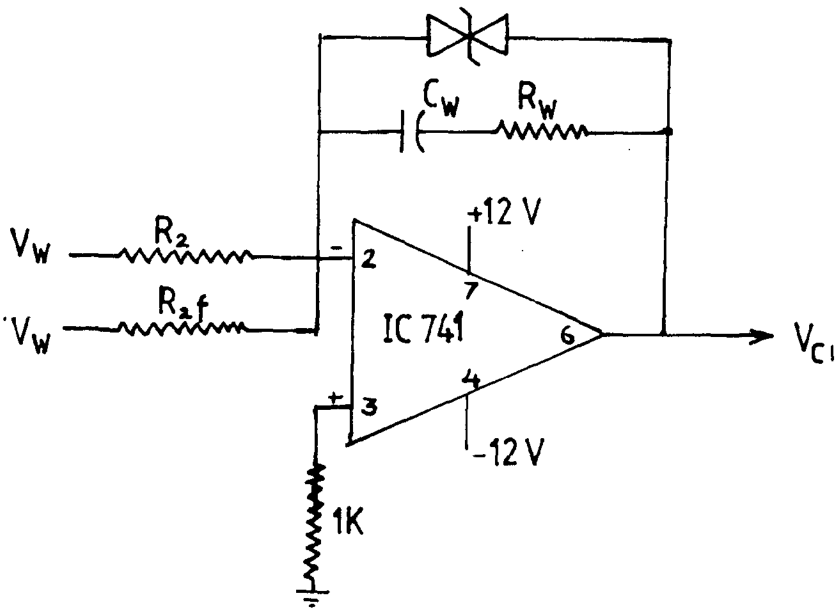

FIG.6.23 SPEED CONTROLLER

is taken from pin 6 and also fed back to the inverting terminal though R_i C_i series circuit. The feedback capacitor C_i is chosen as 0.66 µf and from the values of K_1 and T_{c1} the values selected for R_i and R_{1f} are:

$$R_i = 125 \text{ K ohm}$$

$$R_{1f} = 510 \text{ K ohm}$$

The value of R_1 is selected from the relation

$$\frac{V_{c2}}{R_1} = \frac{V_i}{R_{1f}}$$

For a maximum armature current, the feedback voltage is 4V ($=V_i$). Limiting the value of V_{c2} to 4V in both direction the values of R_1 is choosen as 510 K ohm.

The output of current controller is limited to $\pm$ 9V using 9 volt zeners connected back to back in parallel with R_i-C_i series circuit.

6.6.2 Speed Controller

A PI controller is also used for the speed controller. The transfer function of speed controller is given by $\frac{K_2(1+T_{c2}s)}{T_{c2}s}$. Here, the gain ($K_2$) and time constant ($T_{c2}$) are to be designed. These values are selected on the basis of relative stability as in the case of current controller. The complete speed loop is shown in Fig. 5.4.

The inner current loop is reduced to a single block, the transfer function of which is given as follows:

$$\text{T.F. of current loop} = \frac{G(s)}{1 + G(s)H(s)}$$

where,

$$G(s) = \frac{K_1(1+T_{c1}s)}{T_{c1}s} \cdot \frac{A}{1+sT_{ca}} \quad \frac{(s+B/J)\,\tau_m/R_a}{[1+(1+s\tau_a)(s+B/J)\,\tau_m]}$$

$$= \frac{F_1(s)}{F_2(s)}$$

$$H(s) = H_i$$

$$\text{T.F. of current loop} = \frac{\frac{F_1(s)}{F_2(s)}}{1 + \frac{H_iF_1(s)}{F_2(s)}}$$

$$= \frac{F_1(s)}{F_2(s)+H_iF_1(s)}$$

The characteristic equation of the complete system with this speed loop is then, given by

$$1 + G'(s)H'(s) = 0$$

Where,

$$G'(s) = \frac{K_2(1+T_{c2}s)}{T_{c2}s} \cdot \frac{F_1(s)}{F_2(s)+H_iF_1(s)} \quad \frac{K_b/J}{s+B/J}$$

$$H'(s) = \frac{H_\omega}{1+sT_f}$$

Therefore, the system characteristic equation is

$$1+K_2(1+\frac{1}{T_{c2}s})\ \frac{F_1(s)}{F_2(s)+H_iF_1(s)}\ \frac{K_b/J}{s+B/J}\cdot\frac{H_\omega}{1+sT_f} = 0 \quad ...(6.15)$$

Now defining,

$$F_3(s) = F_1(s)K_bH_\omega/J$$

$$F_4(s) = (F_2(s)+H_iF_1(s))(s+B/J)(1+sT_f)$$

the equation (6.15) can be written as

$$1+K_2(1+\frac{1}{T_{c2}s})\ \frac{F_3(s)}{F_4(s)} = 0$$

or $$\frac{1}{K_2} + (1+\frac{1}{T_{c2}s})\ \frac{F_3(s)}{F_4(s)} = 0 \quad ...(6.16)$$

Again defining, $\frac{1}{K_2} = \alpha'$, $\frac{1}{T_{c2}} = \beta'$, the equation (6.16) become

$$\alpha' sF_4(s) + \beta' F_3(s) + sF_3(s) = 0 \quad ...(6.17)$$

As before, substituting $s = -\sigma+j\omega_d$ and $s = -\xi\omega_n \pm j\omega_n\sqrt{1-\xi^2}$ two sets of D-decomposition boundaries are plotted and the most stable region is found for both sets as shown in Fig. 6.17, 6.18, and 6.19. For checking the relative stability, σ and ξ are increased from minimum values. The resion with highest possible values of σ and ξ are obtained. The stability of this region is checked using frequency scanning technique as shown in Fig. 6.20 and 6.21. For finding the most suitable parameter set, the response of the speed loop for step speed reference input for different parameter sets from the most stable region are calculated using equations (5.14a)

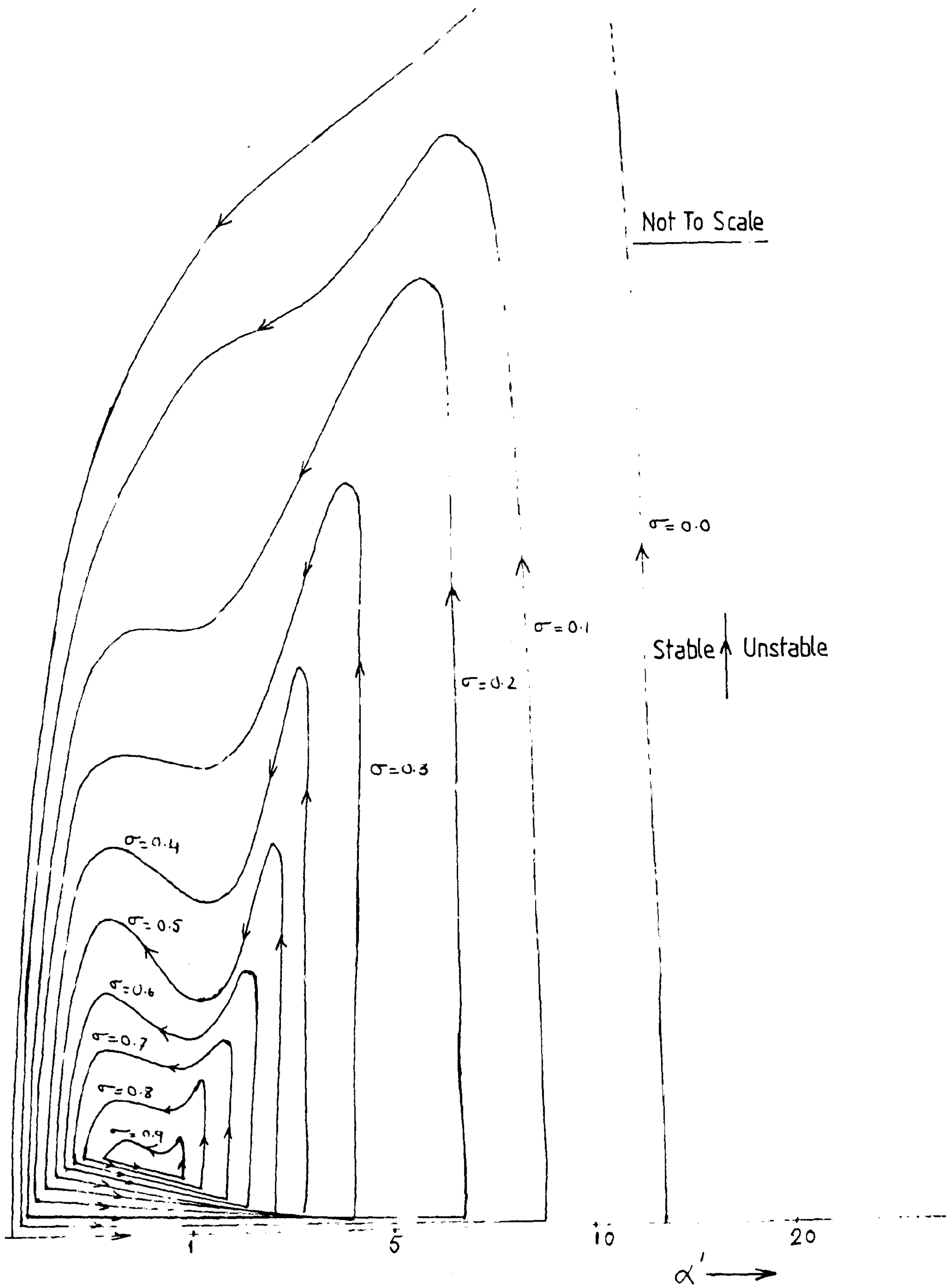

.17 D-PARTITION CURVE FOR SPEED CONTROLLER WITH VARIATION IN σ

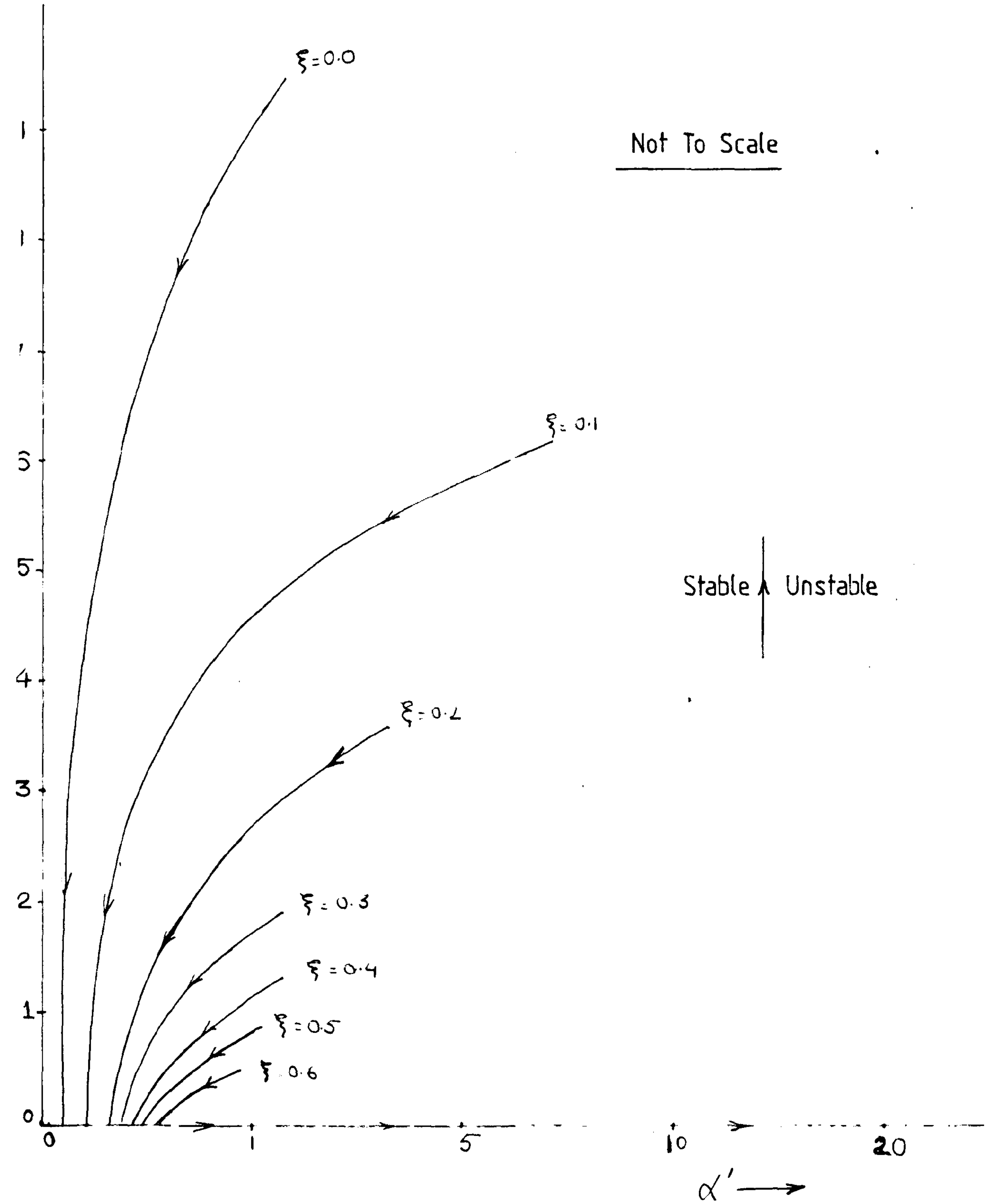

FIG.6.18 D-PARTITION CURVE FOR SPEED CONTROLLER WITH VARIATION IN ξ

Not To Scale

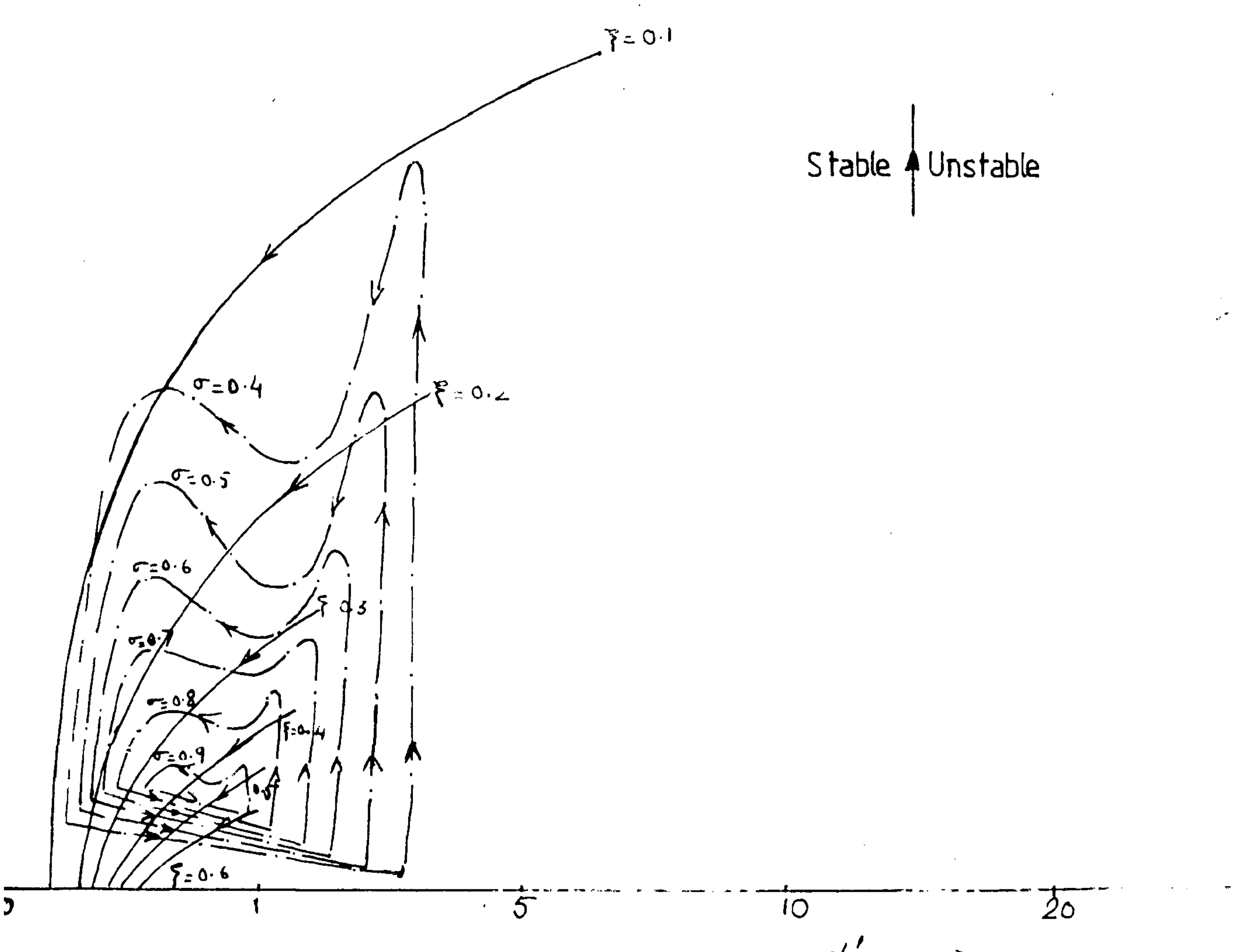

FIG.6.19 COMBINATION OF FIGS.6.17 & 6.18

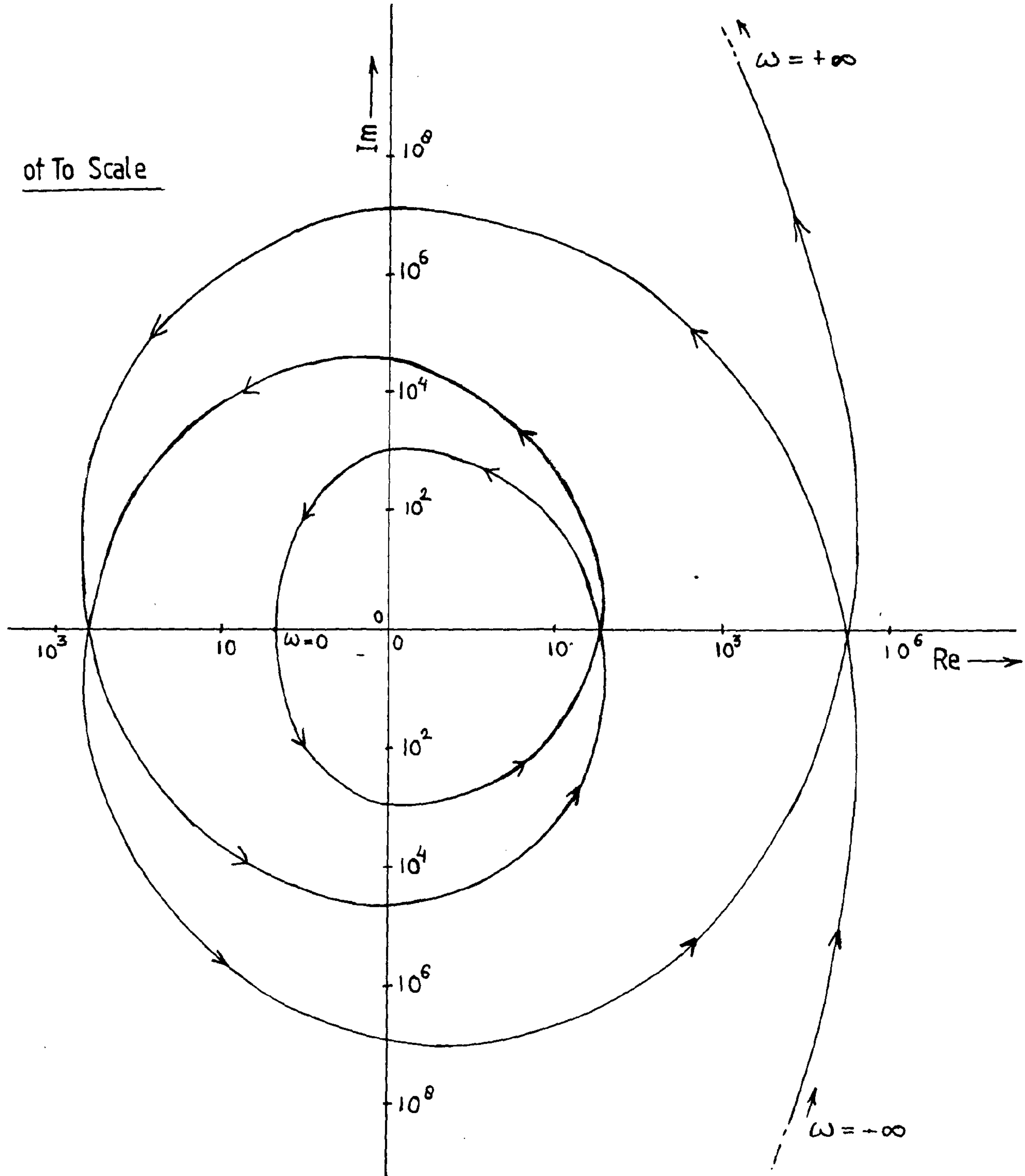

5.20 STABILITY CHECK FOR SPEED CONTROLLER

($\sigma = 0.8, \alpha' = 0.7, \beta' = 0.7$)

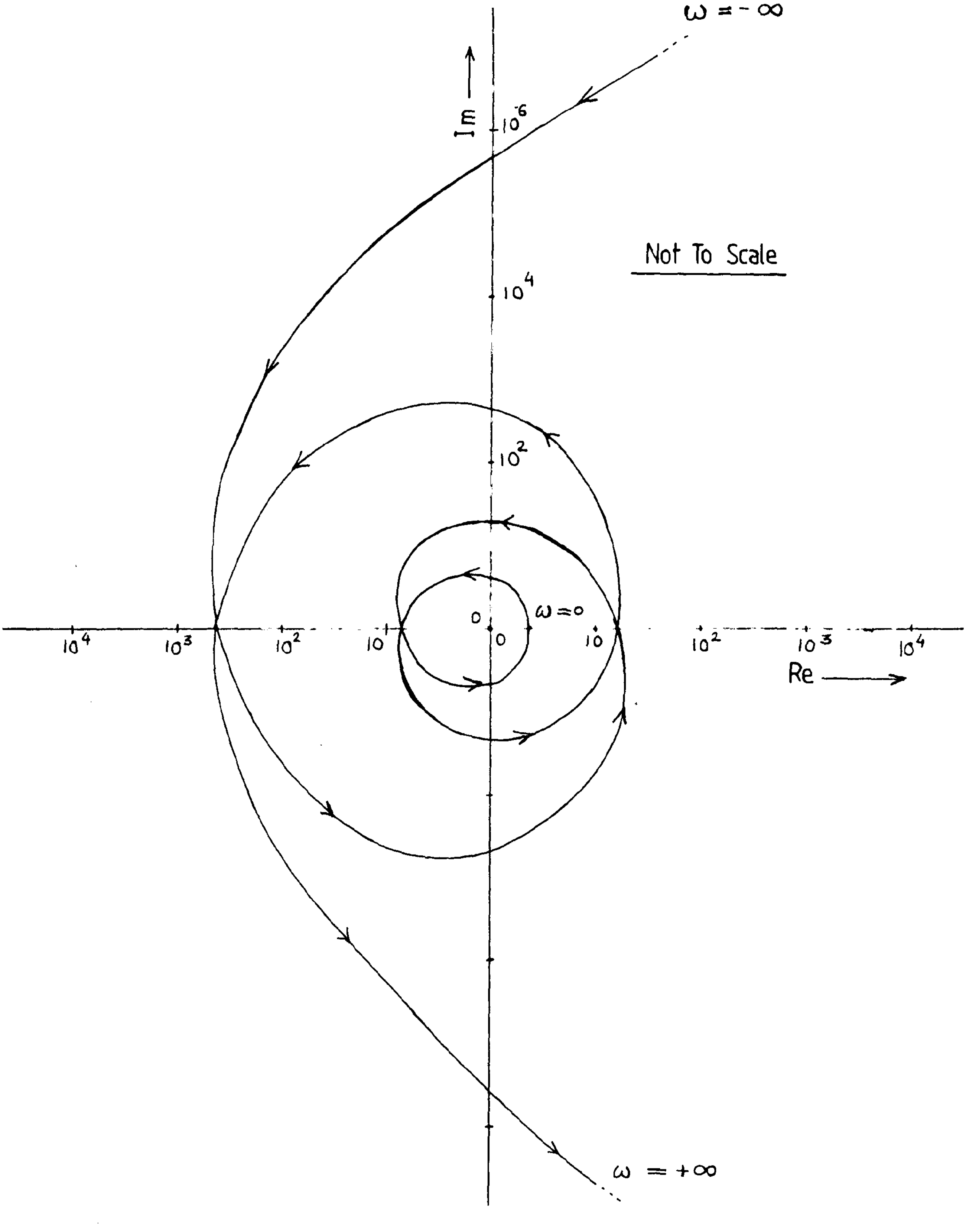

FIG.6.21 STABILITY CHECK FOR SPEED CONTROLLER

($\xi = 0.4$, $\alpha = 0.7$, $\beta = 0.7$)

to (5.14h) and the fourth order Runga-Kutta method. The response of the speed loop (speed ω_m as a function of time t) is plotted for p.u. reference speed input on CALCOMP plotter for various sets of gain and time constant as shown in Fig. 6.22. The response of the speed loop shows that for gain = 1.428, and time constant = 1.428, the response is fast and settling time is nearly 4 secs. Also, the overshoot in speed is less. Therefore, the gain of the speed controller is chosen as 1.428 and time constant of the speed controller is chosen as 1.428. The transfer function of speed controller is given by $\frac{1.428\ (1+1.428s)}{1.428s}$.

The realization of speed controller is shown in Fig. 6.23. OPAMP 741 is used for this realization. Non inverting input is grounded through 1K ohm resistance. The error between reference speed signal V_R and feedback signal V_ω is given at inverting terminal (pin 2). The output is taken from pin 6 and it is fed back to the inverting terminal through R_ω and C_ω series circuit. The feedback capacitor C_ω is chosen as 1.88 μf and from the values of K_2 and T_{c2} the values selected for R_{2f} and R_ω are given by:

$$R_\omega = 760 \text{ K ohm}$$

$$R_{2f} = 530 \text{ K ohm}$$

The input resistance R_2 is chosen from the relation,

$$\frac{V_R}{R_2} = \frac{V_\omega}{R_{2f}}$$

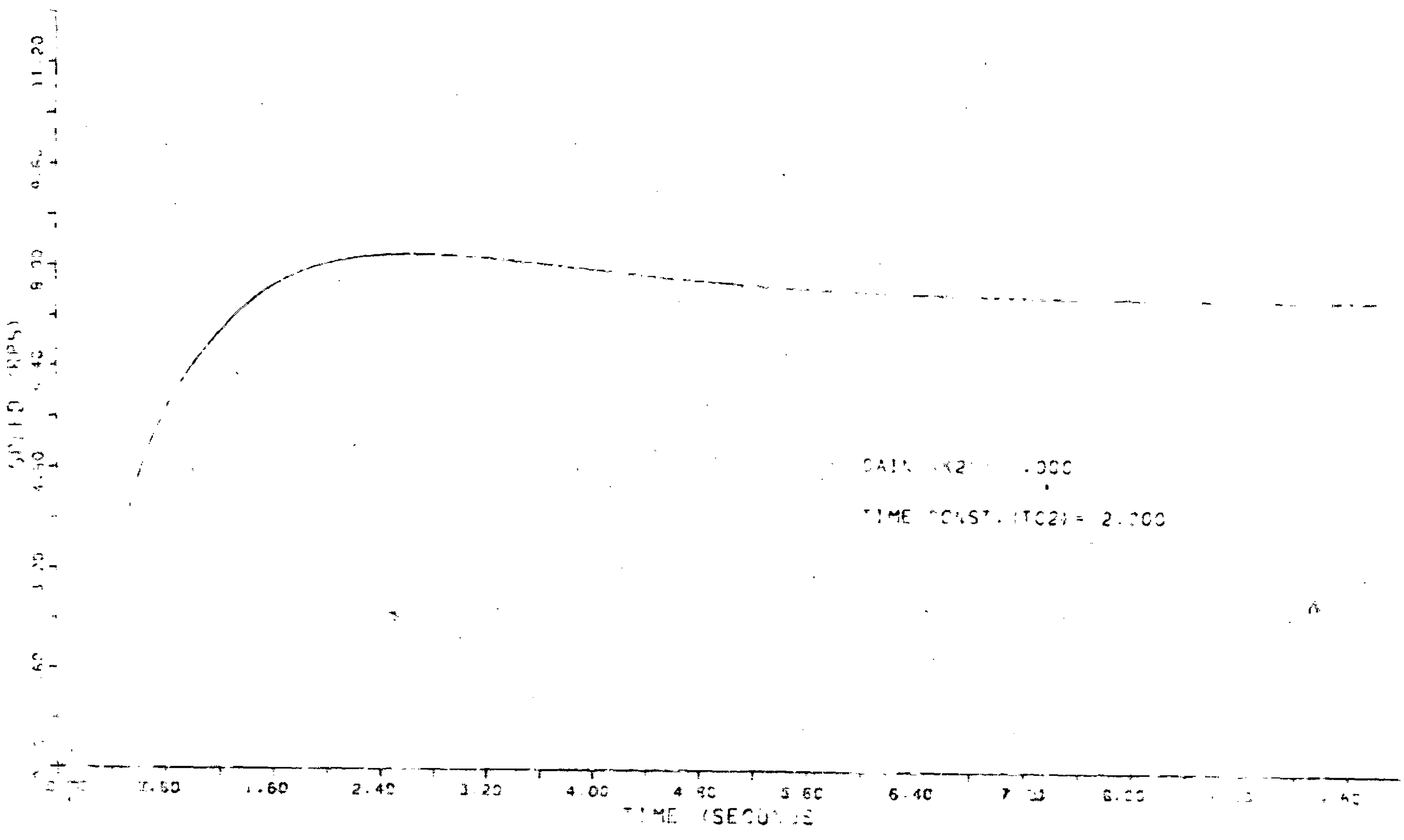

SPEED (RPS)
11.20
8.00
4.80
1.60
.80
1.60
2.40
3.20
4.00
4.80
5.60
6.40
TIME (SECONDS)
GAIN (K2)
TIME CONST. (TC2) = 2.000

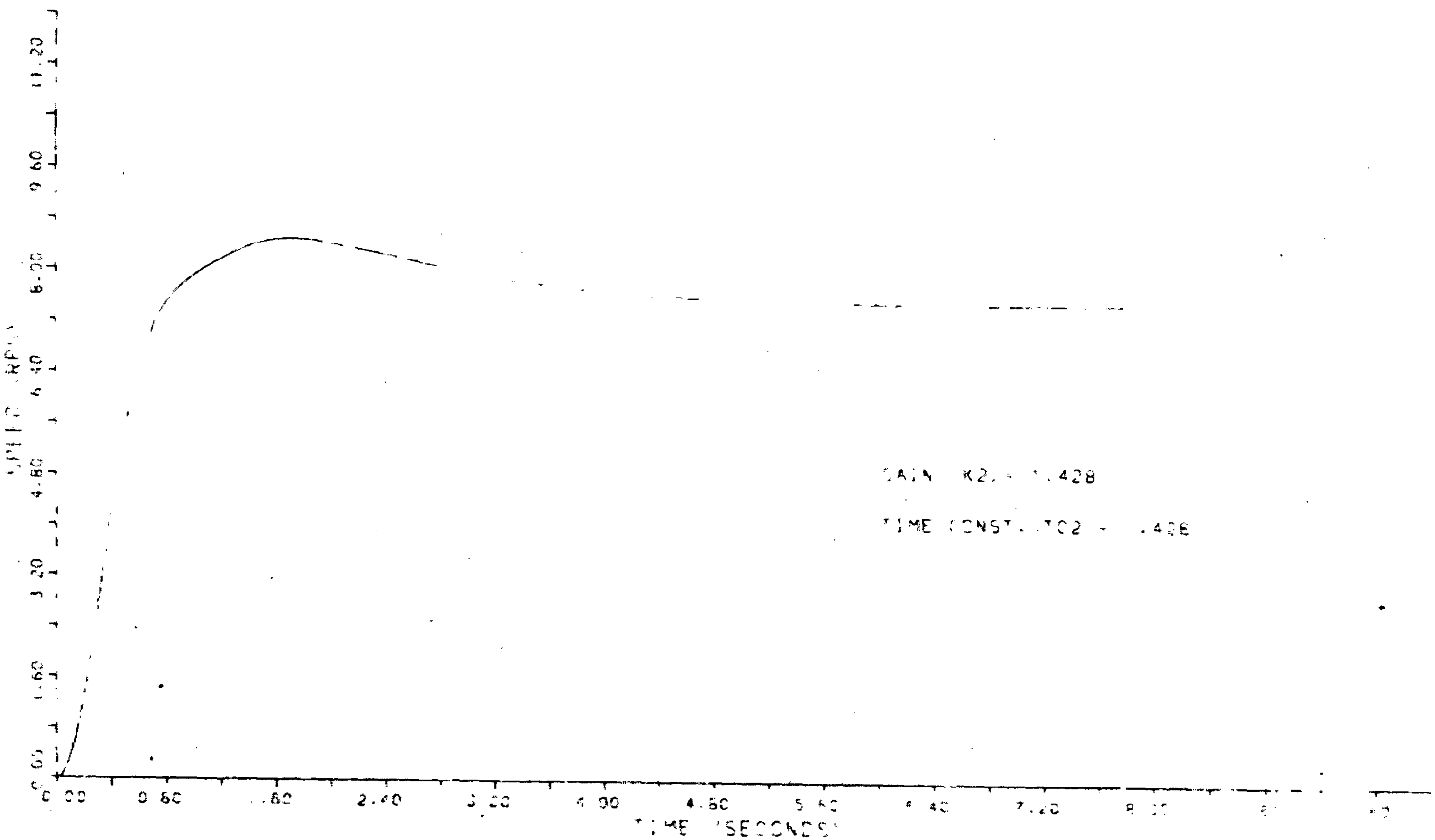

GAIN K2 = 1.428
TIME CONST. TC2 = .428
TIME (SECONDS)
0.00
0.80
2.40
4.00
4.80
5.60
7.20
1.60
3.20
4.80
6.40
8.00
9.60
11.20

FIG. 6 22(c)

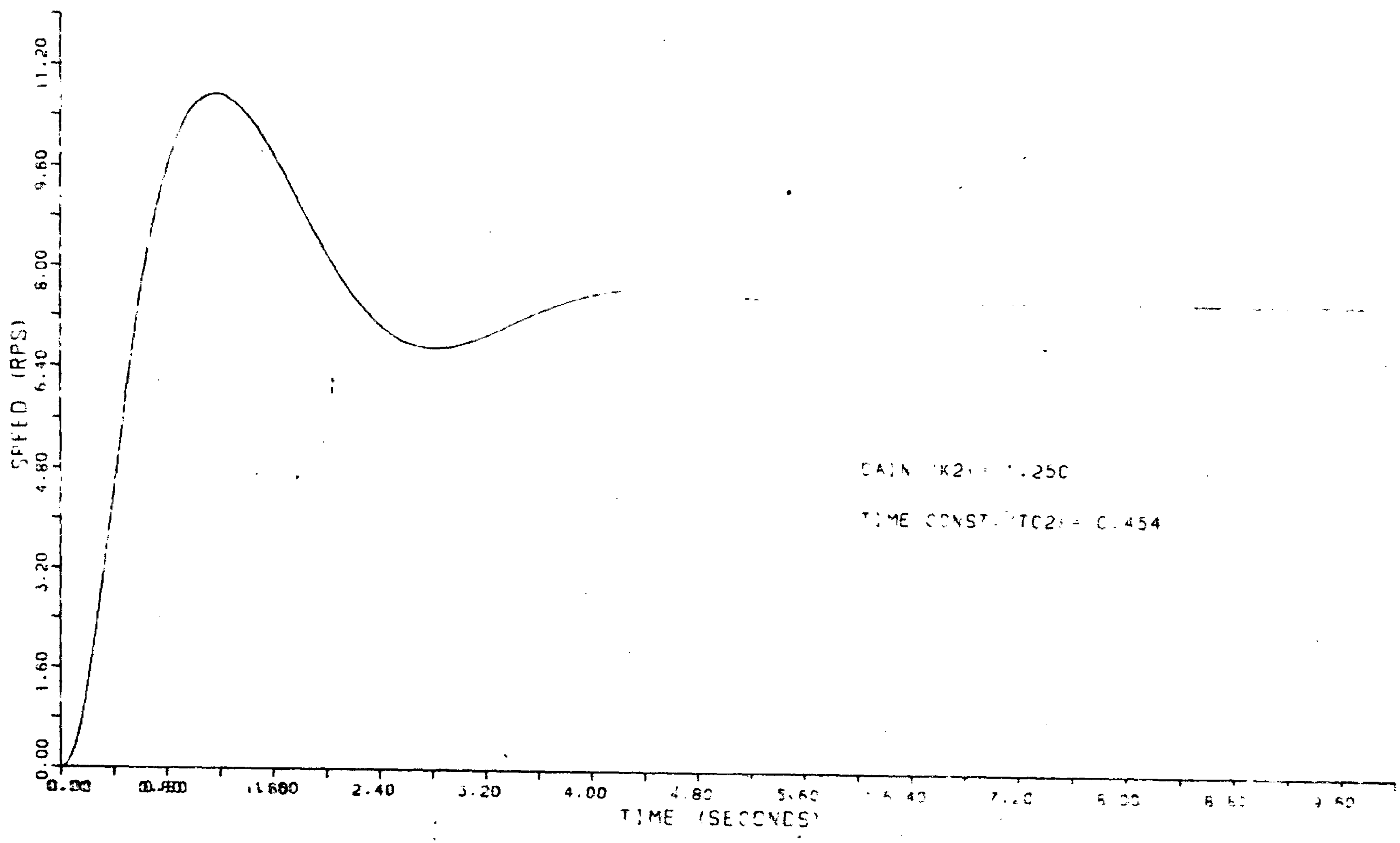
SPEED (RPS)
TIME (SECONDS)
0.00
1.60
3.20
4.80
6.40
8.00
9.60
11.20
2.40
3.20
4.00

FIG. 6.22 (d)

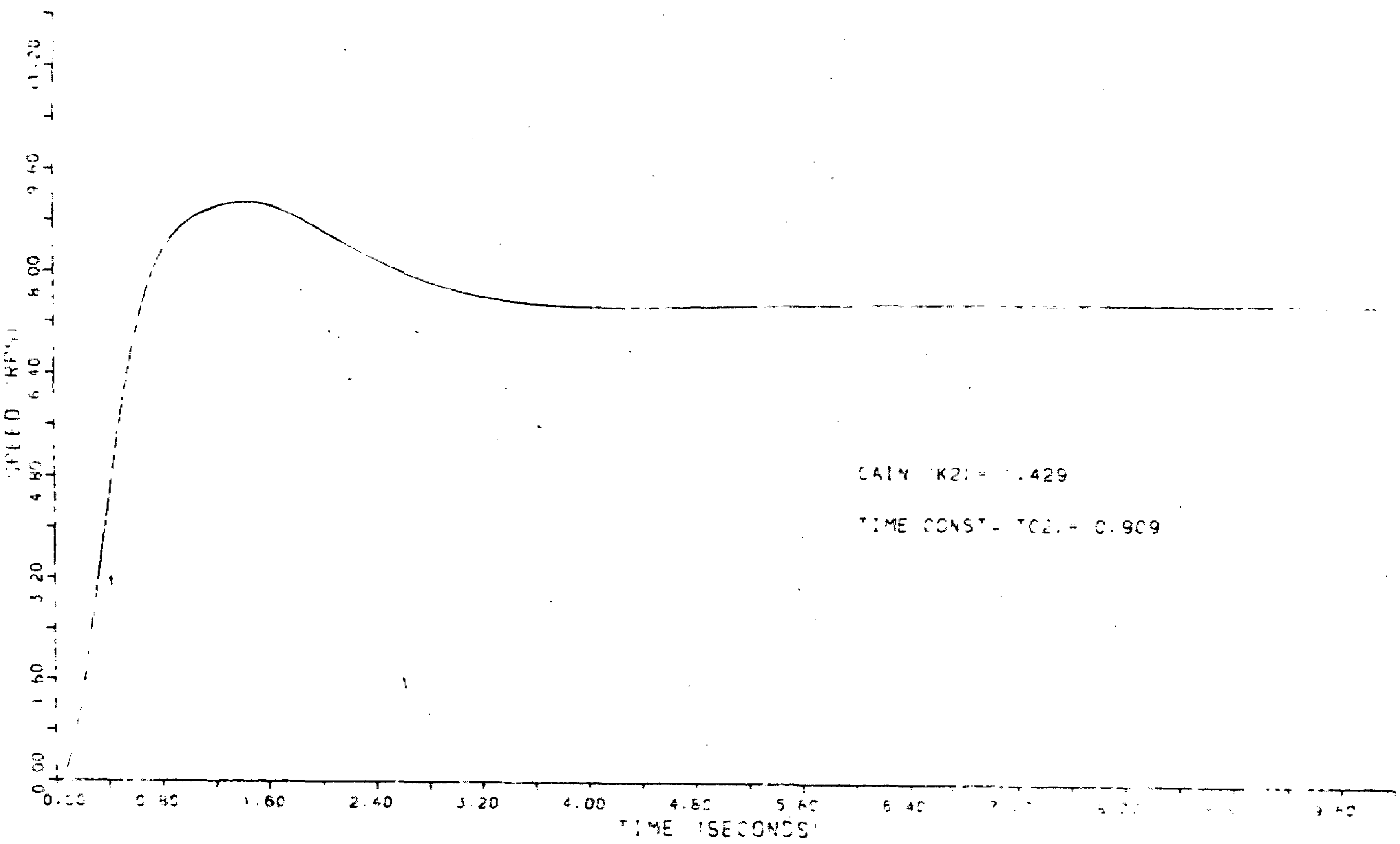

SPEED (RPM)
0.00
1.60
3.20
4.80
6.40
8.00
9.60
11.20
0.00
0.80
1.60
2.40
3.20
4.00
4.80
5.60
6.40
TIME (SECONDS)
GAIN (K2) = .429
TIME CONST. TC2. = 0.909

FIG. 6.22(e)

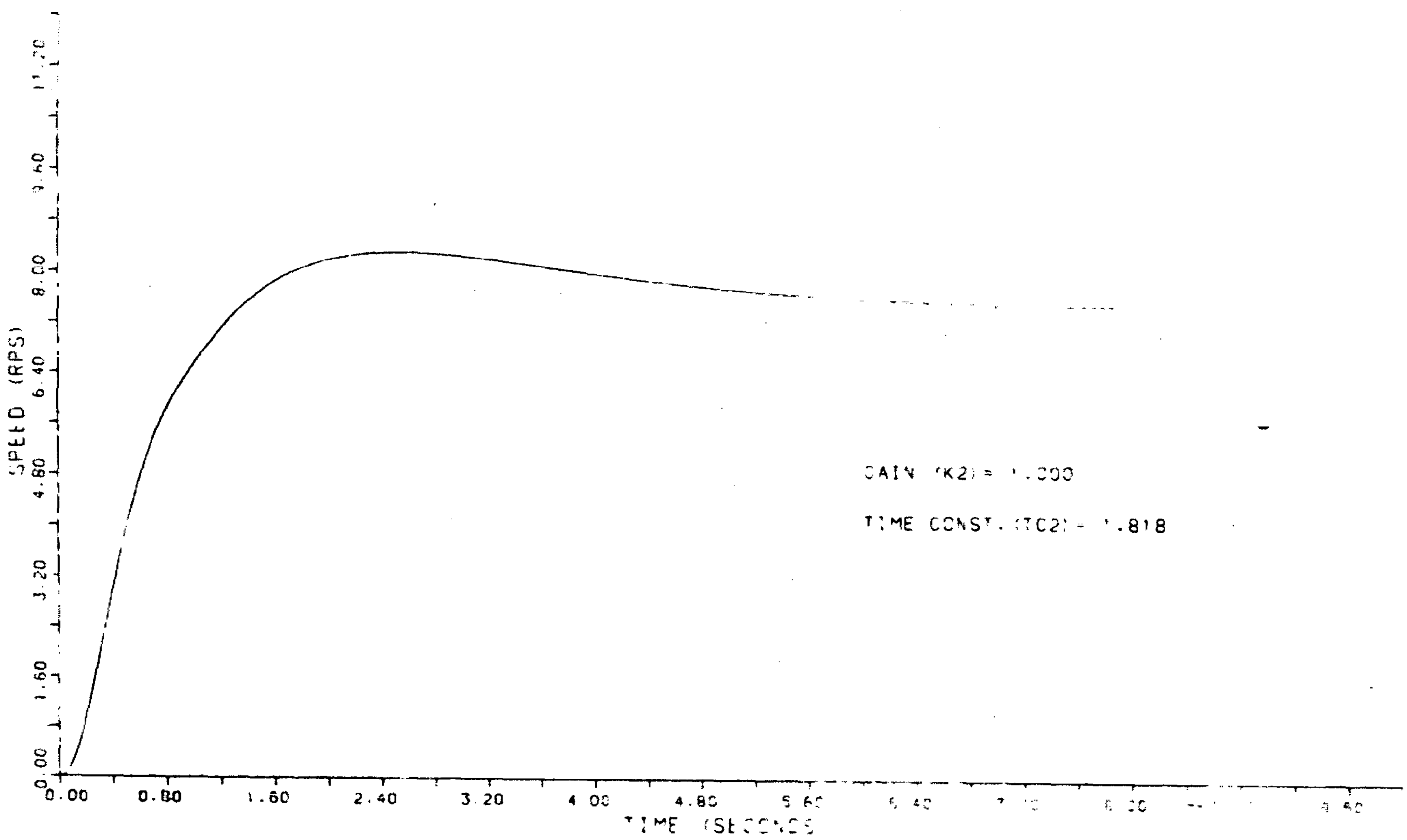

SPEED (RPS)
0.00
1.60
3.20
4.80
6.40
8.00
9.60
11.20
0.00
0.80
1.60
2.40
3.20
4.00
4.80
5.60
TIME (SECONDS)
TIME CONST. (TC2) = 1.818

FIG. 6 22 (f)

For the maximum speed the feedback voltage is 12V and also the corresponding reference speed voltage is 12V.

Therefore, $R_2 = R_{2f} = 530$ K ohm

The output of speed controller is limited to $\pm$ 4 volts using 4 volts zeners connected back to back in feedback circuit across R_ω- C_ω series circuit.

The complete control circuit is shown in Fig. 6.24.

6.7 Conclusion

The power circuit is designed for speed control of 2 h.p. D.C. motor. The thyristor protections are considered while designing the control circuit. The firing circuit is designed carefully. The end-stop pulse generator is developed by author. The speed and current controllers are designed on the basis of relative stability. The response of the system for various gain and time constants are considered while selecting final values of gain and time constants of controllers. The chosen parameters ensure a very fast response current loop (with .4 sec settling time for unit step current reference input) together with a sufficiently fast speed loop response (with a settling time of about 4 sec for a p.u. reference speed setting). Saturation characteristic is provided to both the speed and current controllers to ensure safe operation under starting, sudden change in speed reference setting and sudden loading of the motor.

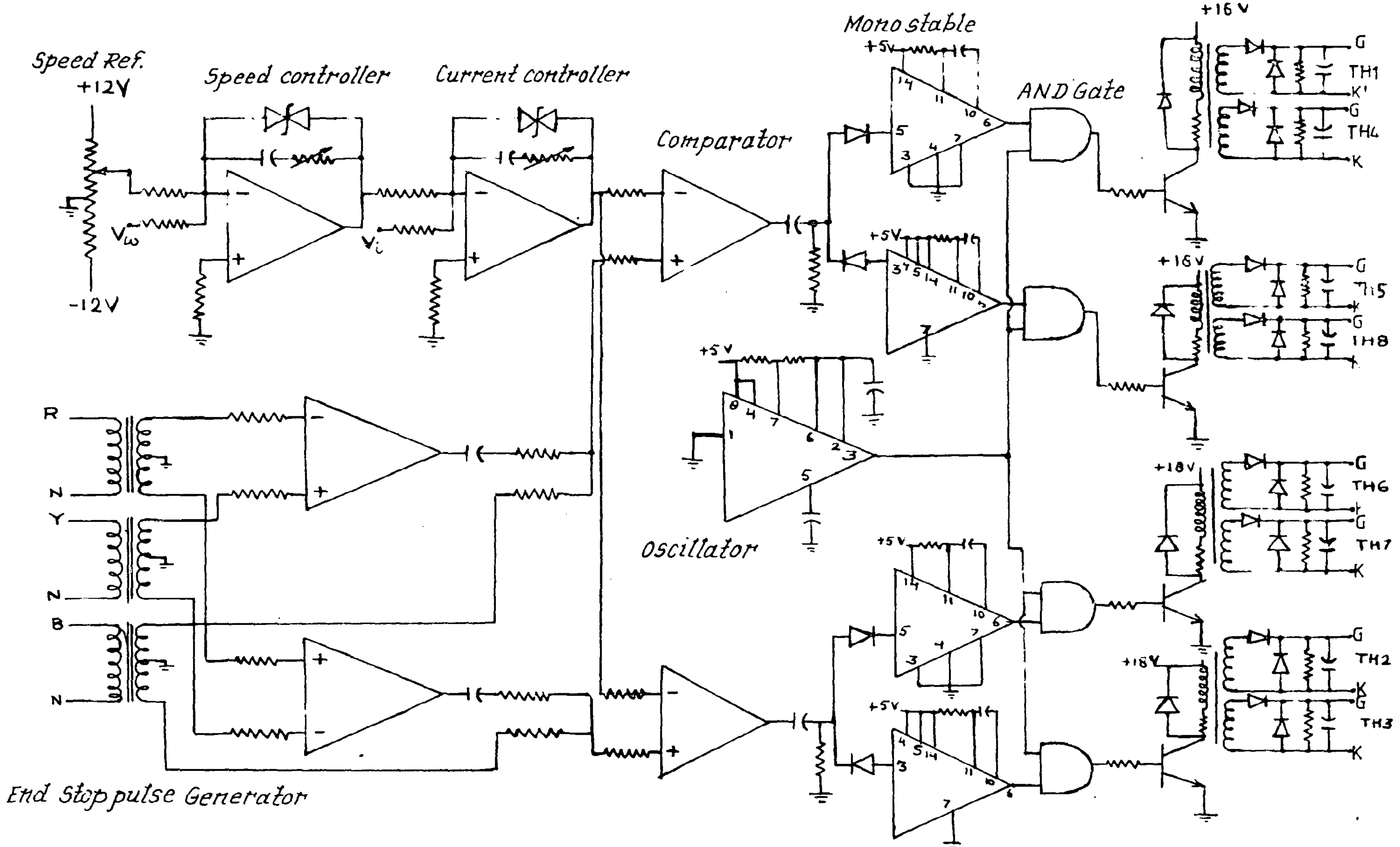

FIG.6.24 COMPLETE FIRING CIRCUIT

Chapter - 7

DRIVE PERFORMANCE

The performance of d.c. motor drive, fed from the dual converter is investigated experimentally in this chapter. The experimental results are compared with the analytical results. Typical waveforms of d.c. output voltage and current are also given for various operating conditions.

7.1 Introduction

In an earlier chapter, the various components of the dual converter have been designed and experimental results in form of waveforms of the firing circuit have been given. The experimental and analytical performance of the d.c. drive, fed from the earlier designed dual converter, is determined now. In order to extensively test the designed converter, its performance both as a single converter and a dual converter under resistive and inductive load conditions is also determined experimentally.

7.2 Performance as a Single Converter

First, both the converters are tested separately on resistive and inductive loads to ensure that both the converters are operating well. Since there is no speed back in these cases, the speed controller output will always be under saturation. Therefore, an external variable voltage is used as a control voltage to fix any firing angle. The photographs of d.c. voltage output and load current at this firing angle are shown in Fig. 7.1. The waveforms seem to be satisfactory.

The converters are now tested separately on the motor load in closed loop mode with both current and speed feedbacks. Table - 7.1 gives the variation of speed of the motor as a function of speed reference voltage.

Table 7.1 D.C. Motor Speed Control With Single Converter

S.No.	Speed reference Voltage (volts)	Speed (rpm)
1	3.5	430
2	4.5	510
3	5.5	570
4	6.0	610
5	6.5	650
6	7.0	680
7	7.5	740
8	8.5	830

A curve is plotted between speed and speed reference voltage as shown in Fig. 7.2. The curve shows that the speed varies almost linearly with reference voltage.

7.3 Performance as a Dual Converter

Now, the converters are connected in dual mode. The dual converter is first tested on resistive load. The

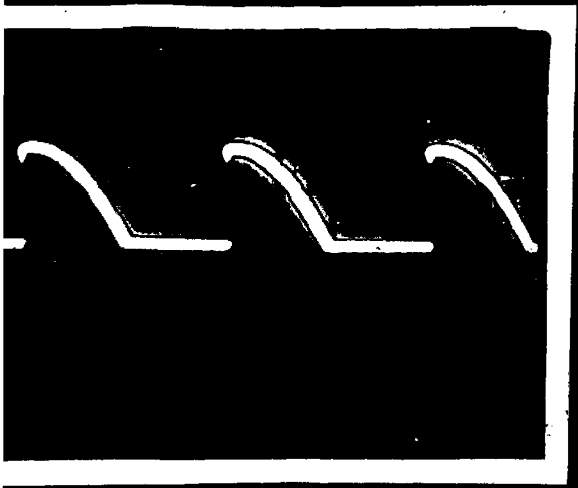

Fig.7.1(a) Voltage Output
With Resistive Load
(Single Converter)

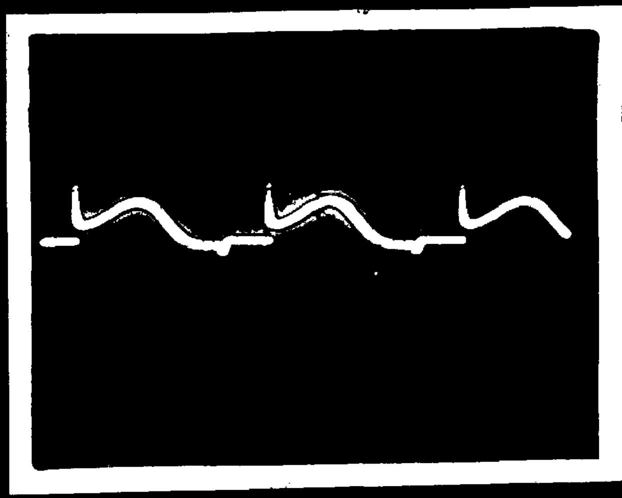

Fig.7.1(b) Load Current
With Resistive Load
(Single Converter)

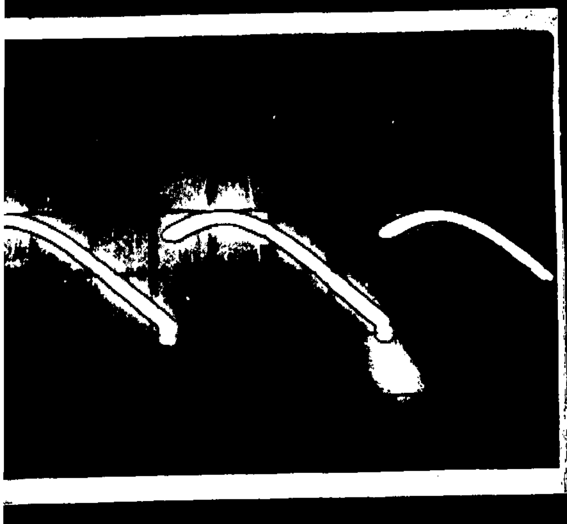

Fig.7.1(c) Voltage Output
With Inductive Load
(Single Converter)

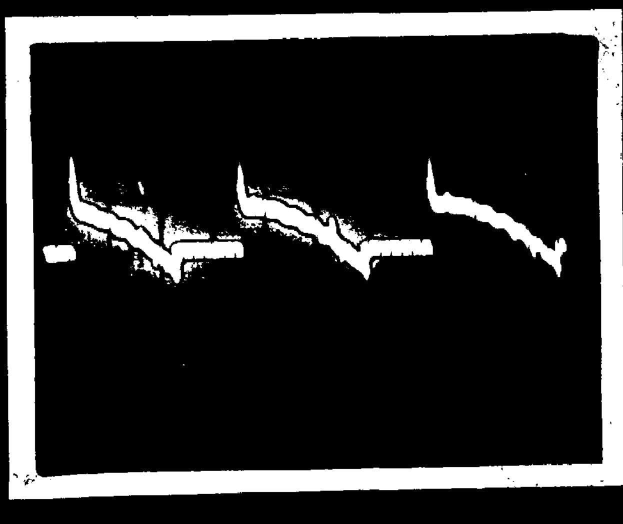

Fig.7.1(d) Load Current
With Inductive Load
(Single Converter)

photographs of d.c. output voltage, and current with a converter operating either in rectification or inversion mode are given in Fig. 7.3. The firing angle is fixed to any desired value using a variable voltage as a control voltage input. The waveforms again seem to be satisfactory. The variation of load voltage as a function of load current is determined. Table 7.2 gives the performance with positive group converter under rectification mode and negative group converter under inversion mode whereas Table 7.3 gives the performance with the positive group converter under inversion mode and negative group converter under rectification mode.

Table 7.2 Dual Converter Performance With Positive Converter in Rectification Mode

S.No.	Input Voltage (Volts)	Input Current (Amps)	Input Power (Watts)	Load Voltage (Volts)	Load Current (Amps)
1	250	0.8	200	228	0.8
2	250	1.6	360	226	1.6
3	250	3.0	680	226	3.0
4	250	4.6	1060	224	4.6
5	250	5.7	1200	222	5.3
6	250	6.7	1480	220	6.7

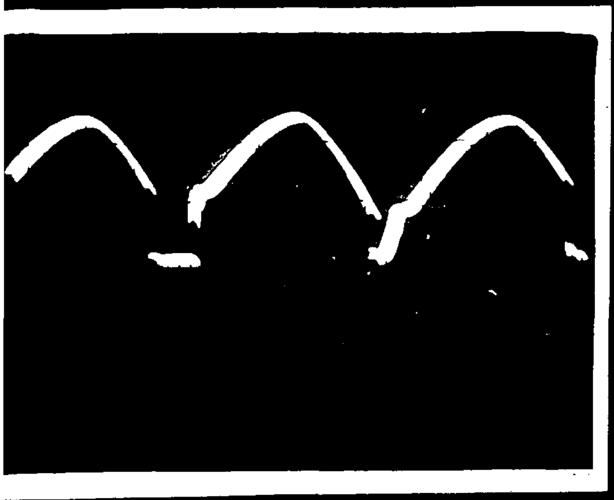

Fig.7.3(a) Voltage Output With Resistive Load (Positive Converter as Rectifier).

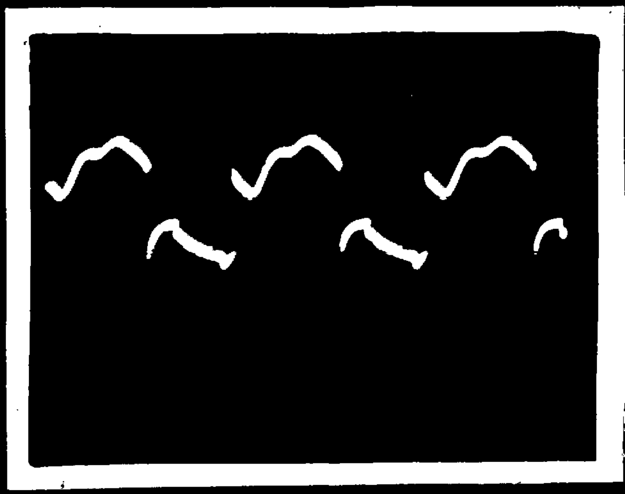

Fig.7.3(b) Load Current With Resistive Load (Positive Converter as rectifier)

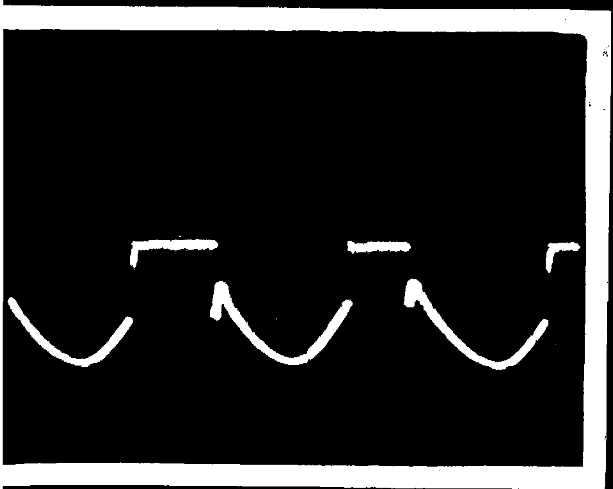

Fig.7.3(c) Voltage Output With Resistive Load (Positive Converter as Inverter)

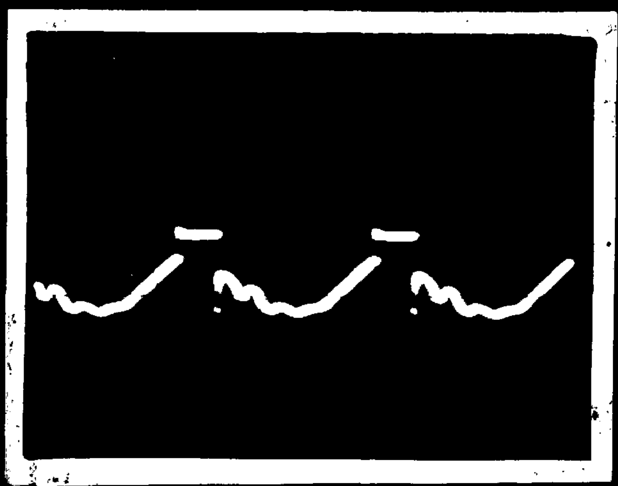

Fig.7.3(d) Load Current With Resistive Load (Positive Converter as Inverter)

Table 7.3 Dual Converter Performance With Positive Converter in Inversion Mode

S.No.	Input Voltage (Volts)	Input Current (Amps)	Input Power (Watts)	Load Voltage (Volts)	Load Current (Amps)
1	200	0.5	140	178	0.5
2	200	1.3	240	177	1.3
3	200	1.95	360	176	1.95
4	200	3.2	600	176	3.2
5	200	4.5	860	175	4.5
6	200	5.7	1060	174	5.7
7	200	6.8	1240	174	6.8

Since no feedback is present, both the controller outputs are in saturation and hence, the firing angle is fixed to minimum value for converter operating in rectifier mode and at maximum value for converter operating in inverter mode. The circulating current is nearly zero and not measurable. The converter is capable of supplying rated converter load.

Lastly, the dual converter is tested on the motor load in closed loop. The photographs of motor terminal voltage and current, and voltage across the reactor with a converter working in either rectification or inversion mode are shown in Fig. 7.4. The waveforms seem to be satisfactory. Table 7.4 gives the variation of speed as a function of speed reference voltage.

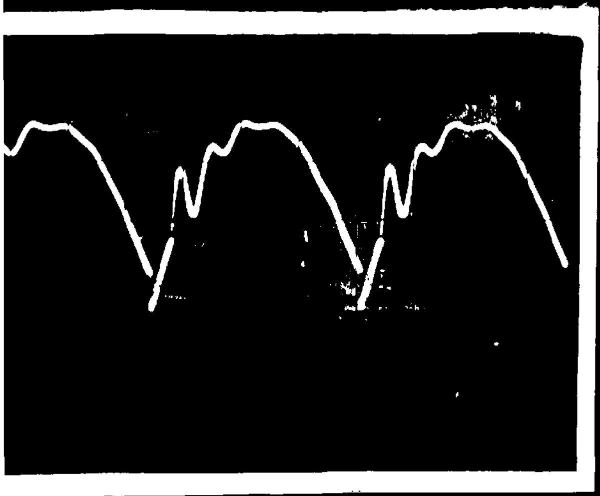

Fig.7.4(a) Motor Voltage (Positive Converter as Rectifier)

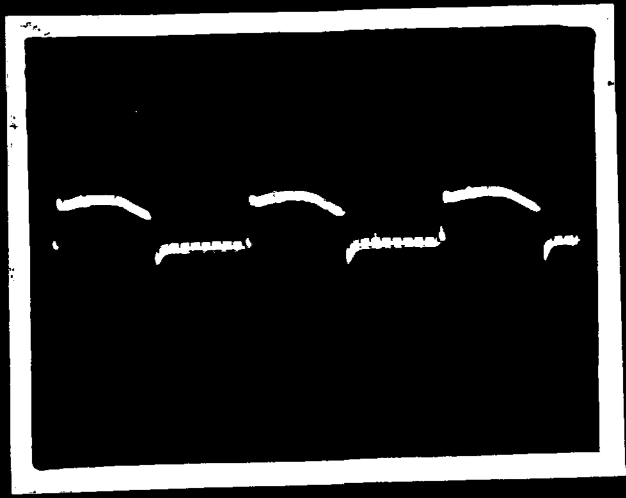

Fig.7.4(b) Motor Armature Current (Positive Converter as rectifier)

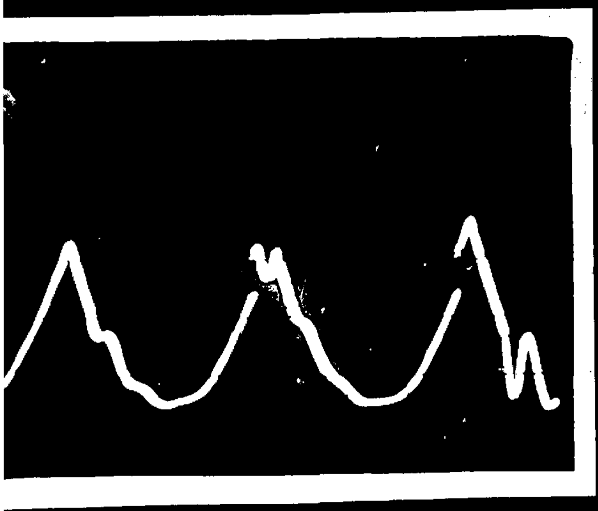

Fig.7.4(c) Motor Voltage (Positive Converter as Inverter)

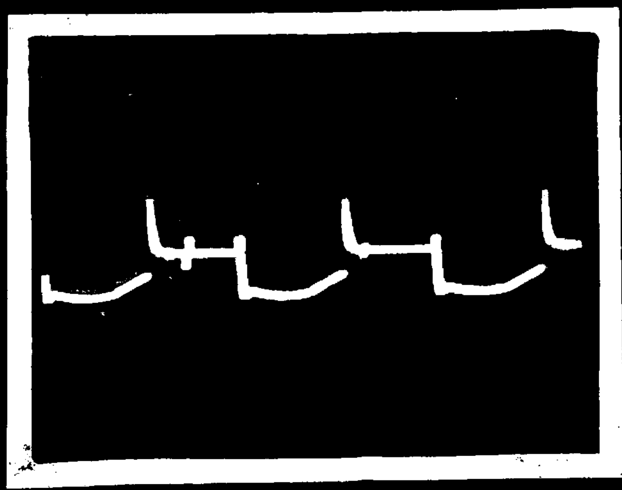

Fig.7.4(d) Motor Armature Current (Positive Converter as Inverter)

Fig.7.4(e) Voltage Across Reactor

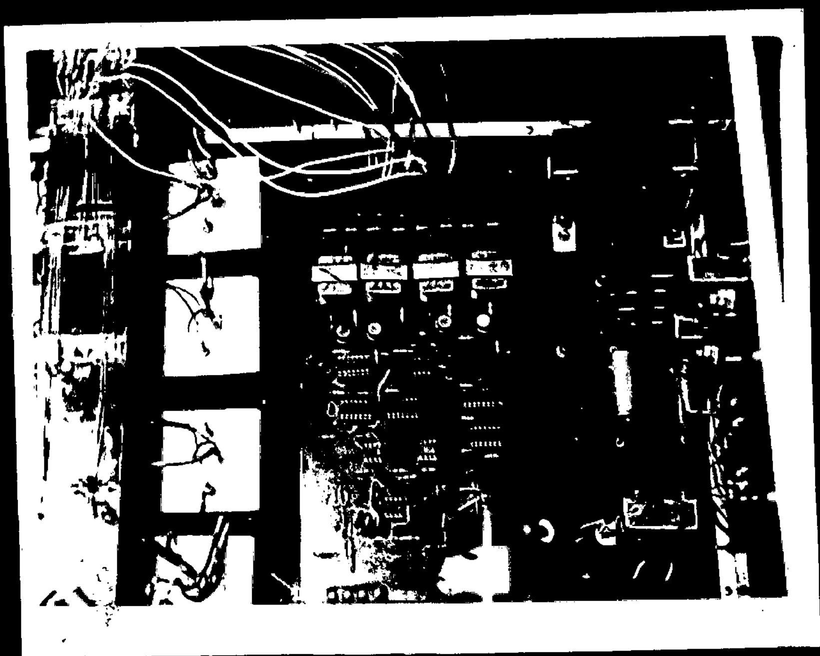

Photograph of the Control Circuit

Table 7.4 Dual Converter Fed D.C. Motor Speed Control

S.No.	Speed Reference Voltage (Volts)	Speed (rpm)
1	4.5	400
2	5.5	500
3	6.0	600
4	7.0	670
5	8.0	750
6	9.25	850
7	10.0	900

A curve is plotted, between speed and speed reference voltage as shown in Fig. 7.5. The curve shows that the speed varies almost linearly with speed reference voltage.

The response of the drive for step speed reference input is plotted on a dual channel recorder and is shown in Fig. 7.6. The response shows that the controllers gain and time constant determined in an earlier chapters are well suited to the drive. The drive takes nearly 5 secs to readh the steady state speed of 480 rpm.

Now, the motor reference speed is fixed at a particular value and the load on the d.c. generator is varied. Table 7.5 gives the variation of speed as a function of load.

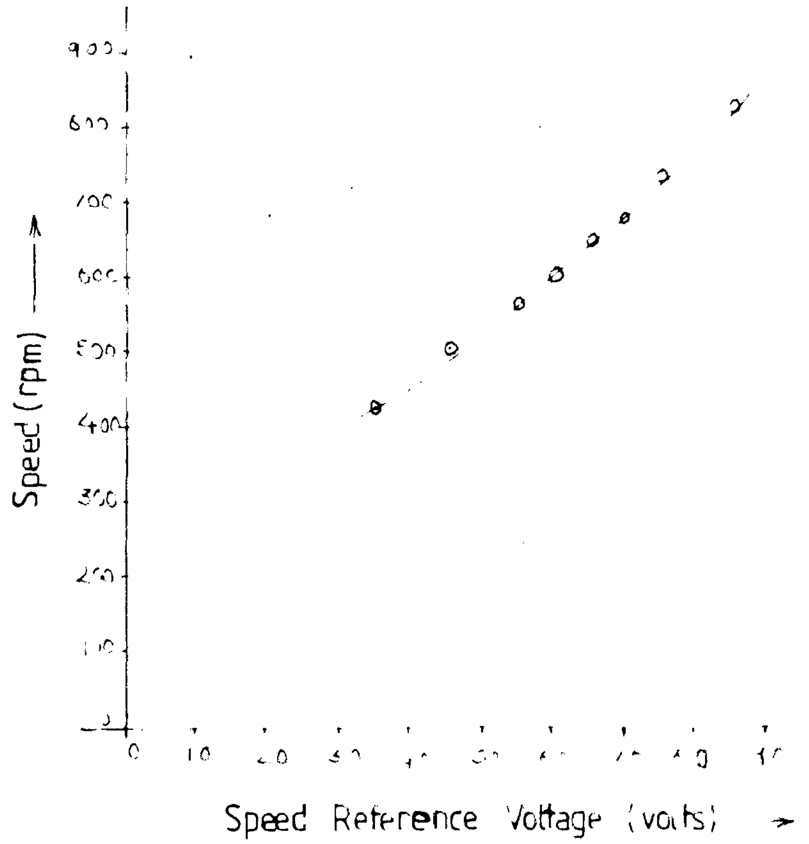

FIG.7.2 D.C. MOTOR SPEED CONTROL WITH SINGLE CONVERTER

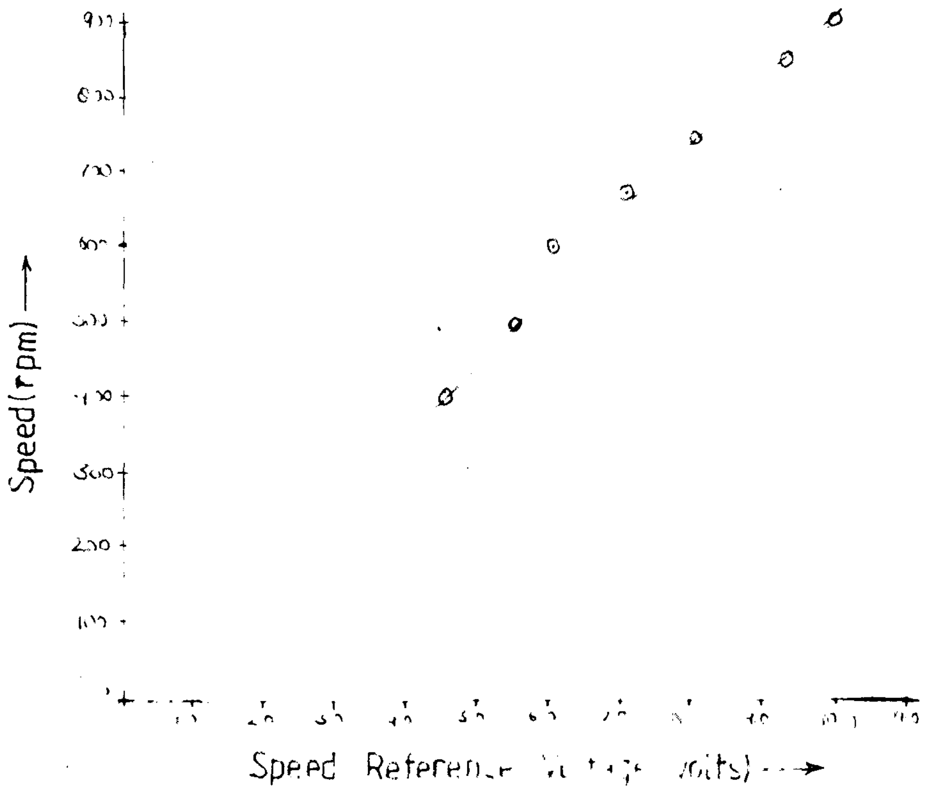

FIG.7.5 D.C MOTOR SPEED CONTROL WITH DUAL CONVERTER

Table 7.6 Speed Regulation of D.C. Motor With Load Variation

S.No.	Input Voltage (Volts)	Input Current (Amps)	Input Power (Watts)	Motor Armature Voltage (Volts)	Motor Armature Current (Amps)	Speed (rpm)	Load Voltage (Volts)	Load Current (Amps
1	300	4.6	880	268	4.6	946	196	2.6
2	300	4.8	920	266	4.8	943	192	2.7
3	300	5.0	1000	262	5.0	940	186	3.3
4	300	5.4	1060	260	5.4	938	164	4.1
5	300	6.2	1120	258	6.2	935	150	4.8

The speed is found to drop by small amount as the load is varied from low value to high value. The speed regulationi is found to be 1.16 %.

The transient response of drive system showing the effect of load variations are plotted theoretically and experimentally as shown in Fig. 7.7 and Fig. 7.8 respectively for 25 % and 50 % step decrease in load. The initial speed of the motor is held at 480 rpm. to obtain the plot. The point 'A' shows the instant of load variation. The initial speed of the motor is held at 480 rpm to obtain the plot. The results shows that such a step variation in load causes negligible variation in drive speed and the drive settles extremely fast.

The transient response of the drive system for step change in speed reference voltage is plotted both theoretically and

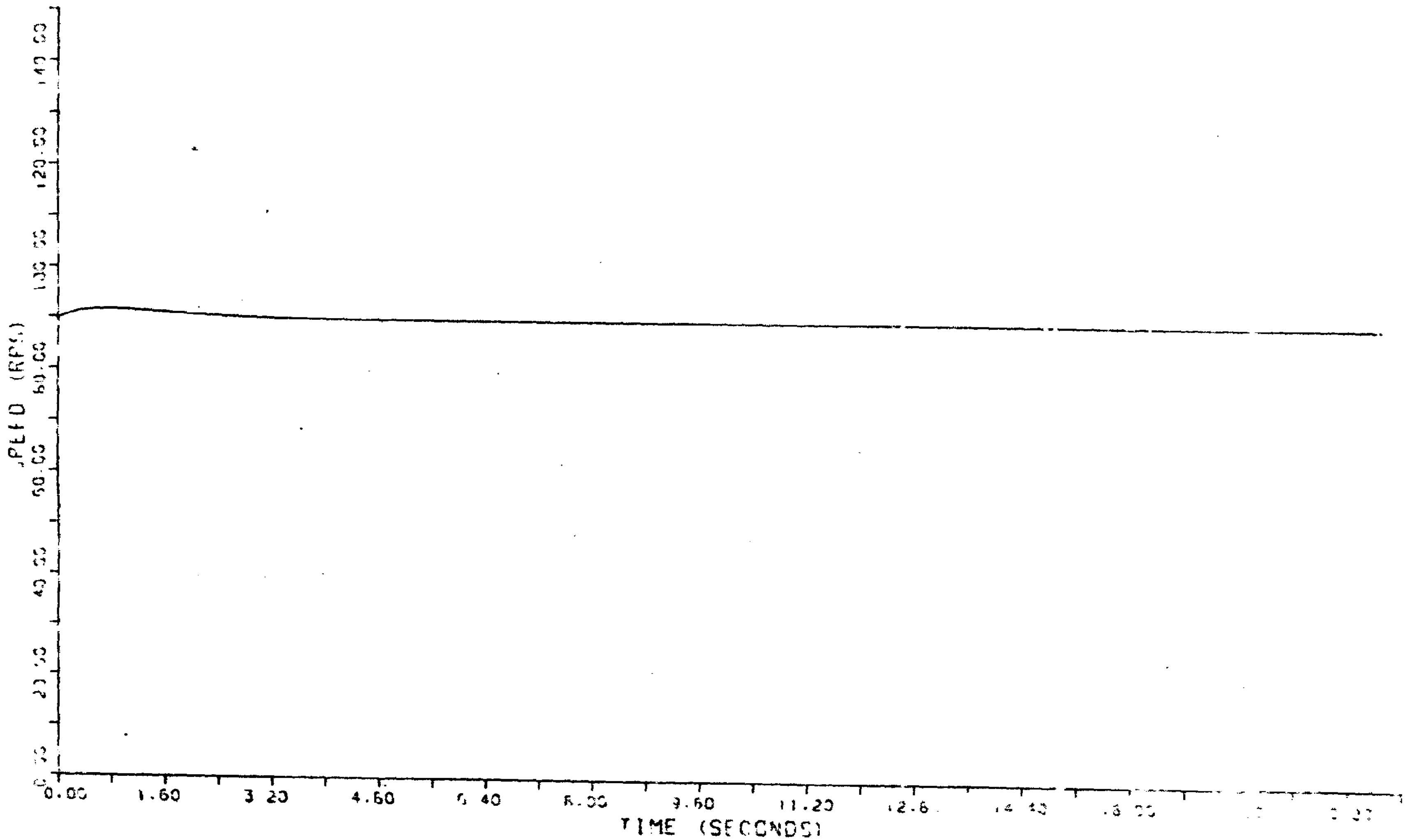

FIG. 7.7 (a) RESPONSE OF THE DRIVE FOR 25% DECREASE IN LOAD TORQUE

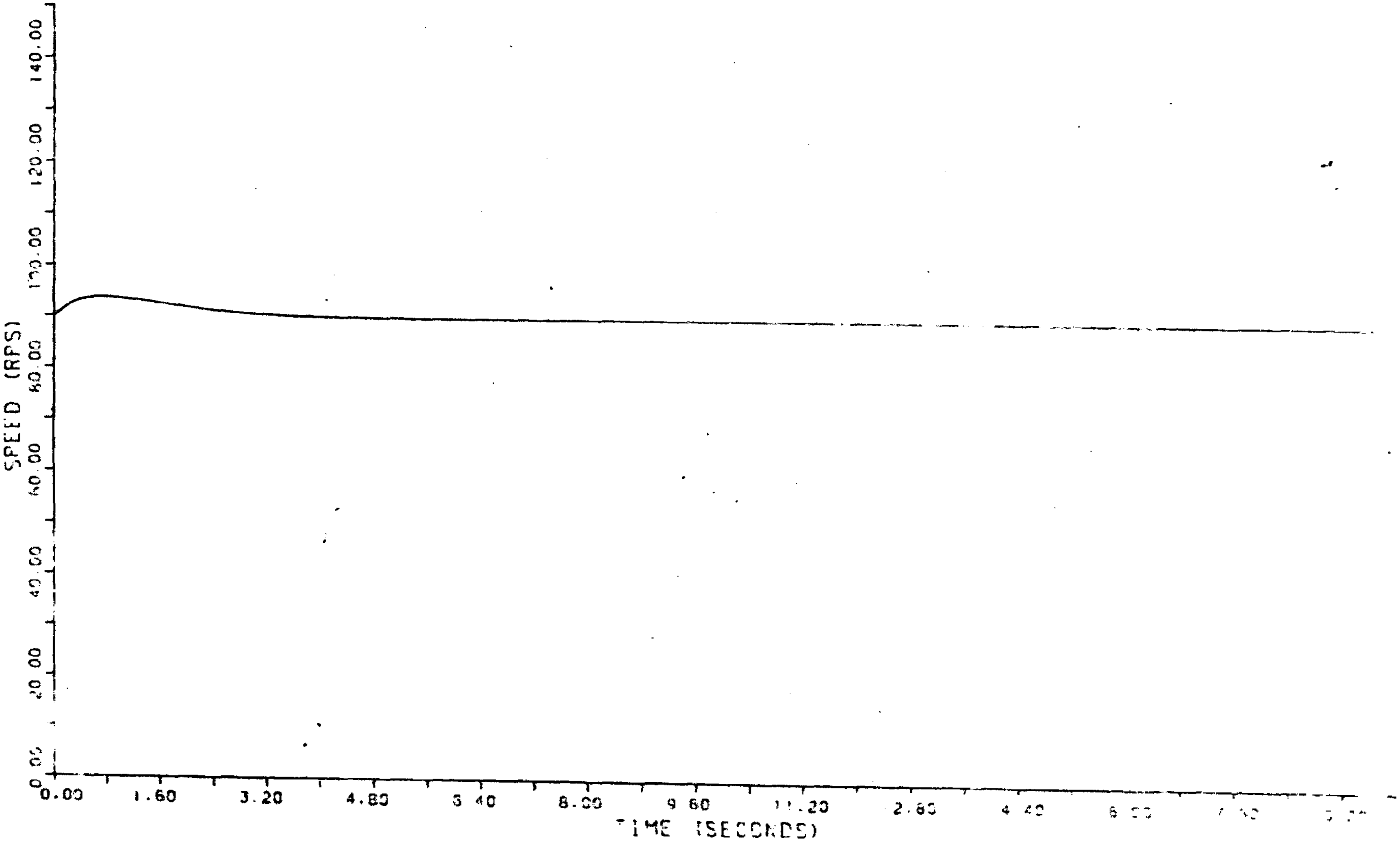

FIG. 27(b) RESPONSE OF THE DRIVE FOR 50% DECREASE IN LOAD TORQUE

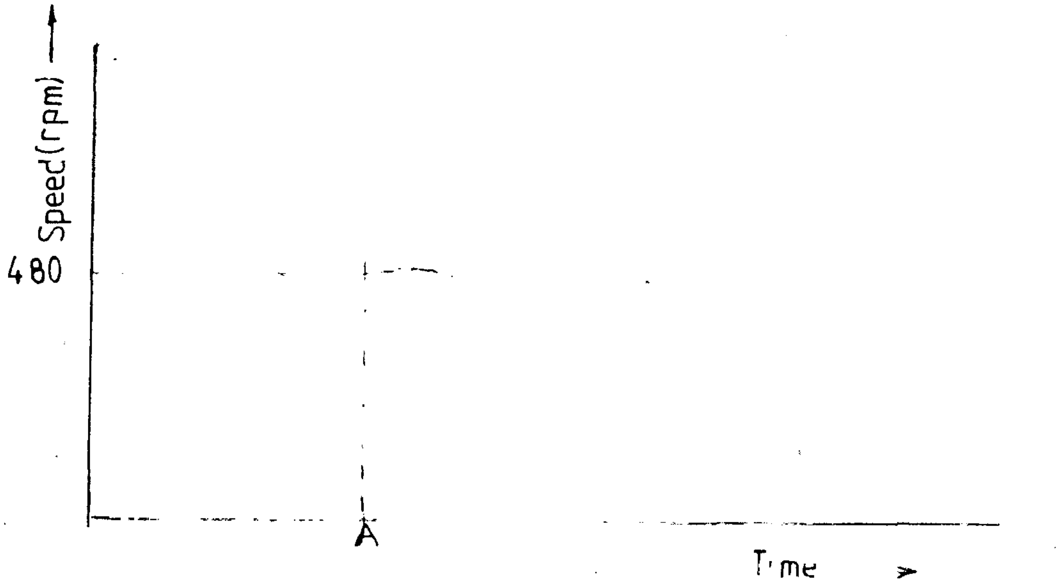

FIG. 7.8(a) RESPONSE OF DRIVE FOR 50 % DECREASE IN [illegible]

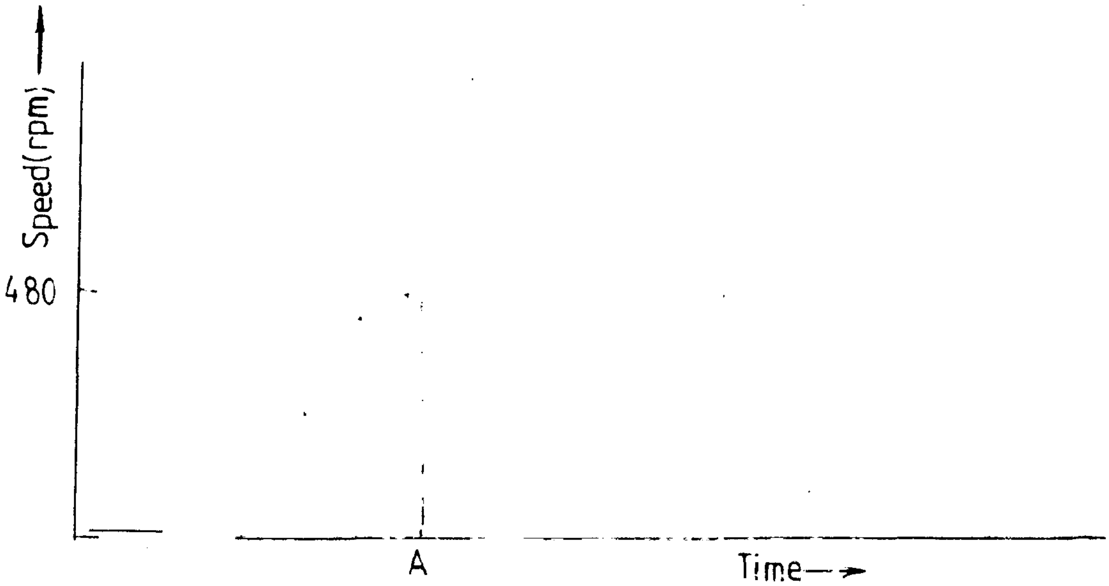

FIG. 7.8(b) RESPONSE OF DRIVE FOR 25 % DECREASE IN [illegible]

experimentally as shown in Fig. 7.9 and 7.10. The initial speed of the motor is held at 480 rpm and the speed is reduced to 300 rpm. It takes nearly 4 secs for the drive to settle to the new speed.

The transient response of the motor for change in speed reference voltage from full forward to full backward and full forward to half the backward are calculated theoretically and plotted as shown in Fig. 7.11 and Fig. 7.12. The author could not plot these responses experimentally because the tachogenerator available is a.c. tachogenerator, the output of which is to be rectified to get d.c. voltage and therefore, the change in direction of rotation will not change the direction of tachogenerator output voltage. The author could run the motor in open loop in both directions and found that by reversing the direction of speed reference voltage, motor changes its direction of rotation.

7.4 Conclusion

The performance of d.c. motor drive fed from the 1 - phase dual converter is investigated. The performance of converter both as a single converter and as dual converter is tested on resistive, inductive and motor load. The analytical and experimental results are compared. The motor takes nearly 5 secs at step reference speed input to reach 480 rpm. The speed of motor drops by a small amount with load variation and speed regulation is found to be 2 % order. The dual

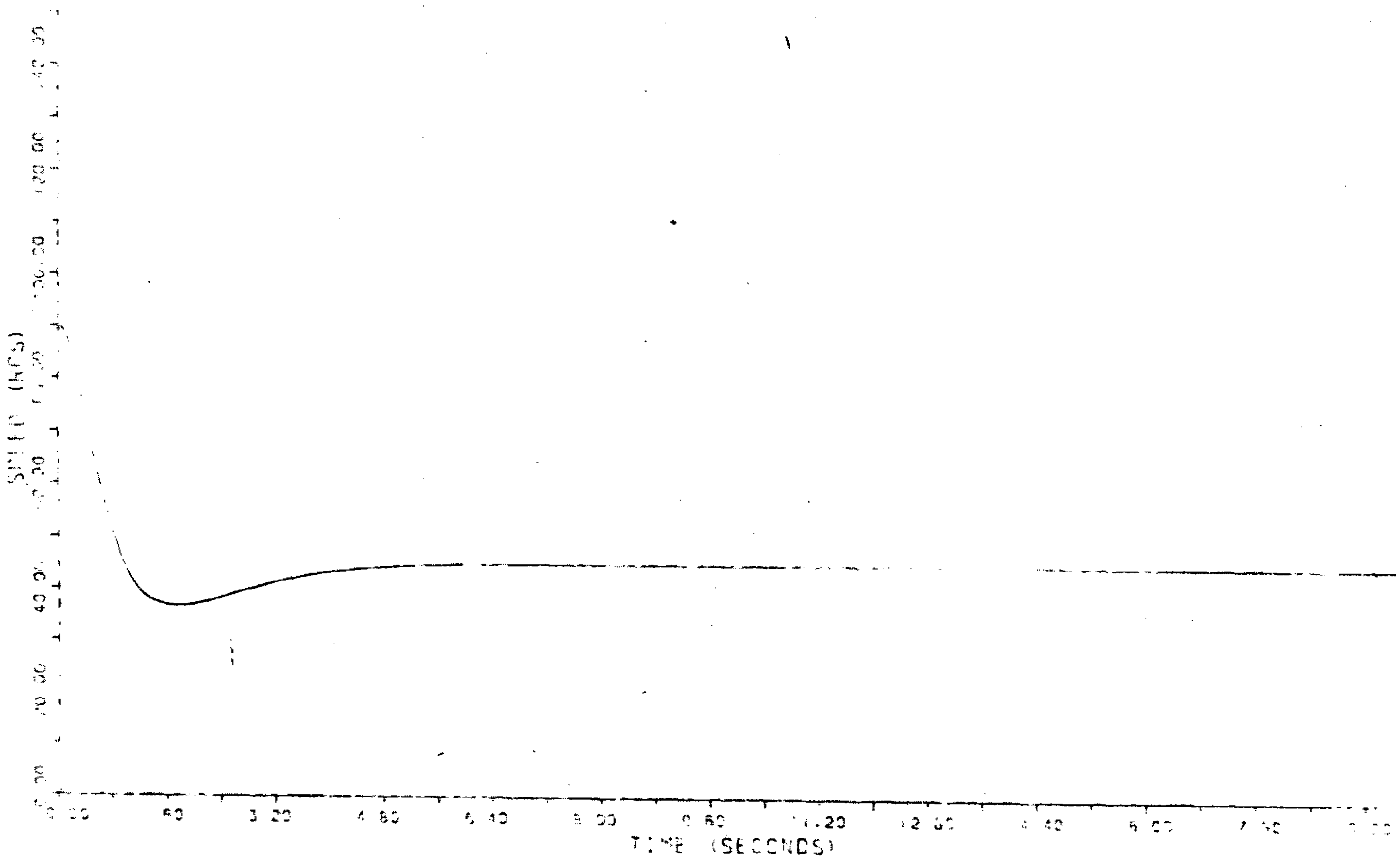

FIG 7.9 RESPONSE OF THE DRIVE FOR STEP CHANGE IN REFERENCE SPEED INPUT
FROM +VE MAX. TO HALF THE +VE MAX.

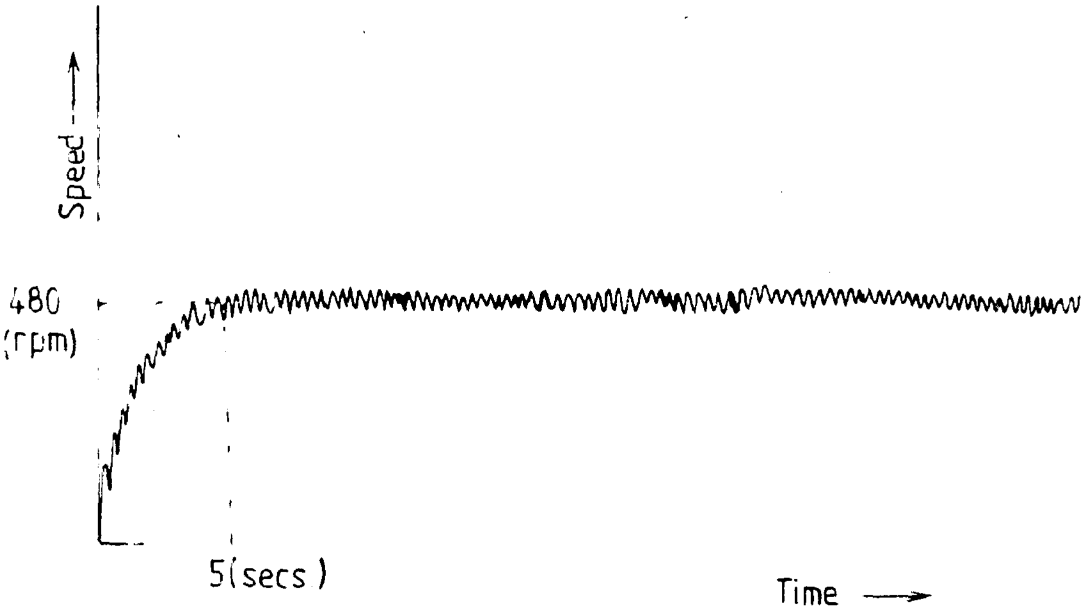

FIG.7.6 RESPONSE OF DRIVE FOR STEP REFERENCE SPEED VOLTAGE

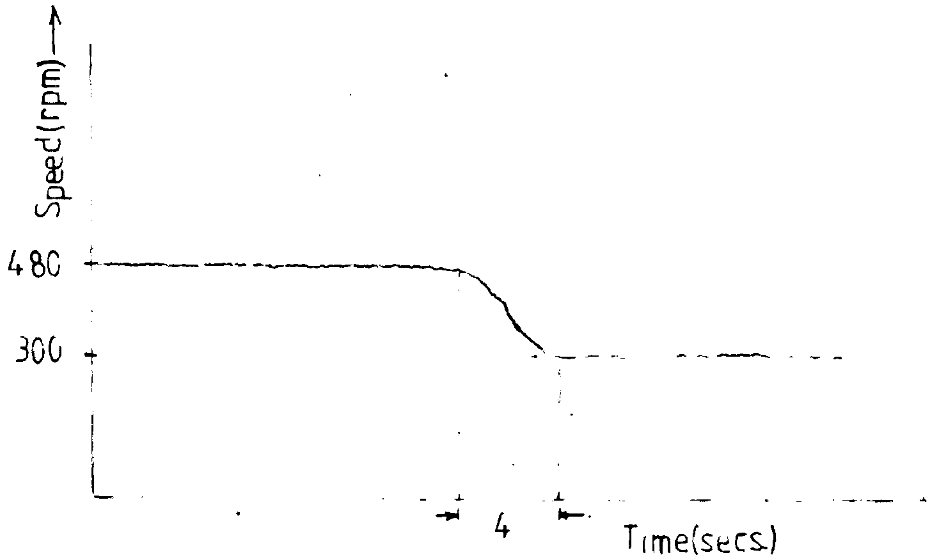

FIG.7.10 RESPONSE OF DRIVE FOR CHANGE IN REFERENCE SPEED VOLTAGE

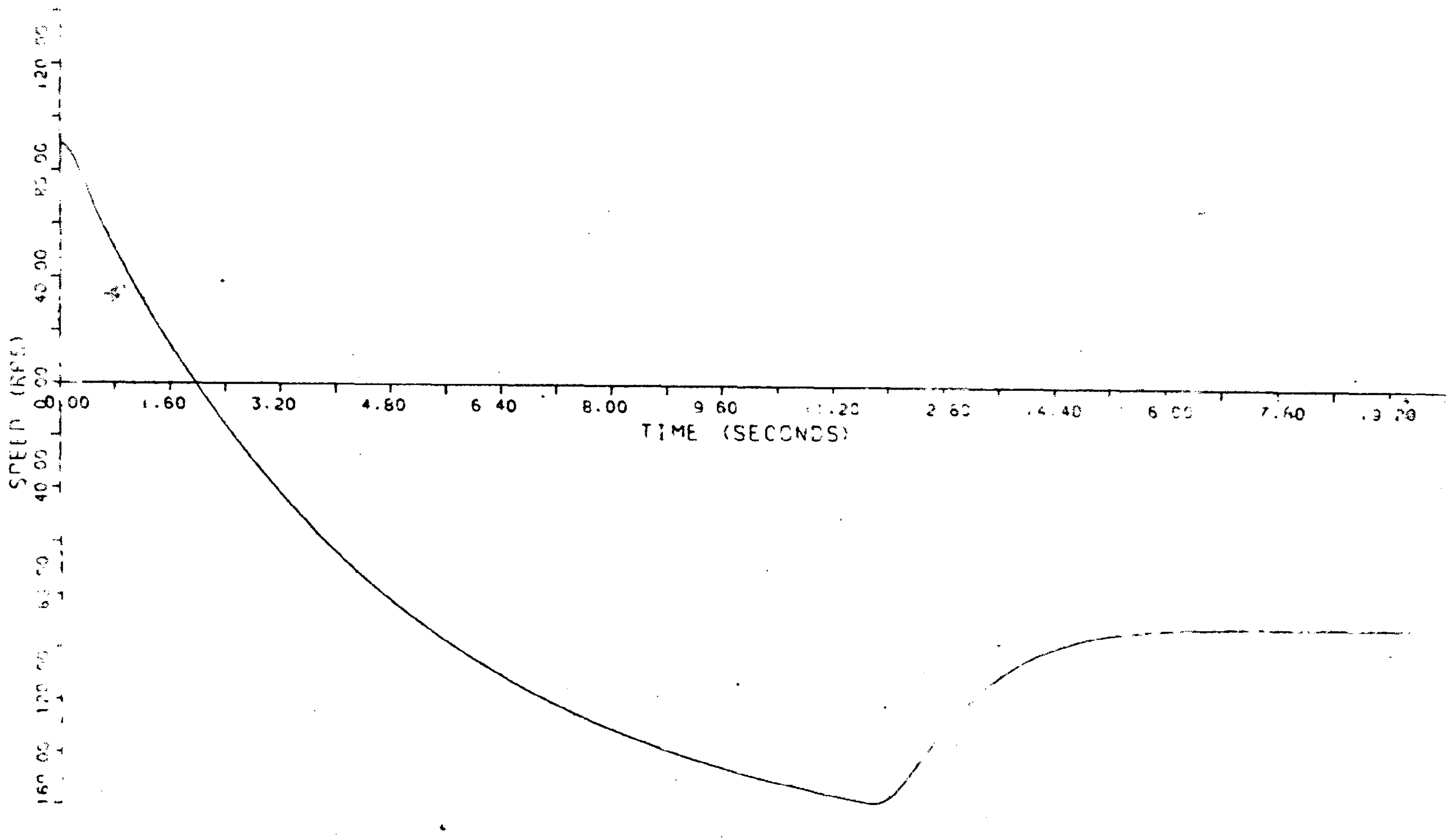

FIG. 7.11 RESPONSE OF THE DRIVE FOR STEP CHANGE IN REFERENCE SPEED INPUT FROM +VE MAX. TO -VE MAX.

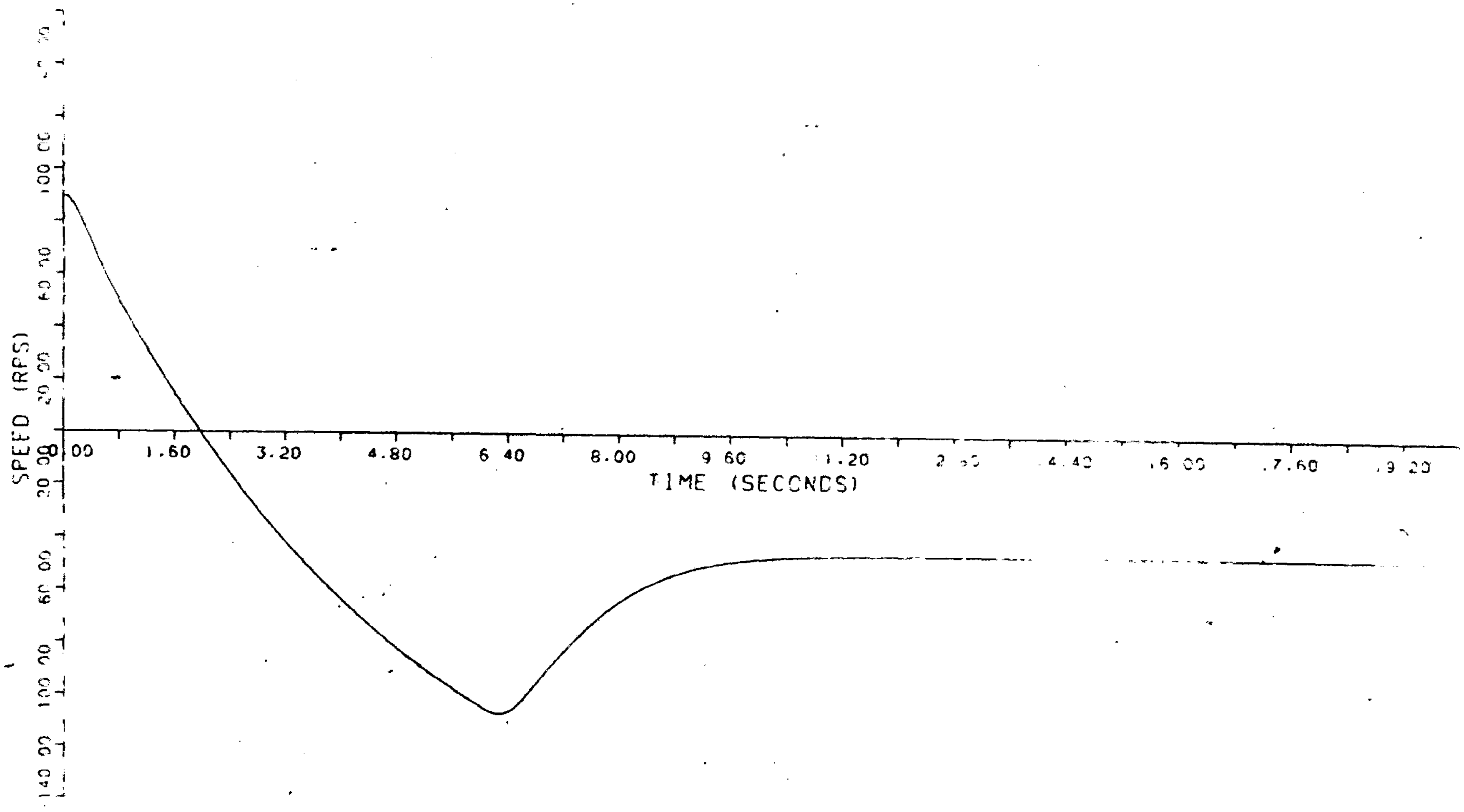

FIG. 7.12 RESPONSE OF THE DRIVE FOR STEP CHANGE IN REFERENCE SPEED INPUT FROM +VE MAX. TO HALF THE -VE MAX.

converter is capable of taking rated load. The motor takes nearly 4 secs for step change in speed reference voltage to change the speed from 480 rpm to 300 rpm. The dual converter is able to run the motor in both directions by reversing the speed reference voltage.

Chapter - 8

CONCLUSION

The design, fabrication and performance investigation of a 4-quadrant speed control of a dual converter fed separately excited d.c. motor has been discussed in this dissertation.

A dual converter consists of two similar fully controlled converters connected in antiparallel and the firing angles of both the converters are varied such that the sumofboth angles is equal to 180°. If one converter operates as a rectifier, then the other operates as inverter. The circulating current is limited to an accepted level using two reactor coils between two converters.

The cosine firing circuit consists of end stop pulse generator, comparator, differentiator, monostable multivibrator, oscillator and output complifiers to fire the thyristors. A ferrite core pulse transformer with two secondaries, is used for isolation between power and firing circuit.

Two proportional plus integral (PI) controllers are used, one as speed controller and other as current controller to provide a fast response. The inner current loop protects the thyristors and d.c. motor from over currents and also provides fast response. It also takes care of supply voltage variations. The current is sensed by means of a low resistance in series with the motor armature circuit. The speed is sensed by means of a tachogenerator mounted on the motor shaft.

In operation, the error between speed reference voltage and speed feedback voltage (V_R - V_ω) is integrated in speed (PI) controller. This automatically sets the current reference voltage and is compared with output of current feedback voltage V_i. The resulting error is integrated in current (PI) controller which is used as a control voltage and sets the firing angles of both the converters. Thr firing angle is controlled by controlling V_{c1}, the output voltage of current controller.

For design of controllers (gains and time constants), a mathematical model is made from the transfer functions of different elements i.e.d.c. motor, thyristor dual converter, current controller, speed controller and feedback transducers. First, the inner current loop is considered and the characteristic equation is derived. The current controller has a transfer function $K_1\ (1 + T_{c1}s)/T_{c1}s$. Its parameters gain K_1 and time constant T_{c1} are found out with the help of D-partition method and checked by frequency scanning technique for variation in σ and ξ to obtain the most stable region. The final selection of parameters are done after checking the response of the current loop at various points in the stable region using Ranga - Kutta method. For this, the state model of the current loop is derived. After determining, the value of K_1 and T_{c1}, a suitable current controller is designed and fabricated.

Next, the characteristic equation of the complete system is derived. The parameters of speed controller gain

K_2 and time constant T_{c2} having the transfer function

$$\frac{K_2(1+T_{c2}s)}{T_{c2}s}$$

are determined in a manner same as for the current controller gain and time constant. The state model of the complete system is also determined.

The complete fabrication of firing circuit, thyristorized dual converter , current controller and speed controller are done and the performance of the drive is investigated. The experiments are performed at resistive, inductive and motor load with converter working as a single connerter or dual converter.

It is evident from the experimental and analytical studies that the closed loop control provides good speed regulation. The speed of motor can be varied by varying the speed reference voltage and it can also run in both direction by reversing the speed reference voltage.

Scope For Further Work

Further work can be done on the following topics:

(i) While deriving the transfer function of thyristor converter the time delay in the firing current is approximated by a simple first order time lag to make the analysis simpler. It can be taken in transdental form which is more accurate.

(ii) A .d.c. tachogenerator can be used to study the 4-quadrant speed control of the d.c. drive.

(iii) The performance can be improved if the single-phase dual converter is replaced by three-phase converter because of various advantages The circulating current is less in case of 3 - ϕ dual converter and also both the converters are in continuous conduction both at no load and loaded condition.

REFERENCES

[1] Fitzgerald, A.E., Kingsley Jr., and Kusko, A.: 'Electric Machinery' (McGraw Hill Kogakusha Ltd., New Delhi 1971)

[2] Schieman, R.G., Wilkes, E.A., and Jordan, H.E.: 'Solid state control of electric drives', Proceedings of the IEEE, Vol. 62, No. 12, Dec. 1974, pp. 1643-1660

[3] Pisecker, H: 'Semiconductor converter for electric drives', Brown Boveri Review, Vol.53, No.10, 1966, pp.672-687

[4] Jacobs, A.P., and Walsh, G.W.: 'Application considerations for SCR drives and associated power system', IEEE Trans. IGA, Vol. 4, July/August 1968, pp. 396-404

[5] Robinson, C.E.: 'Redesign of d.c. motor application with thyristor power supply', IEEE Trans. IGA, Vol. 4, No. 5, Sept./Oct. 1968, pp. 508-514

[6] Arrilage, J., Hisha, H.: 'Fast ON/OFF detection of silicon controlled rectifier and its influence on converter controllability', IEEE Trans. IECI, Vol. 26, No. 1, Feb. 1972, pp.22-26

[7] Palanichamy, S., Subbiah, V.: 'Analysis of a inductance estimation for half controlled thyristor converters', IEEE Trans. IECI, Vol. 28, No. 3, August 1981, pp. 134 - 141

[8] Simard, R., and Raj Gopalan, V.: 'Economical equidistant pulse firing scheme for thyristor d.c. drives', IEEE Trans. IECI, Vol. 22, No. 3, 1975, pp. 425 - 429

[9] Franklin, P.W.: 'Theory of the d.c. motor controlled by power pulses Part I motor operation', IEEE Trans. PAS, Vol. 91, No. 1, Jan./Feb. 1972, pp. 249 - 253

[10] Black, K.G.: 'The effect of rectifier discontinuous current on motor performance', IEEE Trans. AI, Vol. 83, No. 70-75, Nov. 1964, pp. 377 - 382

[11] Farag, A.S.A., Malik, O.P., and Hope, G.S.: 'Studies on a SCR controlled variable speed d.c. shunt motor', IEEE Trans. IA, Feb. 1974, pp. 785 - 792

[12] Brill, J.M., and Rammamorthy, M.: 'Reverssible drive control for elevator doors - Part I', IEEE Trans., IECI, Vol. 22, No. 1, Feb. 1975, pp. 19 - 22

[13] Brill, J.M., and Rammamorthy, M.: 'Reverssible drive control for elevator doors - Part II', IEEE Trans. IECI, Vol. 22, No. 1, Feb. 1975, pp. 23 - 28

[14] Krishnan, T., and Ramaswami, B.: 'A fast response d.c. motor speed control system', IEEE Trans. IA, Vol. 10, No. 5, Sept./Oct. 1974, pp. 643 - 651

[15] Krishnan, T., and Ramaswani, B.: 'Speed control of d.c. motor using thyristor dual converter', IEEE

Trans. IECI, Vol. 23, No. 4, Nov. 1976, pp. 391 - 399

[16] Sen, P.C., and Mac Donald, M.: 'Thyristorized d.c. drives with regenerative braking and speed reversal', IEEE Trans. IECI, Vol. 25, No. 4, Nov. 1978, pp. 347 - 354

[17] Eswaramma, K., Hubli, S.S., and Sharma, P.S.: 'Speed control of d.c. motor by dual converter', IE (I) Journal EL, Vol. 63, August 1982, pp. 19 - 22

[18] Duff, D.L., and Ludbrook, A.: 'Reversing thyristor armature dual converter with logic crossover control', IEEE Trans. IGA, No. 3, 1963, pp. 216 - 222

[19] Revanker, G.N., and Subnis, D.S.: 'Analysis of dual converter system', IEEE Trans. IE (I), Vol. 22, No. 1, Feb. 1975, pp. 55 - 61

[20] Mittal, A.P., and Chatterjee, J.K.: 'Simple method for analysis of circulating current in dual converter operating with off set voltage control', IE (I) Journal-EL, Vol. 64, April 1984, pp. 233 - 240

[21] Srivastava, K.D., and Davies, R.M.: 'A note on the reverse parallel operation of rectifier bridges', Direct Current, Vol. 8, July 1963, pp. 202 - 204

[22] Joobs, G., and Barton, T.H.: 'Four quadrant d.c. variable speed drives Design consideration', Proceeding of IEEE, Vol. 63, No. 12, Dec. 1975, pp. 1660 - 1668

[23] Rice, J.B., and Nicker, L.E.: 'Commutation dv/dt effects in thyristor 3 - Ø bridge converters', IEEE Trans. IGA, Vol. 4, No. 6, Nov./Dec. 1966, pp. 665 - 672

[24] Zwicky, R.: 'Modern development in electric drives', Brown Boveri Review, May/June 1967, pp. 21 - 212

[25] Tyristors Data Book, Vol. 1, Electronics Information Series, 1977

[26] Sen, P.C.: 'Thyristor D.C. Drives' (Wiley, New - York 1981)

[27] Pelly, B.R.: 'Thyristor Phase Controlled Converters and Cycloconverters - Operation, Control and Performance' (Wiley - INTESCIENCE, New York 1971)

[28] Duncan, N.J., and Wilson, D.R.: 'Modern Practice in Servo Design', (Per-gamon Press, Oxford 1970)

[29] Aizerman, M.A.: 'Theory of Automatic Control' (Pergamon Press, New York 1963)

[30] Meerov, M.V.: 'Introduction to Dynamics of Automatic Regulating of Electrical Machines', (London, Butter-worths 1961)

[31] Siljack, D.D.: 'Non-Linear Systems: The Parameter Analysis and Design', (John Wiley and Sons, Inc., U.S.A. 1969)

[32] Anand, M.M.S., and Jain R.P.: 'Digital Electronics Practice Using Integrated Circuits' (Tata - McGraw Hill. Publishing Company Ltd., New Delhi, 1983)

[33] Berde, M.S.: 'Thyristor Engineering', (Khanna Publishers, Delhi 1978)

[34] Malvino, A.P.: 'Electronic Principles', (Tata Mc Grow Hill, New Delhi 1983)

[35] Sharma, M.C.: '555 Timer and its Applications', (Business Promotion Publication, Delhi 1978)

[36] Saraswat, R.K.: 'A Thyristorized Closed Loop D.C. Motor Drive', Thesis, M.E., Electrical Engineering Department, University of Roorkee, Roorkee 1979.

APPENDIX - A

PARAMETER PLANE SYNTHESIS METHOD

A process is said to be stable if for any small initial deviations, the equilibrium is restored to the control system as a result of the action of the controller, and the process is said to be unstable if the controller does not restore operating state which existed in the system before the appearance of these initial deviations. In the case of linear model, if it is stable for small disturbances then it is stable with respect to any other disturbance. The necessary and sufficient condition for the stability of the control process in its linear approximation (i.e. in the case when the process is described by a set of linear differential equations) is that all the real roots of the characteristic equation be negative and all complex roots have a negative real part.

Usually the techniques employed for studying the stability have been the Routh - Hurwitz's criterion, Nyquist method and Root locus method. These methods have been successfully used to study the effect of only one parameter of the control system on the system performance. An improvement over the above methods is the D-partition method. This method was presented first by Neimark in 1948. This method can be used to study the effect of two parameters of the control system on stability and transient performance.

With regard to stability analysis, the method provides a possibility of defining the relative stability of control system as the numbers of roots of characteristic equation relative to a specified s-plane contour of a general shape. The plane with the two adjustable parameters as coordinate axes is termed as 'Parameter Plane'. The parameter plane method can also be extended in case of non-linear and sample data system.

Parameter Mapping

The idea of system design is to obtain a simple correlation between the system parameters and the characteristic roots so that the roots can be set at a desired location by adjusting the system parameters. This can be done by parameter plane synthesis method.

The parameter plane method is based on a mapping procedure that transform points from the complex $s(\sigma, \omega)$ plane on to the parameter α–β plane. In the general case, the mapping function is an n^{th} degree algebric equation

$$F(s) = \sum_{k=0}^{n} a_k s^k = 0$$

where s is the complex variable defined by

$$s = -\sigma + j\omega_d,$$

and a_k are the coefficients that are functions of two real parameters α and β i.e.

$$a_k = a_k(\alpha, \beta), \quad k = 0, 1, 2, \ldots\ldots, n$$

If to a given pair of number (σ_1, ω_{d1}) there corresponds a pair of number (α_1, β_1) so that mapping equation $F(s) = 0$ is satisfied, then for α_1 and β_1, the equation has a root pair $s_1 = -\sigma_1 \pm j\omega_{d1}$. Therefore, the defined mapping can be regarded as a transformation of the points (σ, ω_d) for the complex s-plane, which represents root values of the algebraic equation $F(s) = 0$, to certain points of parameter $\alpha - \beta$ plane. This is referred to as parameter mapping. The same theory is also applicable for $s = -\xi\omega_n \pm j\omega_n\sqrt{1-\xi^2}$ in (ξ, ω_n) plane.

Now, considering the case when two parameters α and β enter into the characteristic equation linearly so that the characteristic equation can be reduced to the form,

$$F(s) = \alpha S(s) + \beta Q(s) + R(s) = 0 \qquad \text{...(A.1)}$$

Substituting $s = -\sigma+j\omega_d$ in equation (A.1) and separating real and imaginary parts, results in following equation.

$$\alpha S(-\sigma+j\omega_d)+\beta Q(-\sigma+j\omega_d)+R(-\sigma+j\omega_d) = 0$$

or $$u(\sigma, \omega_d, \alpha, \beta) + jv(\sigma, \omega_d, \alpha, \beta) = 0 \qquad \text{...(A.2)}$$

In order to construct the boundary of the D-partition it is necessary to determine α and β for each ω_d by solving simultaneously the two equations:

$$u(\sigma, \omega_d, \alpha, \beta) = 0 \qquad \text{...(A.3)}$$

$$v(\sigma, \omega_d, \alpha, \beta) = 0 \qquad \text{...(A.4)}$$

Separating terms containing α and β results in following two equations:

$$u(\sigma,\omega_d,\alpha,\beta) = \alpha S_1(\sigma,\omega_d) + \beta Q_1(\sigma,\omega_d) + R_1(\sigma,\omega_d) = 0 \quad \ldots (A.5)$$

$$v(\sigma,\omega_d,\alpha,\beta) = \alpha S_2(\sigma,\omega_d) + \beta Q_2(\sigma,\omega_d) + R_2(\sigma,\omega_d) = 0 \quad \ldots (A.6)$$

Solving equations (A.5) and(A.6) with respect of α and β for each ω_d give

$$\alpha = \frac{\begin{vmatrix} -R_1 & Q_1 \\ -R_2 & Q_2 \end{vmatrix}}{\begin{vmatrix} S_1 & Q_1 \\ S_2 & Q_2 \end{vmatrix}} = \frac{Q_1 R_2 - Q_2 R_1}{S_1 Q_2 - S_2 Q_1} \quad \ldots (A.7)$$

$$\beta = \frac{\begin{vmatrix} S_1 & -R_1 \\ S_2 & -R_2 \end{vmatrix}}{\begin{vmatrix} S_1 & Q_1 \\ S_2 & Q_2 \end{vmatrix}} = \frac{S_2 R_1 - S_1 R_2}{S_1 Q_2 - S_2 Q_1} \quad \ldots (A.8)$$

The equations (A.5) and (A.6) determine one value of α and one value β as given by equations (A.7) and (A.8) for each ω_d, only when these equations are simultaneous and independent.

If for some value of ω_d, say ω_c, the numerator and denominator becomes zero, then for this value of ω_d, the two equations (A.5) and (A.6) are linearly dependent to each other and a straight line is obtained instead of a point in the α - β plane, known as spatial line. In this case, either of the equations (A.5) or (A.6) is the equation of the straight line when this value of ω_d is substituted. If the coefficient of the highest term of the characteristic equation depends on the parameter α and β, then by equating this coefficient to zero spatial line at $\omega_d = \infty$ is obtained. Similarly, a spatial line at $\omega_d = 0$ is obtained by equating the coefficient of the lowest (free) term of the characteristic equation to zero.

In order to find the number of roots in the various region obtained in the parameter plane by the plotted boundaries it is necessary to know whether a root is leaving or entering the s-plane contour as shown in Figs. (A.1),(A.2), (A.3) at the instant that point goes over a boundary in the parameter plane. In order to know whether the roots are leaving or entering the s-plane contour; the boundary curves should be appropriately shaded. The side of the boundary to be shaded is determined according to sign of the denominator Δ where $\Delta = \begin{vmatrix} S_1 & Q_1 \\ S_2 & Q_2 \end{vmatrix}$. Facing the direction in which ω_d is increasing the boundary curves in the α - β plane are shaded on the left side if $\Delta > 0$ and on the right side if $\Delta < 0$. Usually, the curve is traversed twice, once when ω_d goes from $-\infty$ to 0 and next when it changes from 0 to $+\infty$. It is shaded both the times on the same side, as the sign of Δ changes with change in sign of ω_d (Δ is an odd function of ω_d). After the complex root boundaries are shaded, the

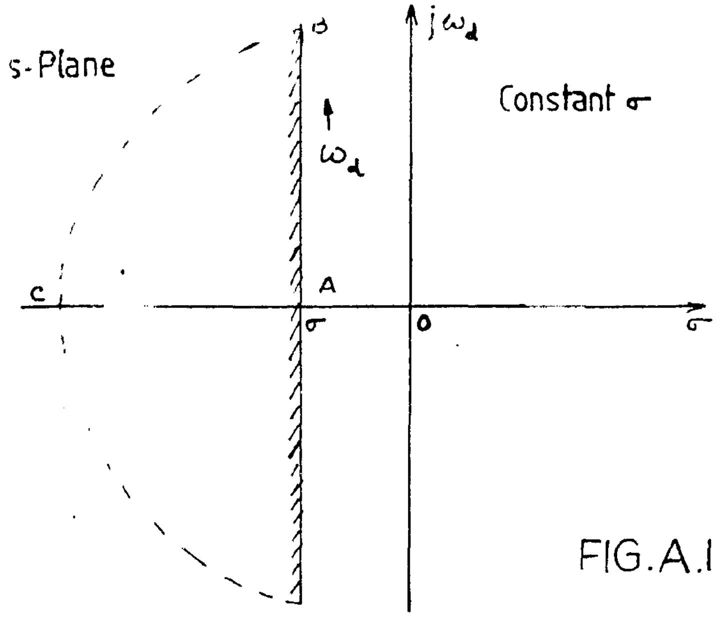

FIG.A.1

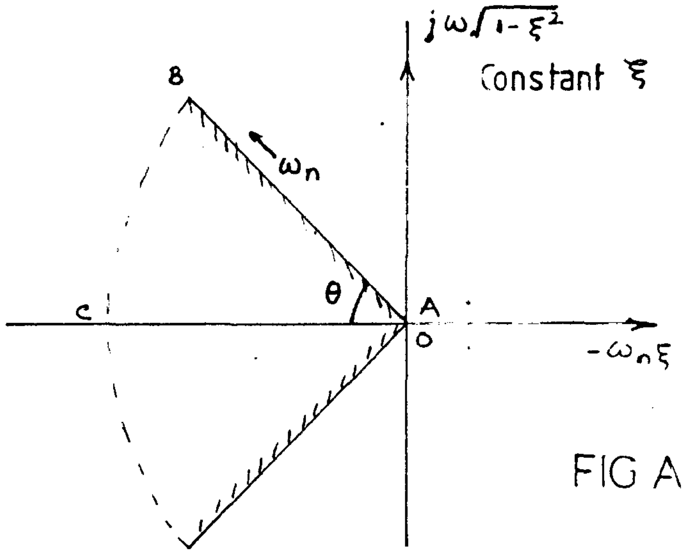

FIG A.2

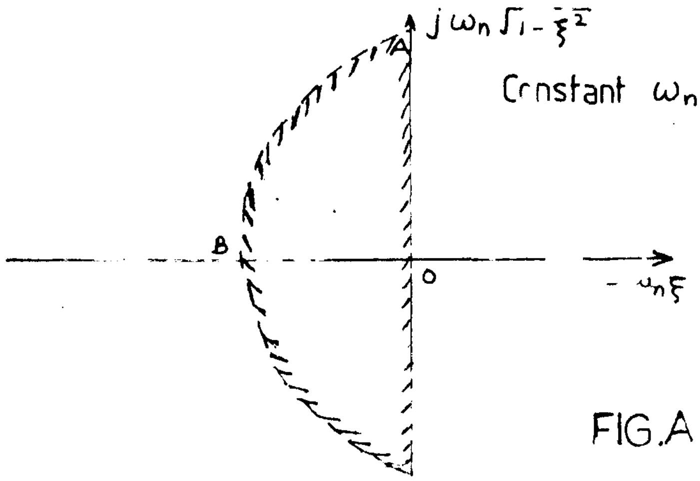

FIG.A.3

S-PLANE CONTOURS

spatial lines (for $\omega_d \neq 0$ or ∞) are simply oriented in accordance with the shading of complex boundaries. The shading of such a spatial line must be done twice on the same side as that on the complex root boundary at their point of intersection. The spatial lines at $\omega_d = 0$ and $\omega_d = \infty$ are also shaded with this rule but they are shaded only once. The root leaves the contour if it goes from a shaded region to the unshaded region and enters the contour if it goes from unshaded to shaded region. After the boundaries are appropriately shaded, the relative number of roots in each bounded region is easily determined. For doing this, firstly the region with maximum values of roots on the left side in the s-plane is established by inspection of the plot. For ascertaining stable region a point in the region with maximum number of roots is selected and the stability of the system is checked by the Frequency Scanning Technique. If the system is stable at this point then this entire enclosed region is also a stable region.

Frequency Scanning Technique (The Mikhailov Criterion)

A system is said stable, provided its characteristic equation

$$F(s) = a_0 s^n + a_1 s^{n-1} + \ldots\ldots + a_n = 0 \qquad \ldots(A.9)$$

where, $s = j\omega$

satisfies the following conditions:

(i) $F(j\omega) \neq 0$ at $\omega = 0$ i.e. $a_n \neq 0$

(ii) The locus of the end points of the vector $F(j\omega)$, when ω varies from 0 to ∞, traverses in succession by 'n' quadrants in anti-clock wise manner for an equation of n^{th} order.

Let the roots of the equation (A.9) be $z_1, z_2, \ldots z_n$. then provided $a_o = 1$, equation (A.9) can be expressed in the form

$$F(s) = (s-z_1)(s-z_2) \ldots (s-z_n)$$

Substituting $s = j\omega$

$$F(j\omega) = (j\omega-z_1)(j\omega-z_2) \ldots \ldots (j\omega-z_n)$$

$F(j\omega)$ constitutes a vector whose modulus is equal to the product of the moduli of all the vectorial factors and whose argument is equal to the sum of the arguments of all the vectorial factors.

At $\omega = 0$, the vector $F(j\omega)$ has a pure real value, $F(0)$ with its arguments equal to zero. As ω is varied from 0 to ∞, the angle of term associated with a real root changes by $\pi/2$, and for each pair of conjugate roots by π. Consequently for an n^{th} order equation, if all the roots lie on the left hand side of imaginary axis, the total angle by which $F(j\omega)$ changes is equal to $n(\pi/2)$.

APPENDIX - B

B.1 Measurement of D.C. Machine Parameters

The armature resistance R_a of motor is measured by D.C. voltmeter-ammeter method and is found to be 6.44 ohms. The impedance Z_a of the armature is measured at a.c. supply frequency by voltmeter-ammeter method and is found to be 44.67 ohms. Therefore, armature inductances is 0.140 H. The back emf constant K_b of the motor is obtained by running the machine as a generator at constant field current and is found to be 1.939 Volts/rad/sec.

The d.c. motor is loaded by means of a d.c. generator (with field excitation constant) supplying a fixed resistor. Therefore, the load torque T_L is propotional to the speed ω_m and the proportionality constant B is defined by the equation

$$T_L = B\ \omega_m$$

The viscous friction only increases this proportionality constant. For the operating condition used, this proportionality constant (viscous friction constant included in load on the motor) is determined experimentally and is found to be 0.0799 Nw-m/rad/sec.

The moment of inertia of the machine together with load generator is determined by the Retardation or Running down test method. In this method, the machine is run slightly above the rated speed and then supply is cut-off from the armature. Consequently the armature slows down and its kinetic energy is used to meet rotational losses i.e. friction, windage and iron loss.

$$\text{Loss due to rotation } P = \frac{d}{dt}(K.E.)$$

$$= \frac{d}{dt}\left(\tfrac{1}{2}J\omega_m^2\right)$$

$$= J\omega_m \frac{d\omega_m}{dt}$$

Since $\omega_m = 2\pi n/60$, n is motor speed in rev/min.

$$\text{and } \frac{d\omega_m}{dt} = \frac{2\pi}{60}\,\frac{dn}{dt}$$

$$\therefore\ P = \left(\frac{2\pi}{60}\right)^2 J\,n\,\frac{dn}{dt} = 0.0109\ J\,n\,\frac{dn}{dt}$$

For calculating P, a curve between n and t is determined.

$$\text{Average load current during retardation } I_a = \frac{1.8+1.7}{2}$$

$$= 1.75\ A$$

The time is measured for approximately 5 % drop in speed i.e. from 210 V to 200 V variation in the armature voltage at fixed field excitation. The tests give following readings:

(a) Without additional load $t = 0.3$ sec

(b) With additional load $t' = 0.2$ sec

$$\text{Rotational losses } P = P' \times \frac{t'}{t-t'}$$

where, P' = losse due to additional load

$$\therefore P = P' \times \frac{0.2}{0.3-0.2} = 2P'$$

Average voltage during retsrdation test $= \frac{210+200}{2}$

$= 205$ V

also $P' = I_a V$

$= 1.75 \times 205 = 358.75$ watts

$\therefore$ $P = 2 \times 358.75 = 717.5$ watts

For determination of $\frac{dn}{dt}$, a graph is plotted between armature voltage (proportionally to speed) as a function of time as shown in Fig. B.1.

The speed of the motor $n = 1050$ rpm

Since 220 V corresponds to 1080 rpm, hence 1 V corresponds to 4.909 rpm.

From graph,

$$\frac{dn}{dt} = \frac{4 \times 4.909}{0.1} = 196.36 \text{ rpm/sec}$$

$$\therefore J = \frac{P}{0.0109\, n\, (dn/dt)}$$

$$= \frac{717.5}{0.0109 \times 1050 \times 196.36}$$

$$= 0.3192 \text{ Kg-m}^2$$

The mechanical time constant $_m = \frac{JR_a}{K_b^2}$

$$= \frac{0.3192 \times 6.44}{(1.939)^2} = 0.546 \text{ sec}$$

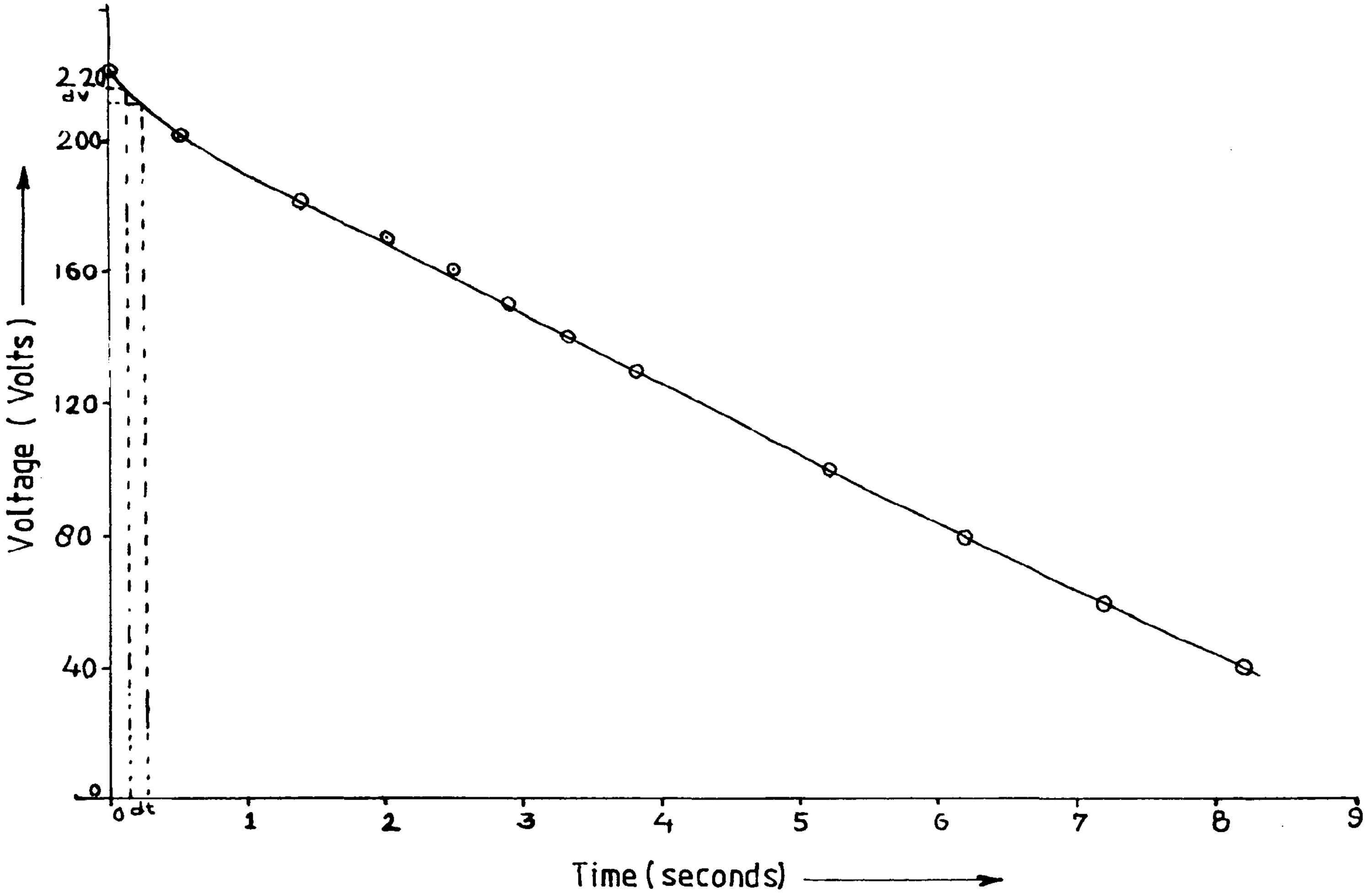

FIG. B.1 DETERMINATION OF $d\omega/dt$

Electrical time constant $_a$ is found to to 0.022 sec or 22 msec.

B.2 Measurement of Transducers Gain

(A) Speed Transducer

The tachogenerator mounted on the motor shaft provides the speed feedback signal. The gain V_ω/ω is found experimentally from its definition:

Speed		Tachogenerator voltage output
rpm	rad/sec	Volts
1020	106.81	11.5
970	101.58	11.0
880	92.15	10.0
815	85.38	9.0
740	77.49	8.5

A graph is plotted between speed and Tachogenerator output voltage as shown in Fig. B.2. The slope of the curve gives the gain H_ω.

$$H_\omega = \frac{V_\omega}{\omega_m} = \frac{11.0 - 10.0}{9.43} \text{ V/rad/sec}$$

$$= 0.1060 \text{ volts/rad/sec}$$

Filter time constant = 55 msec

(B) Current Transducer

The gain of current transducer is V_i/I_a and is found from an experiment based on the definition of the gain:

Armature Current (amps)	Output Voltage of current Transducer (volts)
1.45	0.75
2.5	1.45
4.1	2.15
5.5	3.0
6.8	3.6
8.1	4.4
9.4	5.0

A graph is plotted between V_i and I_a as shown in Fig. B.3. The slope of the curve gives the gain H_i.

$$H_i = \frac{V_i}{I_a} = \frac{4.3 - 1.6}{8-3} \text{ V/amp}$$

$$= 0.54 \text{ V/amp}$$

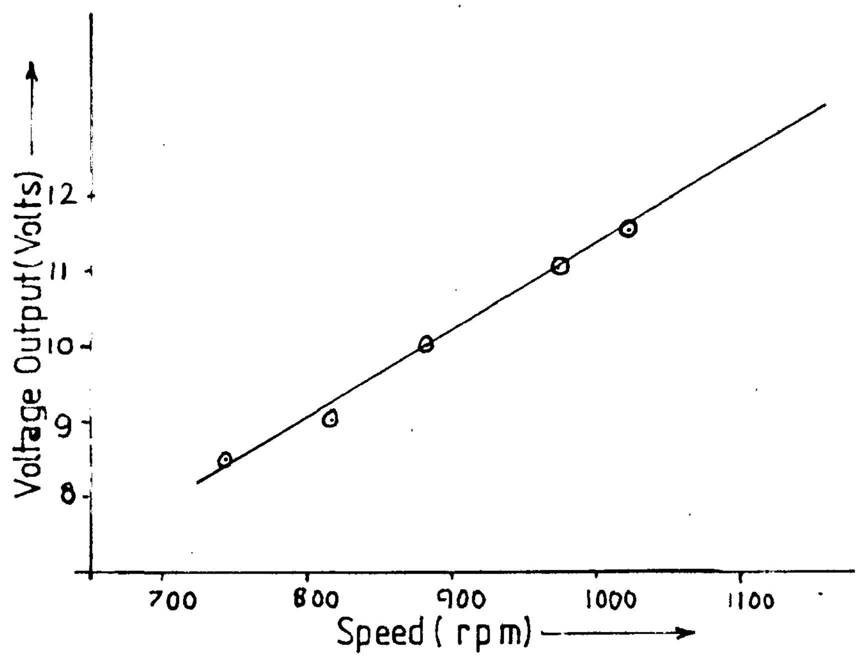

FIG. B.2 TACHO-GENERATOR VOLTAGE VS SPEED

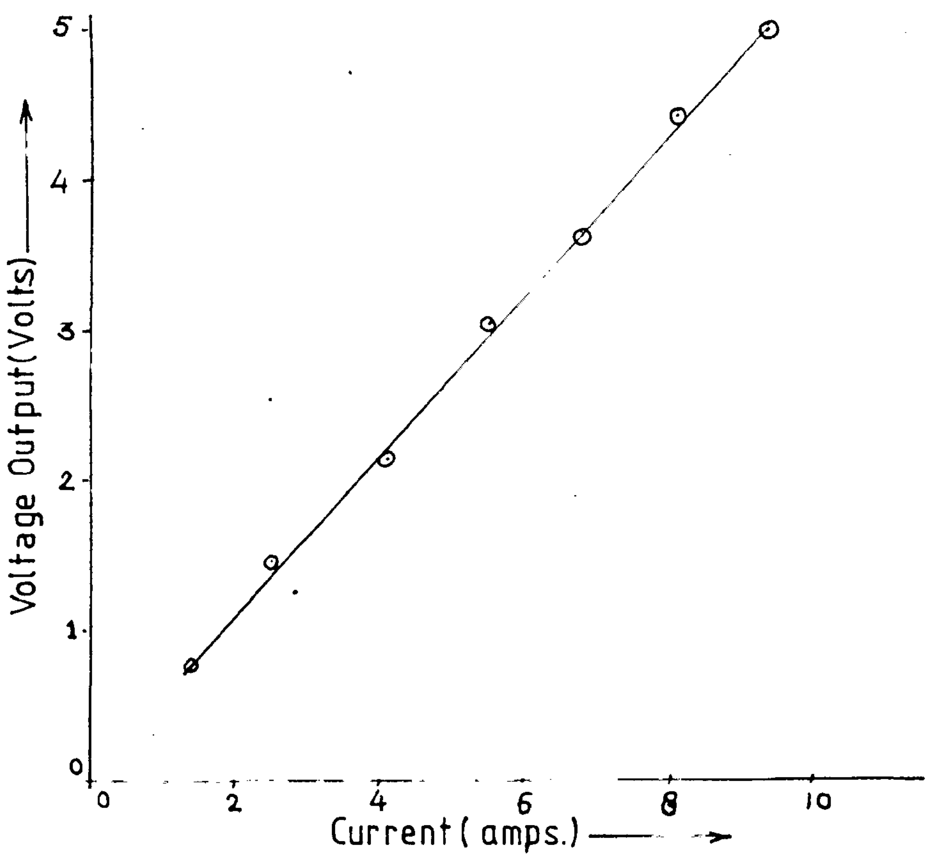

FIG. B.3 DETERMINATION OF CURRENT TRANSDUCER GAIN

APPENDIX - C

DESCRIPTION OF I.C. CHIPS

C.1 IC741

It is a 8 pin integrated circuit. Pins 1, 5 and 8 are used for compensation. Pin 2 is inverting terminal and pin 3 is non-inverting terminal. Pins 4 and 7 are for supply. Pin 7 is for + ve supply and pin 4 is for -ve supply. Pin 6 is for output. The pin connection is shown in Fig. C.1.

C.2 IC74121

It is a 14 pin integrated circuit. The functional diagram and function table of the commonly used one-shot TTL IC74121 are given in Fig. C.2.

C.3 IC555

The 555 IC timer is a very popular and versatile integrated circuit which can be used as an oscillator, pulse generator, ramp generator, voltage controlled oscillator, frequency divider, etc. The internal structure of the timer is shown in Fig. C.3.

C.4 IC7408

It is a 14 pin Quad 2-input AND Gate. The pin connection is shown in Fig. C.4.

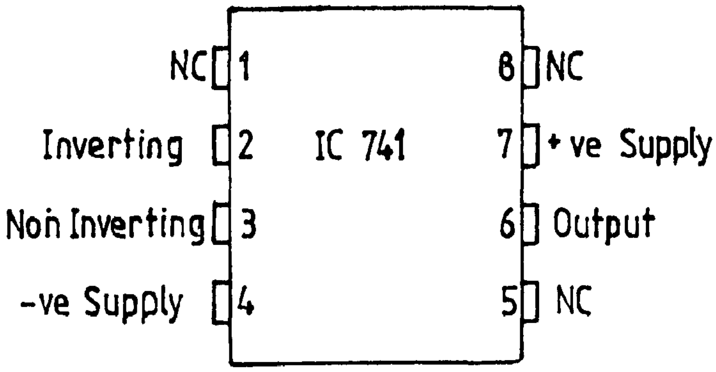

FIG. C.1 OPERATIONAL AMPLIFIER

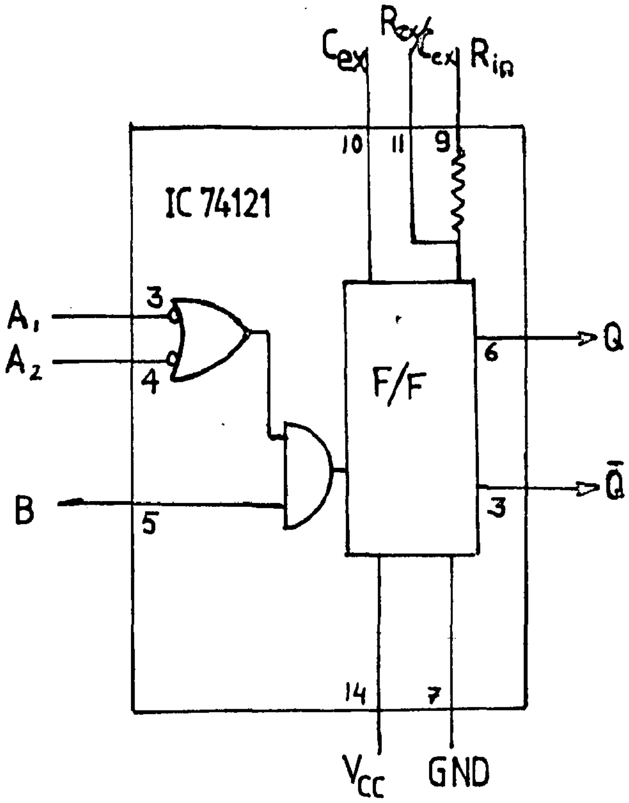

Table C.1

Inputs			Output	
A_1	A_2	B	Q	$\bar{Q}$
0	X	1	0	1
X	0	1	0	1
X	X	0	0	1
1	1	X	0	1
1	↓	1	⊓	⊔
↓	1	1	⊓	⊔
0	X	↑	⊓	⊔
X	0	↑	⊓	⊔
↓	↓	1	⊓	⊔

FIG. C.2 MONOSTABLE MULTIVIBRATOR

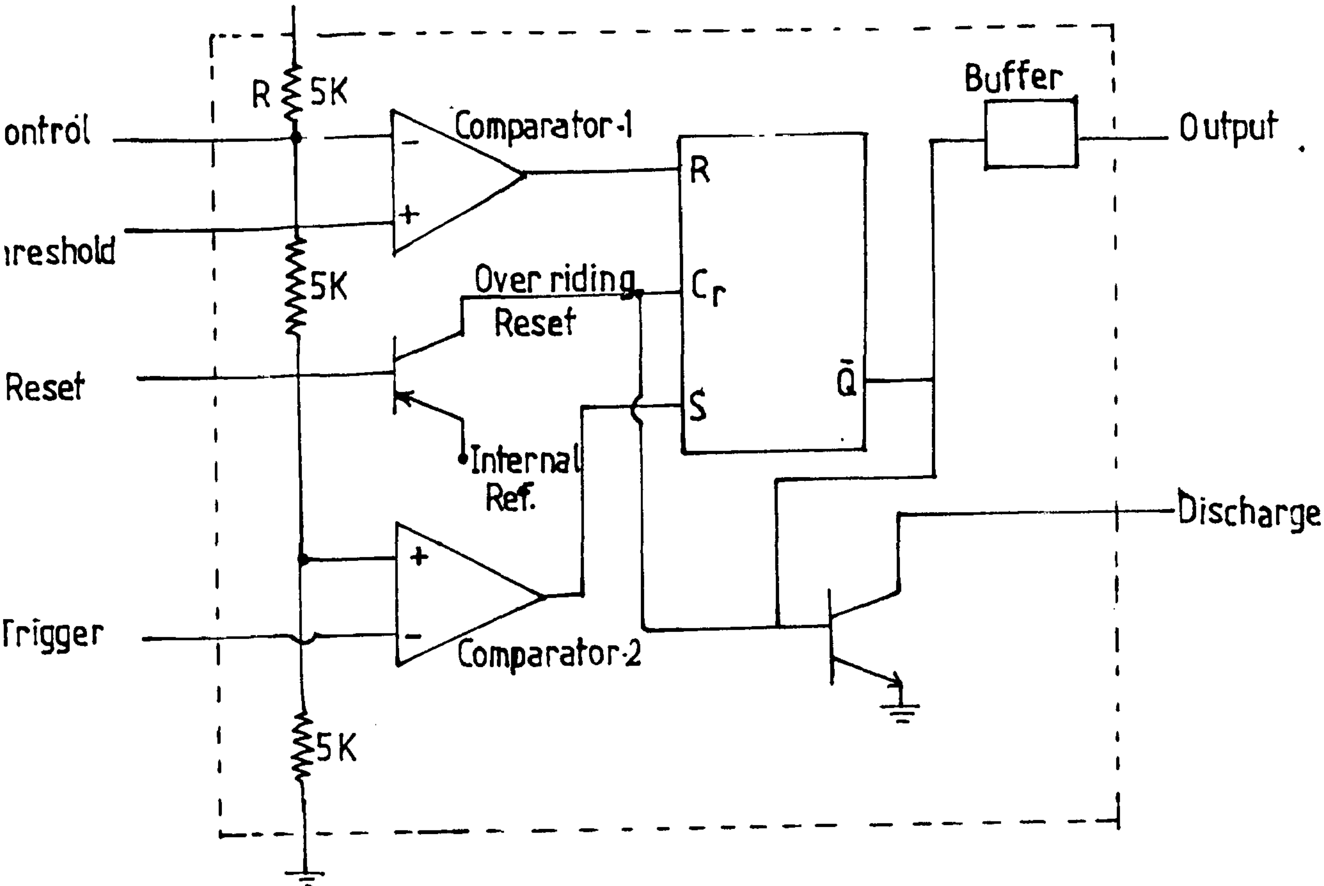

FIG.C.3 TIMER 555

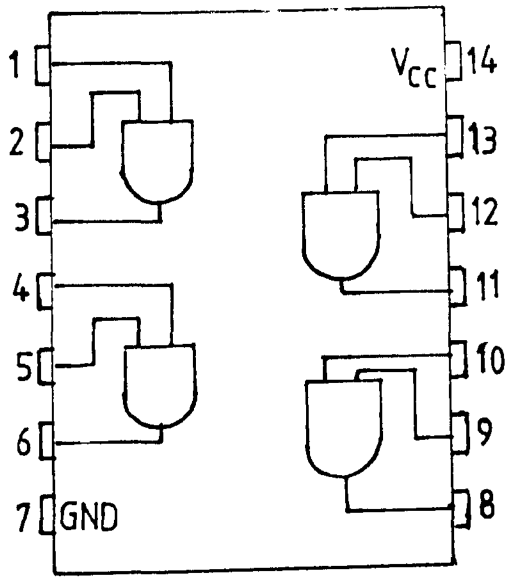

FIG.C.4 AND GATE

APPENDIX - D

```
C         PROGRAM NO.1
C         ****************************************************
C         DETERMINATION OF THE REGION OF RELATIVE STABILITY
C         OF CURRENT LOOP IN THE PLANE OF TWO PARAMETERS
C         ALPHA AND BETA WITH THE VARIATION IN SIGMA
C         USING D-DECOMPOSITION METHOD
C         ****************************************************
C         VARIABLES USED
C         **************
C         ALPHA=INVERSE OF GAIN K1
C         BETA=INVERSE OF TIME CONSTANT TC1
C         S=COMPLEX FREQUENCY
C         ALR=COEFF. OF ALPHA OF REAL EQUATION
C         ALI=COEFF. OF ALPHA OF IMAGINARY EQUATION
C         BTR=COEFF. OF BETA OF REAL EQUATION
C         BTI=COEFF. OF BETA OF IMAGINARY EQUATION
C         COEFR=CONSTANT TERM IN REAL EQUATION
C         COEFI=CONSTANT TERM IN IMAGINARY EQUATION
C         *******************************************************
          COMPLEX S,F1,F2,SF1,SF2,D
          F1(S)=A*TM*HI*(S+B/AJ)/RA
          F2(S)=(1.+(1.+S*TA)*(S+B/AJ)*TM)*(1.+S*TCA)
          OPEN(UNIT=1,FILE='CURENT.DAT')
          READ(1,*)A,TCA,B,AJ,TM,RA,TA,HI
          PRINT*,A,TCA,B,AJ,TM,RA,TA,HI
          SIGMA=0.0
          DO 50 ICOUNT=1,8
          PRINT 76,SIGMA
          PRINT 35
          OMEGA=0.0
20        S=CMPLX(SIGMA,OMEGA)
          SF2=S*F2(S)
          SF1=S*F1(S)
          ALR=REAL(SF2)
          ALI=AIMAG(SF2)
          BTR=REAL(F1(S))
```

```
      BTI=AIMAG(F1(S))
      COEFR=REAL(SF1)
      COEFI=AIMAG(SF1)
      DEN=BTI*ALR-BTR*ALI
      ANUM=BTR*COEFI-BTI*COEFR
      BNUM=ALI*COEFR-BTI*COEFI
      IF(DEN.NE.0.)GO TO 10
      IF(ANUM.NE.0.)GO TO 200
C     ******************************************************
C     CALCULATION OF SPATIAL LINE COORDINATES
C     ******************************************************
      PRINT 60,OMEGA,ALR,BTR,COEFR
      AL=0.
      DO 25 K=1,60
      BT=-(AL*ALR+COEFR)/BTR
      PRINT 26,AL,BT
   25 AL=AL+2.
C     *******************************************************
      GO TO 200
   10 ALPHA=ANUM/DEN
      BETA=BNUM/DEN
      PRINT30,OMEGA,ALPHA,BETA,DEN
      IF(OMEGA.GE.1000.) GO TO 70
  200 OMEGA=OMEGA+2.
      GO TO 20
   70 IF(OMEGA.GE.1.0E5) GO TO 50
      OMEGA=OMEGA+200.
      GO TO 20
   50 SIGMA=SIGMA-.1
   30 FORMAT(4(5X,E12.5))
   76 FORMAT(5X,'SIGMA=',F5.2/5X,'============')
   60 FORMAT(5X,'A SPATIAL LINE EXIST AT THIS POINT WHERE
     1 OMEGA=',F9.4/5X,'COEFFICENT OF ALPHA ='E15.8/5X
     2 ,'COEFFICENT OF BETA ='E15.8/5X,'CONSTANT TERM =',
     3 E15.8)
   26 FORMAT(5X,'AL=',E12.5,5X,'BT=',E12.5)
```

```
   35  FORMAT(7X,'OMEGA',12X,'ALPHA',13X,'BETA',14X,'DENOMINATER'
       STOP
       END
```

```
PROGRAM NO.2
***************************************************
DETERMINATION OF THE REGION OF RELATIVE STABILITY
OF CURRENT LOOP IN THE PLANE OF TWO PARAMETERS
ALPHA AND BETA WITH THE VARIATION IN DAMPING RATIO
USING D-DECOMPOSITION METHOD
***************************************************
VARIABLES USED
**************
ZHI=DAMPING RATIO
ALPHA=INVERSE OF GAIN K1
BETA=INVERSE OF TIME CONSTANT TC1
S=COMPLEX FREQUENCY
ALR=COEFF. OF ALPHA OF REAL EQUATION
ALI=COEFF. OF ALPHA OF IMAGINARY EQUATION
BTR=COEFF. OF BETA OF REAL EQUATION
BTI=COEFF. OF BETA OF IMAGINARY EQUATION
COEFR=CONSTANT TERM IN REAL EQUATION
COEFI=CONSTANT TERM IN IMAGINARY EQUATION
******************************************************
COMPLEX S,F1,F2,SF1,SF2,D
F1(S)=A*TM*HI*(S+B/AJ)/RA
F2(S)=(1.+(1.+S*TA)*(S+B/AJ)*TM)*(1.+S*TCA)
OPEN(UNIT=1,FILE='CURENT.DAT')
READ(1,*)A,TCA,B,AJ,TM,RA,TA,HI
PRINT*,A,TCA,B,AJ,TM,RA,TA,HI
ZHI=0.0
DO 50 ICOUNT=1,8
PRINT 76,ZHI
PRINT 35
OMEGA=0.0
RR=-ZHI*OMEGA
AA=OMEGA*SQRT(1.-ZHI*ZHI)
S=CMPLX(RR,AA)
SF2=S*F2(S)
SF1=S*F1(S)
```

```
      ALR=REAL(SF2)
      ALI=AIMAG(SF2)
      BTR=REAL(F1(S))
      BTI=AIMAG(F1(S))
      COEFR=REAL(SF1)
      COEFI=AIMAG(SF1)
      DEN=BTI*ALR-BTR*ALI
      ANUM=BTR*COEFI-BTI*COEFR
      BNUM=ALI*COEFR-BTI*COEFI
      IF(DEN.NE.0.)GO TO 10
      IF(ANUM.NE.0.)GO TO 200
      ****************************************************
      CALCULATION OF SPATIAL LINE COORDINATES
      ****************************************************
      PRINT 60,OMEGA,ALR,BTR,COEFR
      AL=0.
      DO 25 K=1,60
      BT=-(AL*ALR+COEFR)/BTR
      PRINT 26,AL,BT
      AL=AL+2.
      *****************************************************
      GO TO 200
      ALPHA=ANUM/DEN
      BETA=BNUM/DEN
      PRINT30,S,OMEGA,ALPHA,BETA,DEN
      IF(OMEGA.GE.1000.) GO TO 70
0     OMEGA=OMEGA+2.
      GO TO 20
      IF(OMEGA.GE.1.0E5) GO TO 50
      OMEGA=OMEGA+200.
      GO TO 20
      ZHI=ZHI+.1
      FORMAT(1X,2E12.5,4(5X,E12.5))
      FORMAT(5X,'ZHI=',F5.2/5X,'=============')
      FORMAT(5X,'A SPATIAL LINE EXIST AT THIS POINT WHERE
   1  OMEGA=',F9.4/5X,'COEFFICENT OF ALPHA ='E15.8/5X
```

```
    2  ,'COEFFICENT OF BETA ='E15.8/5X,'CONSTANT TERM =',
    3  E15.8)
26     FORMAT(5X,'AL=',E12.5,5X,'BT=',E12.5)
35     FORMAT(13X,'S',22X,'OMEGA',12X,'ALPHA',13X,'BETA',14X,'DENOMINATER')
       STOP
       END
```

```
C       PROGRAM NO.3
C       ***********************************************
C       FREQUENCY SCANNING TECHNIQUE FOR CURRENT LOOP WITH
C       THE VARITION IN SIGMA
C       *************************************************
        COMPLEX S,F1,F2,SF1,SF2,D
        F1(S)=A*TM*HI*(S+B/AJ)/RA
        F2(S)=(1.+(1.+S*TA)*(S+B/AJ)*TM)*(1.+S*TCA)
        OPEN(UNIT=1,FILE='CURENT.DAT')
        READ(1,*)A,TCA,B,AJ,TM,RA,TA,HI
        PRINT*,A,TCA,B,AJ,TM,RA,TA,HI
        SIGMA=-7.
        ALPHA=4.
        BETA=12.
        PRINT*,ALPHA,BETA
        OMEGA=0.
        PRINT 140
  140   FORMAT(5X,'  OMEGA',15X,'D')
        DO 150 I=1,200
        S=CMPLX(SIGMA,OMEGA)
        D=ALPHA*S*F2(S)+BETA*F1(S)+S*F1(S)
        PRINT 160,OMEGA,D
  160   FORMAT(5X,E12.5,15X,2E13.5)
  150   OMEGA=OMEGA+.2
        STOP
        END
```

```
C     PROGRAM NO.4
C     ************************************************
C     FREQUENCY SCANNING TECHNIQUE FOR CURRENT LOOP WITH
C     THE VARITION IN DAMPING RATIO
C     **************************************************
      COMPLEX S,F1,F2,SF1,SF2,D
      F1(S)=A*TM*HI*(S+B/AJ)/RA
      F2(S)=(1.+(1.+S*TA)*(S+B/AJ)*TM)*(1.+S*TCA)
      OPEN(UNIT=1,FILE='CURENT.DAT')
      READ(1,*)A,TCA,B,AJ,TM,RA,TA,HI
      PRINT*,A,TCA,B,AJ,TM,RA,TA,HI
      ZHI=0.5
      ALPHA=4.0
      BETA=12.0
      PRINT*,ALPHA,BETA
      OMEGA=0.
      PRINT 140
140   FORMAT(5X,'  OMEGA',15X,'D')
      DO 150 I=1,200
      RR=-ZHI*OMEGA
      AA=OMEGA*SQRT(1.-ZHI*ZHI)
      S=CMPLX(RR,AA)
      D=ALPHA*S*F2(S)+BETA*F1(S)+S*F1(S)
      PRINT 160,OMEGA,D
160   FORMAT(5X,E12.5,15X,2E13.5)
150   OMEGA=OMEGA+2.
      STOP
      END
```

```
C      PROGRAM NO.5
C      ******************************************************************
C      TRANSIENT RESPONSE OF CURRENT LOOP WITH A STEP CURRENT REFERENCE
C      INPUT FOR DIFFERENT VALUES OF CURRENT CONTROLLER GAIN AND
C      TIME CONSTANT
C      ******************************************************************
C      VARIABLES USED
C      ******************************************************************
C      T=INDEPENDENT VARIABLE (TIME)
C      DT=DESIRED TIME STEP FOR NUMERICAL INTEGRATION
C      NEQ=NUMBER OF FIRST ORDER DIFFERENTIAL EQUATIONS
C      NSTEP=NUMBER OF STEPS FOR INTEGRATION
C      XX=ARRAY OF DIMENSION NEQ WHICH CONTAINS THE CURRENT VALUES OF
C      STATE VARIABLES X1,X2,X3
C      F=ARRAY OF DIMENSION NEQ WHICH CONTAINS THE VALUES OF FUNCTION
C      COMPUTED AT TIME T BY ASUBROUTINE FTN(XX,F,NEQ,T)
C      YI,YJ,YK,YL,UU=DUMMY ARRAYS OF DIMENSION NEQ
C      ******************************************************************
       DIMENSION TIME(500),X(500,3),XX(3),F(3),YI(3),
      1YJ(3),YK(3),YL(3),UU(3)
C      *************************************************************
C      INITIAL VALUES OF STATE VARIABLES
C      *****************************************************************
       OPEN (UNIT=1,FILE='A.DAT')
       XX(1)=0.0
       XX(2)=1.0
       XX(3)=0.0
       NEQ=3
       NSTEP=500
       DT= .0004
       PRINT 33,DT
33     FORMAT(5X,'DT=',F9.7)
       T=0.0
       PRINT 10
10     FORMAT(2X,'PRINT OUT OF SOLUTION '//2X,'STEP',3X,'TIME',
      15X,'X(1)',7X,'X(2)',7X,' X(3)')
```

```
      I=0
      PRINT 30,I,T,(XX(J),J=1,NEQ)
      DO 40 I=1,NSTEP
      CALL RUNGE (T,DT,NEQ,XX,F,YI,YJ,YK,YL,UU)
      TIME(I)=T
      DO 20 J=1,NEQ
20    X(I,J)=XX(J)
      PRINT 30,I,TIME(I),(X(I,J),J=1,NEQ)
30    FORMAT(2X,I4,F8.6,3E12.5)
40    CONTINUE
      WRITE(1,111)(X(I,3),TIME(I),I=1,NSTEP)
111   FORMAT(2F10.2)
      END
C     ***************************************************
      SUBROUTINE RUNGE(T,DT,NEQ,XX,F,YI,YJ,YK,YL,UU)
C     ***************************************************
      DIMENSION YI(NEQ),YJ(NEQ),YK(NEQ),YL(NEQ),
     1UU(NEQ),XX(NEQ),F(NEQ)
      DO 10 I=1,NEQ
10    UU(I)=XX(I)
      CALL FTN(XX,F,NEQ,T)
      DO 20 I=1,NEQ
      YI(I)=F(I)*DT
20    XX(I)=UU(I)+YI(I)/2.0
      T=T+DT/2.0
      CALL FTN (XX,F,NEQ,T)
      DO 30 I=1,NEQ
      YJ(I)=F(I)*DT
30    XX(I)=UU(I)+YJ(I)/2.0
      CALL FTN(XX,F,NEQ,T)
      DO 40 I=1,NEQ
      YK(I)=F(I)*DT
40    XX(I)=UU(I)+YK(I)
      T=T+DT/2.0
      CALL FTN(XX,F,NEQ,T)
      DO 50 I=1,NEQ
```

```
      YL(I)=F(I)*DT
50    XX(I)=UU(I)+(YI(I)+2.0*YJ(I)+2.0*YK(I)+YL(I))/6.0
      RETURN
      END
C     ******************************************************
      SUBROUTINE FTN(XX,F,NEQ,T)
C     ******************************************************
      DIMENSION XX(NEQ),F(NEQ)
      OPEN(UNIT=2,DEVICE='DSK',FILE='X1.DAT')
      READ(2,*)AK1,TC1,HI,A,TCA,AL,RA
      VC2=1.0
      F(1)=AK1*(VC2-HI*XX(3))/TC1
      VC1=XX(1)+AK1*(VC2-HI*XX(3))
      IF(VC1.GT.9.0)VC1=9.0
      IF(VC1.LT.-9.0)VC1=-9.0
      F(2)=(A*VC1-XX(2))/TCA
      F(3)=(XX(2)-RA*XX(3))/AL
      RETURN
      END
```

```
C         PROGRAM NO.6
C         ******************************************************
C         PLOTTING OF TRANSIENT REAPONSE FOR CURRENT LOOP WITH
C         A STEP CURRENT REFERENCE INPUT
C         ******************************************************
          DIMENSION CURENT(502),TIME(502)
          OPEN(UNIT=1,DIALOG)
          CALL PLOTS(0.,0.,5)
          READ(1,10)(CURENT(J),TIME(J),J=1,500)
10        FORMAT(2F10.6)
          TIME(501)=0.
          TIME(502)=0.1
          CURENT(501)=0.0
          CURENT(502)=0.25
          DO 30 I=1,2
          CALL AXIS(0.,0.,'TIME',-4,21.,0.,TIME(501),TIME(502))
          CALL AXIS(0.,0.,'CURRENT',7,10.,90.,CURENT(501),CURENT(502))
30        CONTINUE
          CALL LINE(TIME,CURENT,500,1,0,0)
          DO 20 J=1,3
          CALL SYMBOL(9.0,-2.,0.25,'FIG.',0.,4)
          CALL SYMBOL(10.0,3.,0.25,'GAIN(K1)= 0.250',0.,15)
          CALL SYMBOL(10.0,2.0,0.25,'TIME CONST.(TC1)= 0.111',0.,23)
20        CONTINUE
          CALL PLOT(0.,0.,-999)
          STOP
          END
```

```
C        PROGRAM NO.7
C        ********************************************************
C        DETERMINATION OF THE REGION OF RELATIVE STABILITY
C        OF SPEED LOOP IN THE PLANE OF TWO PARAMETERS.
C        ALPHA AND BETA WITH THE VARIATION IN SIGMA
C        USING D-DECOMPOSITION METHOD
C        ********************************************************
C        VARIABLES USED
C        **************
C        ALPHA=INVERSE OF GAIN K2
C        BETA=INVERSE OF TIME CONSTANT TC2
C        S=COMPLEX FREQUENCY
C        ALR=COEFF. OF ALPHA OF REAL EQUATION
C        ALI=COEFF. OF ALPHA OF IMAGINARY EQUATION
C        BTR=COEFF. OF BETA OF REAL EQUATION
C        BTI=COEFF. OF BETA OF IMAGINARY EQUATION
C        COEFR=CONSTANT TERM IN REAL EQUATION
C        COEFI=CONSTANT TERM IN IMAGINARY EQUATION
C        *******************************************************
         COMPLEX S,F1,F2,SF3,SF4,F3,F4
         F1(S)=AK1*A*TM/RA*(1.+S*TC1)*(S+B/AJ)
         F2(S)=S*TC1*(1.+(1.+S*TA)*(S+B/AJ)*TM)*(1.+S*TCA)
         F3(S)=F1(S)*AKB*HW/AJ
         F4(S)=(F2(S)+HI*F1(S))*(S+B/AJ)*(1.+S*TF)
         OPEN(UNIT=1,FILE='SPEED.DAT')
         READ(1,*)A,TCA,B,AJ,TM,RA,TA,HI,AK1,TC1,HW,AKB,TF
         PRINT*,A,TCA,B,AJ,TM,RA,TA,HI,AK1,TC1,HW,AKB,TF
         SIGMA=0.0
         DO 50 ICOUNT=1,10
         PRINT 76,SIGMA
         PRINT 35
         OMEGA=0.0
 20      S=CMPLX(SIGMA,OMEGA)
         SF4=S*F4(S)
         SF3=S*F3(S)
         ALR=REAL(SF4)
```

```
      ALI=AIMAG(SF4)
      BTR=REAL(F3(S))
      BTI=AIMAG(F3(S))
      COEFR=REAL(SF3)
      COEFI=AIMAG(SF3)
      DEN=BTI*ALR-BTR*ALI
      ANUM=BTR*COEFI-BTI*COEFR
      BNUM=ALI*COEFR-BTI*COEFI
      IF(DEN.NE.0.)GO TO 10
      IF(ANUM.NE.0.)GO TO 200
C     *****************************************************
C     CALCULATION OF SPATIAL LINE COORDINATES
C     *****************************************************
      PRINT 60,OMEGA,ALR,BTR,COEFR
      AL=0.
      DO 25 K=1,60
      BT=-(AL*ALR+COEFR)/BTR
      PRINT 26,AL,BT
25    AL=AL+1.
C     *****************************************************
      GO TO 200
10    ALPHA=ANUM/DEN
      BETA=BNUM/DEN
      PRINT30,OMEGA,ALPHA,BETA,DEN
200   IF(OMEGA.GE.1000.)GO TO 70
      OMEGA=OMEGA+2.00
      GO TO 20
70    IF(OMEGA.GE.1.0E5) GO TO 50
      OMEGA=OMEGA+200.
      GO TO 20
50    SIGMA=SIGMA-0.1
30    FORMAT(4(5X,E12.5))
35    FORMAT(7X,'OMEGA',13X,'ALPHA',14X,'BETA',14X,'DENOMINATER')
76    FORMAT(5X,'SIGMA=',F5.2/5X,'============')
26    FORMAT(5X,'AL=',E12.5,5X,'BT=',E12.5)
60    FORMAT(5X,'A SPATIAL LINE EXIST AT THIS POINT WHERE
```

```
     1 OMEGA=',F9.4/5X,'COEFFICENT OF ALPHA ='E15.8/5X
     2 ,'COEFFICENT OF BETA ='E15.8/5X,'CONSTANT TERM =',
     3 E15.8)
 800  STOP
      END
```

```
C      PROGRAM NO.8
C      ***********************************************************
C      DETERMINATION OF THE REGION OF RELATIVE STABILITY
C      OF SPEED LOOP IN THE PLANE OF TWO PARAMETERS
C      ALPHA AND BETA WITH THE VARIATION IN DAMPING RATIO
C      USING D-DECOMPOSITION METHOD
C      ***********************************************************
C      VARIABLES USED
C      **************
C      ALPHA=INVERSE OF GAIN K2
C      BETA=INVERSE OF TIME CONSTANT TC2
C      S=COMPLEX FREQUENCY
C      ALR=COEFF. OF ALPHA OF REAL EQUATION
C      ALI=COEFF. OF ALPHA OF IMAGINARY EQUATION
C      BTR=COEFF. OF BETA OF REAL EQUATION
C      BTI=COEFF. OF BETA OF IMAGINARY EQUATION
C      COEFR=CONSTANT TERM IN REAL EQUATION
C      COEFI=CONSTANT TERM IN IMAGINARY EQUATION
C      ***********************************************************
       COMPLEX S,F1,F2,SF3,SF4,F3,F4
       F1(S)=AK1*A*TM/RA*(1.+S*TC1)*(S+B/AJ)
       F2(S)=S*TC1*(1.+(1.+S*TA)*(S+B/AJ)*TM)*(1.+S*TCA)
       F3(S)=F1(S)*AK8*HW/AJ
       F4(S)=(F2(S)+HI*F1(S))*(S+B/AJ)*(1.+S*TF)
       OPEN(UNIT=1,FILE='SPEED.DAT')
       READ(1,*)A,TCA,B,AJ,TM,RA,TA,HI,AK1,TC1,HW,AKB,TF
       PRINT*,A,TCA,B,AJ,TM,RA,TA,HI,AK1,TC1,HW,AKB,TF
       ZHI=0.0
       DO 50 ICOUNT=1,10
       PRINT 76,ZHI
       PRINT 35
       OMEGA=0.0
2      RR=-ZHI*OMEGA
       AA=OMEGA*SQRT(1.-ZHI*ZHI)
       S=CMPLX(RR,AA)
       SF4=S*F4(S)
```

```
      SF3=S*F3(S)
      ALR=REAL(SF4)
      ALI=AIMAG(SF4)
      BTR=REAL(F3(S))
      BTI=AIMAG(F3(S))
      COEFR=REAL(SF3)
      COEFI=AIMAG(SF3)
      DEN=BTI*ALR-BTR*ALI
      ANUM=BTR*COEFI-BTI*COEFR
      BNUM=ALI*COEFR-BTI*COEFI
      IF(DEN.NE.0.)GO TO 10
      IF(ANUM.NE.0.)GO TO 200
C     ******************************************************
C     CALCULATION OF SPATIAL LINE COORDINATES
C     ******************************************************
      PRINT 60,OMEGA,ALR,BTR,COEFR
      AL=0.
      DO 25 K=1,60
      BT=-(AL*ALR+COEFR)/BTR
      PRINT 20,AL,BT
25    AL=AL+1.
C     ******************************************************
      GO TO 200
10    ALPHA=ANUM/DEN
      BETA=BNUM/DEN
      PRINT30,OMEGA,ALPHA,BETA,DEN
200   IF(OMEGA.GE.1000.)GO TO 70
      OMEGA=OMEGA+2.00
      GO TO 20
70    IF(OMEGA.GE.1.0E5) GO TO 50
      OMEGA=OMEGA+200.
      GO TO 20
50    ZHI=ZHI+0.1
30    FORMAT(4(5X,E12.5))
35    FORMAT(7X,'OMEGA',13X,'ALPHA',14X,'BETA',14X,'DENOMINATOR')
75    FORMAT(5X,'ZHI=',F5.2/5X,'============')
```

```
      26   FORMAT(5X,'AL=',E12.5,5X,'BT=',E12.5)
      6    FORMAT(5X,'A SPATIAL LINE EXIST AT THIS POINT WHERE
         1 OMEGA=',F9.4/5X,'COEFFICENT OF ALPHA ='E15.8/5X
         2 ,'COEFFICENT OF BETA ='E15.8/5X,'CONSTANT TERM =',
         3 E15.8)
           STOP
           END
```

```
C       PROGRAM NO.9
C       ***********************************************
C       FREQUENCY SCANNING TECHNIQUE FOR SPEED LOOP WITH
C       THE VARITION IN SIGMA
C       ***********************************************
        COMPLEX S,F1,F2,SF3,SF4,F3,F4,D
        F1(S)=AK1*A*TM/RA*(1.+S*TC1)*(S+B/AJ)
        F2(S)=S*TC1*(1.+(1.+S*TA)*(S+B/AJ)*TM)*(1.+S*TCA)
        F3(S)=F1(S)*AKB*HW/AJ
        F4(S)=(F2(S)+HI*F1(S))*(S+B/AJ)*(1.+S*TF)
        OPEN(UNIT=1,FILE='SPEED.DAT')
        READ(1,*)A,TCA,B,AJ,TM,RA,TA,HI,AK1,TC1,HW,AKB,TF
        PRINT*,A,TCA,B,AJ,TM,RA,TA,HI,AK1,TC1,HW,AKB,TF
        SIGMA=-0.8
        ALPHA=1.0
        BETA=0.5
        PRINT*,ALPHA,BETA
        OMEGA=0.
        PRINT 140
140     FORMAT(5X,'  OMEGA',15X,'D')
        DO 150 I=1,200
        S=CMPLX(SIGMA,OMEGA)
        D=ALPHA*S*F4(S)+BETA*F3(S)+S*F3(S)
        PRINT 160,OMEGA,D
160     FORMAT(5X,E12.5,15X,2E13.5)
150     OMEGA=OMEGA+.2
        STOP
        END
```

```
C       PROGRAM NO.10
C       ************************************************
C       FREQUENCY SCANNING TECHNIQUE FOR SPEED LOOP WITH
C       THE VARITION IN DAMPING RATIO
C       ************************************************
        COMPLEX S,F1,F2,SF3,SF4,F3,F4,D
        F1(S)=AK1*A*TM/RA*(1.+S*TC1)*(S+B/AJ)
        F2(S)=S*TC1*(1.+(1.+S*TA)*(S+B/AJ)*TM)*(1.+S*TCA)
        F3(S)=F1(S)*AKB*HW/AJ
        F4(S)=(F2(S)+HI*F1(S))*(S+B/AJ)*(1.+S*TF)
        OPEN(UNIT=1,FILE='SPEED.DAT')
        READ(1,*)A,TCA,B,AJ,TM,RA,TA,HI,AK1,TC1,HW,AKB,TF
        PRINT*,A,TCA,B,AJ,TM,RA,TA,HI,AK1,TC1,HW,AKB,TF
        ZHI=0.7
        ALPHA=1.
        BETA=0.5
        PRINT*,ALPHA,BETA
        OMEGA=0.
        PRINT 140
140     FORMAT(5X,'  OMEGA',15X,'D')
        DO 150 I=1,200
        RR=-ZHI*OMEGA
        AA=OMEGA*SQRT(1.-ZHI*ZHI)
        S=CMPLX(RR,AA)
        D=ALPHA*S*F4(S)+BETA*F3(S)+S*F3(S)
        PRINT 160,OMEGA,D
160     FORMAT(5X,E12.5,15X,2E13.5)
150     OMEGA=OMEGA+.2
        STOP
        END
```

```
C     PROGRAM NO.11
C     ******************************************************************
C     TRANSIENT RESPONSE OF SPEED LOOP WITH A STEP SPEED REFERENCE
C     INPUT FOR DIFFERENT VALUES OF SPEED CONTROLLER GAIN AND
C     TIME CONSTANT
C     ******************************************************************
C     VARIABLES USED
C     ******************************************************************
C     T=INDEPENDENT VARIABLE (TIME)
C     DT=DESIRED TIME STEP FOR NUMERICAL INTEGRATION
C     NEQ=NUMBER OF FIRST ORDER DIFFERENTIAL EQUATIONS
C     NSTEP=NUMBER OF STEPS FOR INTEGRATION
C     XX=ARRAY OF DIMENSION NEQ WHICH CONTAINS THE CURRENT VALUES OF
C     STATE VARIABLES X1,X2,X3
C     F=ARRAY OF DIMENSION NEQ WHICH CONTAINS THE VALUES OF FUNCTION
C     COMPUTED AT TIME T BY ASUBROUTINE FTN(XX,F,NEQ,T)
C     YI,YJ,YK,YL,UU=DUMMY ARRAYS OF DIMENSION NEQ
C     ******************************************************************
      DIMENSION TIME(2500),X(2500,6),XX(6),F(6),YI(6),
     1YJ(6),YK(6),YL(6),UU(6)
      OPEN (UNIT=1,FILE='PA.DAT')
      XX(1)=0.0
      XX(2)=0.0
      XX(3)=0.0
      XX(4)=0.0
      XX(5)=0.0
      XX(6)=0.0
      NEQ=6
      NSTEP=2500
      DT=.0049
     PRINT 33,DT
33    FORMAT(5X,'DT=',F9.7)
      T=0.0
     PRINT 10
10    FORMAT(2X,'PRINT OUT OF SOLUTION '//2X,'STEP',3X,'TIME',
     15X,'X(1)',7X,'X(2)',7X,' X(3)',7X,'X(4)',7X,'X(5)',7X,'X(6)')
```

```
      I=0
      PRINT 30,I,T,(XX(J),J=1,NEQ)
      DO 40 I=1,NSTEP
      CALL RUNGE (T,DT,NEQ,XX,F,YI,YJ,YK,YL,UU)
      TIME(I)=T
      DO 20 J=1,NEQ
20    X(I,J)=XX(J)
      PRINT 30,I,TIME(I),X(I,5)
30    FORMAT(2X,I4,F8.6,E12.5)
40    CONTINUE
      WRITE(1,111)(X(I,5),TIME(I),I=1,NSTEP)
111   FORMAT(2F10.6)
      END
C     ************************************************
      SUBROUTINE RUNGE(T,DT,NEQ,XX,F,YI,YJ,YK,YL,UU)
C     ************************************************
      DIMENSION YI(NEQ),YJ(NEQ),YK(NEQ),YL(NEQ),
     1UU(NEQ),XX(NEQ),F(NEQ)
      DO 10 I=1,NEQ
10    UU(I)=XX(I)
      CALL FTN(XX,F,NEQ,T)
      DO 50 I=1,NEQ
      YI(I)=F(I)*DT
50    XX(I)=UU(I)+YI(I)/2.0
      T=T+DT/2.0
      CALL FTN (XX,F,NEQ,T)
      DO 30 I=1,NEQ
      YJ(I)=F(I)*DT
30    XX(I)=UU(I)+YJ(I)/2.0
      CALL FTN(XX,F,NEQ,T)
      DO 80 I=1,NEQ
      YK(I)=F(I)*DT
80    XX(I)=UU(I)+YK(I)
      T=T+DT/2.0
      CALL FTN(XX,F,NEQ,T)
      DO 90 I=1,NEQ
```

```
      YL(I)=F(I)*DT
90    XX(I)=UU(I)+(YI(I)+2.0*YJ(I)+2.0*YK(1)+YL(I))/6.0
      RETURN
      END
C     ************************************************
      SUBROUTINE FTN(XX,F,NEQ,T)
C     ************************************************
      DIMENSION XX(NEQ),F(NEQ)
      OPEN(UNIT=2,DEVICE='DSK',FILE='PX1.DAT')
      READ(2,*)AK1,TC1,HI,A,TCA,AL,RA,AJ,B,AKB,HW,TF,AK2,TC2
      VR=12.0
      VC1=XX(2)+AK1*(VC2-HI*XX(4))
      IF(VC1.GT.9.0)VC1=9.0
      IF(VC1.LT.-9.0)VC1=-9.0
      VC2=XX(1)+AK2*(VR-XX(6))
      IF(VC2.LT.-4.0) VC2=-4.0
      IF(VC2.GT.4.0) VC2=4.0
      F(1)=AK2/TC2*(VR-XX(6))
      F(2)=AK1/TC1*(VC2-HI*XX(4))
      F(3)=(A*VC1-XX(3))/TCA
      F(4)=(XX(3)-RA*XX(4)-AKB*XX(5))/AL
      F(5)=(AKB*XX(4)-B*XX(5))/AJ
      F(6)=(HW*XX(5)-XX(6))/TF
      RETURN
      END
```

```
C        PROGRAM NO.12
C        **************************************************************
C        PLOTTING OF TRANSIENT RESPONSE OF SPEED LOOP WITH
C        A STEP SPEED REFERENCE INPUT
C        **************************************************************
         DIMENSION SPEED(2002),TIME(2002)
         OPEN(UNIT=1,DIALOG)
         READ (1,20)(SPEED(J),TIME(J),J=1,2000)
   20    FORMAT(2F10.6)
         CALL PLOTS(0.,0.,5)
         TIME(2001)=0.
         TIME(2002)=0.4
         SPEED(2001)=0.
         SPEED(2002)=0.8
         DO 30 I=1,2
         CALL AXIS(0.,0.,'TIME (SECONDS)',-14,25.,0.,TIME(2001),TIME(2002))
         CALL AXIS(0.,0.,'SPEED (RPS)',11,15.,90.,SPEED(2001),SPEED(2002))
   30    CONTINUE
         CALL LINE(TIME,SPEED,2000,1,0,0)
         DO 24 J=1,3
         CALL SYMBOL(12.,-2.,0.25,'FIG.',0.,4)
         CALL SYMBOL(15.,6.,0.25,'GAIN (K2)= 0.813',0.,16)
         CALL SYMBOL(15.,5.,0.25,'TIME CONST.(TC2)= 2.000',0.,23)
   24    CONTINUE
         CALL PLOT(0.,0.,-999)
         STOP
         END
```

```
C       PROGRAM NO.13
C       ****************************************************************
C       CALCULATION OF AVERAGE CIRCULATING CURRENT WITH VARITION
C       IN TRIGGER ANGLE AT DIFFERENT REACTOR INDUCTANCE
C       ****************************************************************
C       VARIBLES USED
C       **************
C       ALPHA1,ALPHA2=FIRING ANGLES IN DEGREE OF CONVERTERS
C       ALRAD1,ALRAD2=FIRING ANGLES IN RADIAN OF CONVERTERS
C       VM=SUPPLY VOLTAGE(RMS)
C       FQ=SUPPLY FREQUENCY(HZ)
C       AL=REACTOR INDUCTANCE
C       AVGIC=AVERAGE CIRCULATING CURRENT
C       ****************************************************************
        OPEN(UNIT=1,DEVICE='DSK',FILE='CCC.DAT')
        DATA VM,FQ/400.0,50.0/
        PRINT*,VM,FQ
        PI=3.1415927
        AL=1.0
        DO 50 I=1,3
        PRINT 4,AL
        PRINT 5
        CONST=2.8284271*VM/(2.*PI*PI*FQ*AL)
        ALPHA1=0.
        DO 43 JK=1,181
        ALRAD1=ALPHA1*PI/180.
        IF(ALPHA1.GT.90.) GO TO 30
        AVGIC=CONST*(-ALRAD1*COS(ALRAD1)+SIN(ALRAD1))
        GO TO 60
30      ALPHA2=180.-ALPHA1
        ALRAD2=ALPHA2*PI/180.
        AVGIC=CONST*(-ALRAD2*COS(ALRAD2)+SIN(ALRAD2))
60      PRINT 20,ALPHA1,AVGIC
        WRITE(1,25)ALPHA1,AVGIC
43      ALPHA1=ALPHA1+1.0
        PRINT 6
```

```
C     PROGRAM NO.14
C     ************************************************
C     PLOTTING OF CIRCULATING CURRENT
C     ************************************************
      DIMENSION  CURENT(183),DEGREE(183)
      OPEN(UNIT=1,DIALOG)
      CALL PLOTS(0.,0.,5)
      DEGREE(182)=0.
      DEGREE(183)=9.0
      CURENT(182)=0.0
      CURENT(183)=0.075
      DO 30 I=1,2
      CALL AXIS(0.,0.,'FIRING ANGLE ALPHA1 (DEGREES)',
     1-29,21.,0.,DEGREE(182),DEGREE(183))
      CALL AXIS(0.,0.,'AVERAGE CIRCULATING CURRENT (IC)',
     1 32,20.,90.,CURENT(182),CURENT(183))
   30 CONTINUE
      DO 22 KI=1,3
      READ(1,20)(DEGREE(J),CURENT(J),J=1,181)
   20 FORMAT(2F10.6)
      CALL LINE(DEGREE,CURENT,181,1,0,0)
      CALL PLOT(0.0,0.,-3)
   22 CONTINUE
      DO 24 J=1,3
      CALL SYMBOL(9.0,-2.,0.25,'FIG.',0.,4)
      CALL SYMBOL(15.,15.,0.25,'L=1.0H',0.,6)
      CALL SYMBOL(15.,14.,0.25,'L=1.5H',0.,6)
      CALL SYMBOL(15.,13.,0.25,'L=2.0H',0.,6)
   24 CONTINUE
      CALL PLOT(0.,0.,-999)
      STOP
      END
```